AFCRC-TN-56-656
ASTIA Document No. AD 98712

**NEW YORK UNIVERSITY**
Institute of Mathematical Sciences
Division of Electromagnetic Research

RESEARCH REPORT No. MH-5

# Resolution of an Initial Shear Flow Discontinuity in One-Dimensional-Hydromagnetic Flow

JACK BAZER

CONTRACT NO. AF 19(604)-926
JUNE, 1956

c.2

NEW YORK UNIVERSITY
Institute of Mathematical Sciences
Division of Electromagnetic Research

Research Report No. MH-5

# RESOLUTION OF AN INITIAL SHEAR FLOW DISCONTINUITY IN ONE-DIMENSIONAL HYDROMAGNETIC FLOW

Jack Bazer

Jack Bazer
Jack Bazer

Morris Kline
Morris Kline
Project Director

June, 1956

*The research reported in this document has been made possible through support and sponsorship extended by the Geophysics Research Directorate of the Air Force Cambridge Research Center, under Contract No. AF 19(604)-926. It is published for technical information only and does not necessarily represent recommendations or conclusions of the sponsoring agency.*

New York, 1956

# Table of Contents

Page

Abstract (i)-(iv)

1. Introduction 1

2. Survey of known results. Formulation of the problem 9
  - 2.1 The equations of one-dimensional hydromagnetic motion 9
  - 2.2 Hydromagnetic shocks 11
  - 2.3 Hydromagnetic simple waves 14
  - 2.4 Formulation of the problem 18

3. Switch-on and fast gas dynamical shocks 26
  - 3.1 Introductory remarks 26
  - 3.2 Switch-on shocks 27
  - 3.3 Fast gas dynamical shocks 32

4. Slow and fast simple waves 35
  - 4.1 Preliminary comments - Terminology 35
  - 4.2 Slow and fast simple rarefaction waves 37
  - 4.3 Approximate expressions for $\kappa(s/s_{tr};s_{tr})$ and $\lambda(s/s_{tr};s_{tr})$ 44

5. Resolution of the shear flow discontinuity 51
  - 5.1 Preliminary considerations; notation 51
  - 5.2 The state behind the fast shocks assuming the pressure ratio and state in front is prescribed 54
    - 5.21 The switch-on shock 54
    - 5.22 The fast gas shock 56
  - 5.3 The state in the simple wave region (Region (2)) behind the shock 57
    - 5.31 The RS combination 57
    - 5.32 The RG combination 59
  - 5.4 Program for establishing the dependence of $\eta (= s_1/s_o)$ on $(u_{y,0}/b_o)$ for several values of $s_o$ 61
    - 5.41 Preliminary remarks 61
    - 5.42 The program for the RG combination 63
    - 5.43 The program for the RS combination 66
  - 5.5 Approximate expressions for $\eta$ , $s_3/s_1$ and $(H_{y,3}/H_x)$ 68
    - 5.51 Approximate expressions for $\eta$, $(H_{y,3}/H_x)$ when $(u_{y,0}/b_o)$ is very large 68
    - 5.52 Approximate expressions for $\eta$ , $s_3/s_{tr}$ and $(H_{y,3}/H_x)$ when $(u_{y,0}/b_o)$ is small 70

## Table of Contents
(cont'd)

Page

6. Interpretation of the results 75

6.1 Introductory remarks 75

6.2 Some general features of the solution in Region (1), behind the shock 76

6.21 Some general features of the solution in Region (1) behind the pure gas shock 77

6.22 Some general features of the motion in Region (1) behind the switch-on shock 80

6.3 Some general features of the motion in Region (3) between the rarefaction waves 81

Acknowledgments 84

## Figures

Figure 1 1

Figure 2 2

Figures 3 - 13 86-96

Figure 14 103

Figures 15a-15c 97-102

Figures 16 - 19 104-109

Appendix I 110

Appendix II 115

References 117

## Abstract

We are concerned here with the nonlinear one-dimensional hydromagnetic flow problem of the resolution of an initial shear flow discontinuity in a perfectly conducting, electrically neutral, compressible fluid. By one-dimensional hydromagnetic flow we mean a hydromagnetic flow in which the dependent variables, the magnetic intensity, fluid velocity, density, pressure and entropy per unit mass, are functions of one space variable, x say, and time t; no restriction need be imposed as to the presence or absence of the y- and z-components of the magnetic intensity and fluid velocity. Consider a plane surface normal to the x-axis across which a component, the y-component say, of the velocity is discontinuous and across which no fluid passes. In addition, let it be assumed that these variables are independent of x initially and, moreover, that the transverse component of the magnetic field (i.e., the component normal to the x-axis), vanishes initially. Such a flow discontinuity is referred to as a shear flow discontinuity. Since the basic hydromagnetic equations are invariant under galilean transformations we may, without loss of generality, assume that the longitudinal component of the velocity (i.e., the component parallel to the x-axis), and the z-component of the velocity also vanish and that the y-component of the velocity in the region $x > 0$ is equal and opposite to that in the region $x < 0$. Hereafter, we shall assume this to be the case. Now if the longitudinal component of the magnetic field, $H_x$, is assumed not to vanish, it can be shown that a shear flow discontinuity is not an admissible hydromagnetic contact discontinuity. The existence of an initial shear flow discontinuity in the presence of a longitudinal magnetic field must therefore be accommodated by a suitable motion of the medium. We refer to this motion as being a 'resolution' of the initial shear flow discontinuity. The object of this work is to construct the solution of this nonlinear initial-value problem, to discuss some of the general features of this solution and to provide for each time $t > 0$ the numerical basis

for obtaining the waveforms of the variables which characterize the flow.

An idealized physical situation in which a shear flow discontinuity occurs is the following. Consider a layer of perfectly conducting, compressible fluid with faces transverse to the x-direction. Assume, at the initial instant, that the fluid within the layer moves uniformly in the negative y-direction, that only the fluid within the layer is in motion, and that the pressure and density are continuous across the layer faces and are independent of x. Such an initial motion may be regarded as an idealization of a jet proceeding in the negative y-direction and much wider in the z-direction than in the x-direction. At each face of the jet we encounter a shear flow discontinuity. The waves resulting from the resolution of the shear flow discontinuity at each face will interact only after a certain time. Before this time the situation may be described by a wave motion resulting from a single interface. It is this motion that is considered here.

The methods employed to determine the motion parallel those employed in one-dimensional gas dynamical problems. It is shown that the initial discontinuity is resolved by two fast shocks moving away from the position of the initial discontinuity followed by slow, centered hydromagnetic rarefaction waves. These rarefaction waves connect the constant state immediately behind the moving shock fronts either to the endpoints of an expanding zone in which the thermodynamic state is constant and the medium is motionless or to the endpoints of a vacuum zone which expands with an appropriate 'escape speed'. The fast shocks in question are fast gas dynamical shocks unless the square ratio between the sound the Alfvén disturbance speed in the undisturbed medium is less than unity and the shock strength is less than a certain 'critical' value. In this last case the resolution is effected by switch-on shocks. Fast gas dynamical shocks are gas shocks in which the speed of the shock front is greater than the Alfvén characteristic speed behind the shock. Switch-on shocks are shocks having a vanishing transverse magnetic field ahead of the shock front but nevertheless a non-vanishing transverse magnetic field component behind the shock.

Switch-on shocks, fast gas shocks, and slow simple wave solutions, the basic building blocks entering into the construction of the solution, are investigated in detail. It is then shown that a complete quantitative description of the motion may be obtained from the knowledge of how two pressure ratios, $p_1/p_0$ and $p_3/p_0$, depend on the magnitude of the initial discontinuity $2u_{y,0}$, the sound speed, and the Alfvén disturbance speed, in the medium in front of the advancing shocks. Here, $p_0$ and $p_1$ are the pressures in front of and behind the shocks and $p_3$ is the pressure at the rails of the simple waves.

A result of particular interest is that in the region between the rarefaction waves a transverse component, $H_{y,3}$, of the magnetic field is created, even though such a component was nowhere present initially. When the magnitude of the initial discontinuity of the velocity $2u_{y,0}$ is small, it is shown that $H_{y,3}$ is proportional to the product of $u_{y,0}$ and the square root of $\rho_0$, the density in the undisturbed medium. When $u_{y,0}$ is large - that is, when the nonlinear terms in the basic equations are operative, it is shown that $H_{y,3}$ is proportional to the product of the square root of $u_{y,0}$, of the fixed longitudinal magnetic field $H_x$, and of the fourth root of the density $\rho_0$ in front of the waves. Thus, even when $H_x$ is very small, a large transverse magnetic field is created behind the rarefaction waves if the magnitude of the initial shear flow discontinuity $2u_{y,0}$ is large enough. Associated with this result is the fact that the motion of the medium differs radically from the corresponding gas dynamical steady-state shear flow motion, even when $H_x$ is small, if $2u_{y,0}$ is large enough. As already indicated above, a longitudinal motion results while no such motion occurs in the gas dynamical case. Moreover, this longitudinal motion is such that cavitation is produced whenever $u_{y,0}$ exceeds a certain minimum value which depends on the ratio of the sound speed and the Alfvén disturbance speed in the medium in front of the advancing shocks.

The exact nature of the dependence of $p_3/p_1$, $p_1/p_0$, $H_{y,3}/H_x$ and other quantities of interest on the parameters which characterize the state in front of the advancing shocks is obtained by a combination of graphical and numerical methods. In addition, approximate expressions for these quantities are developed for small and large values of the initial discontinuity. From an analysis of these results we then ascertain some of the general features of the motion.

## 1. Introduction

We are concerned here with the nonlinear one-dimensional hydromagnetic flow problem of the resolution of a shear flow discontinuity in a perfectly conducting, electrically neutral, compressible fluid. By one-dimensional hydromagnetic flow we mean a hydromagnetic flow in which the dependent variables, the magnetic intensity, fluid velocity, density, pressure and entropy per unit mass, are functions of one space variable, x say, and the time t; no restriction need be imposed as to the presence or absence of the x and z-components of the magnetic intensity and fluid velocity. Because the flow depends only on the single space variable x, it is clear that shock and contact discontinuities, when present, appear only across planes

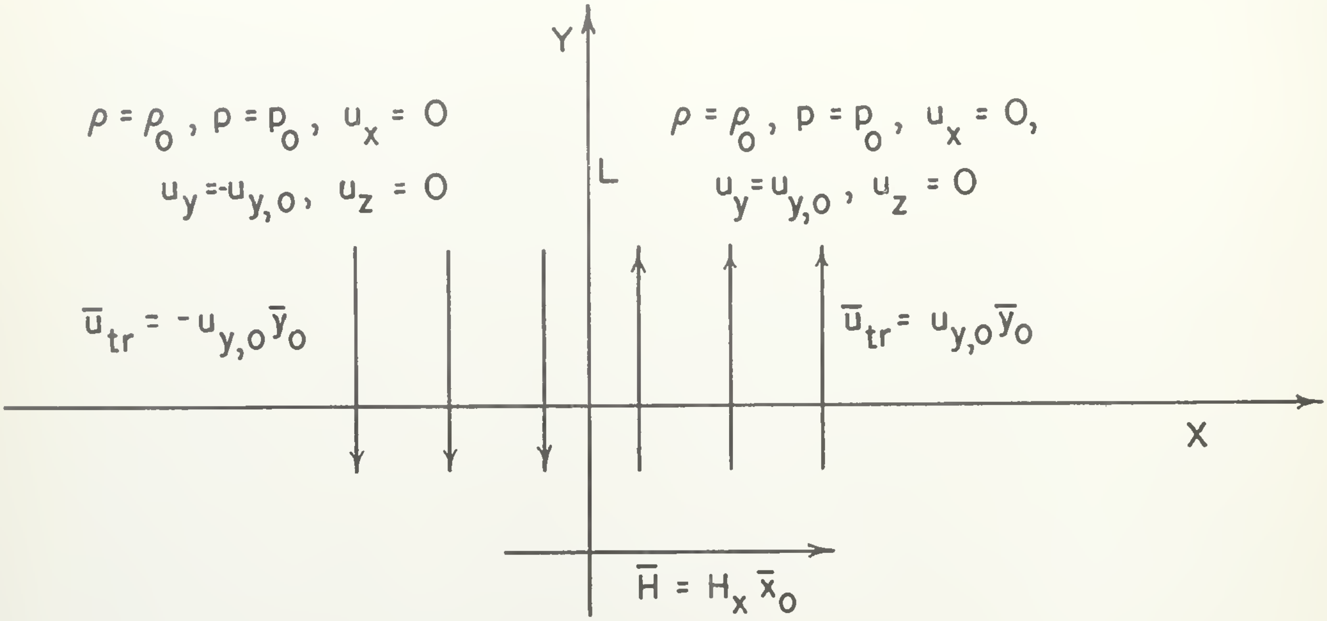
Y
$\rho = \rho_0$, $p = p_0$, $u_x = 0$
$u_y = -u_{y,0}$, $u_z = 0$
L
$\rho = \rho_0$, $p = p_0$, $u_x = 0$,
$u_y = u_{y,0}$, $u_z = 0$
$\overline{u}_{tr} = -u_{y,0}\overline{y}_0$
$\overline{u}_{tr} = u_{y,0}\overline{y}_0$
X
$\overline{H} = H_x \overline{x}_0$

FIG. 1. Symmetrical shear flow discontinuity in the transverse velocity, $\overline{u}_{tr}$. L is the planar surface x = 0, which separates the regions of equal and opposite transverse flow. The quantity $\rho_0$ is the density of the fluid, $p_0$ the pressure of the fluid, and $H_x > 0$ the fixed longitudinal component of the magnetic field. These quantities are assumed to be continuous across L. The transverse magnetic field $\overline{H}_{tr}$ and the longitudinal fluid velocity is assumed to be zero throughout. The magnitude of the initial discontinuity is $2u_{y,0}$. Unsymmetrical shear flow discontinuities in $\overline{u}_{tr}$ may be reduced to the present symmetrical case by means of a galilean transformation.

normal to the x-axis. Consider a plane surface across which a component, the y-component say, of the transverse velocity is discontinuous and across which no fluid passes. In addition, let it be assumed that the remaining variables are continuous across the surface, that these variables are independent of x initially, and moreover, that the transverse component of the magnetic field as well as the longitudinal fluid velocity vanish initially - here the longitudinal and transverse components of any vector quantity are the components of this quantity parallel and perpendicular to the x-axis, respectively. Such a flow discontinuity will be referred to as a shear flow discontinuity. If the component of the magnetic field normal to the discontinuity surface vanishes, the discontinuity reduces to a contact discontinuity in one-dimensional gas dynamical flow. As is well known, such a discontinuity may persist, theoretically, for all time. If, on the other hand, the longitudinal component of the magnetic field does not vanish, it can be shown that this discontinuity is not an admissible hydromagnetic contact discontinuity.

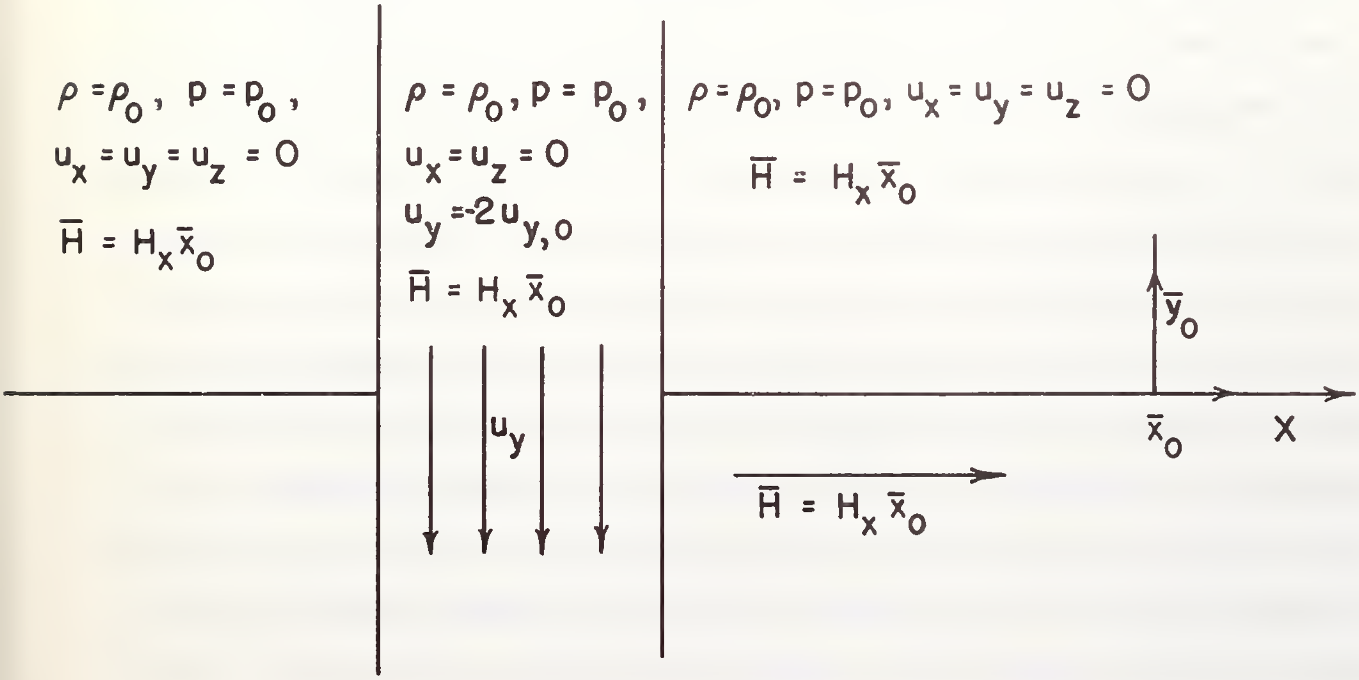
$\rho = \rho_0$, $p = p_0$,
$u_x = u_y = u_z = 0$
$\bar{H} = H_x \bar{x}_0$
$\rho = \rho_0$, $p = p_0$,
$u_x = u_z = 0$
$u_y = -2u_{y,0}$
$\bar{H} = H_x \bar{x}_0$
$u_y$
$\rho = \rho_0$, $p = p_0$, $u_x = u_y = u_z = 0$
$\bar{H} = H_x \bar{x}_0$
$\bar{y}_0$
$\bar{x}_0$
X
$\bar{H} = H_x \bar{x}_0$

FIG. 2. Jet proceeding in the negative y-direction. At each face of the jet we have a shear flow discontinuity.

The existence of an initial shear flow discontinuity in the presence of a longitudinal magnetic field must therefore be accommodated by a suitable motion of the medium. We refer to this motion as being a 'resolution' of the initial shear flow discontinuity, or as the motion which 'resolves' the initial shear flow discontinuity. The object of the present work is to construct such a resolution, to describe the general features of this motion, and to provide, for each $t > 0$, the numerical basis for obtaining the waveforms of the variables which characterize the flow. Here and in subsequent sections we may assume, without loss or generality, that the transverse velocity on one side of the discontinuity surface is equal and opposite to that on the other side and that it is parallel to the y-axis. In Figure 1 we have depicted one such symmetrical initial situation. Non-symmetrical shear flow discontinuities may be reduced to the symmetrical cas by means of a galilean transformation. In Figure 3 we have sketched the waveforms of the motion corresponding to a shear flow discontinuity of the type shown in Figure 1.

An idealized physical situation in which a shear flow discontinuity occurs is the following. Consider a layer of perfectly conducting, compressible fluid with faces transverse to the x-direction [see Figure 2]. Assume, at the initial instant, that the fluid within the layer moves uniformly in the negative y-direction, that only the fluid in the layer is in motion, and that the pressure and density are continuous across the layer faces and are independent of x. Such an initial motion may be regarded as an idealization of a jet proceeding in the negative y-direction and much wider in the z-direction than in the x-direction. A similar situation was described by Alfvén[1], in explaining the possible origin of hydromagnetic waves. At each face of the slab we encounter a shear flow discontinuity. The waves resulting from the resolution of the discontinuities at each face will interact only after a certain time. Before this time the situation may be described by a wave motion resulting from a single interface. It is this motion that is considered here.

The methods employed to determine the motion parallel those used in one-dimensional gas dynamical problems. In such problems initial discontinuities of a sufficiently simple character are resolved by means of shocks and simple waves. As will be recalled, the usefulness of simple waves is a consequence, primarily, of the fact that a flow region adjacent to a region of constant state is always a simple wave. The corresponding simple-wave and shock-wave building blocks are also available in the theory of one-dimensional hydromagnetic flow. The situation here, however, is complicated by the fact that there are three possible types of shocks, the so-called transverse shocks and the slow and fast shocks, and in addition, the corresponding types of simple waves. Nevertheless, from an examination of the known properties of the various shocks and simple waves one is led, in the present problem, to a resolution consisting of a combination of fast shocks and slow, centered, simple waves. Because of the initial conditions the transverse components of the magnetic field must vanish ahead of the shocks. As will be seen later this implies that the fast shocks must reduce either to fast gas dynamical shocks or the so-called switch-on shocks. Switch-on shocks are fast shocks having a vanishing transverse magnetic field ahead of the shock front but nevertheless a non-vanishing transverse magnetic field behind the shock front. Fast gas dynamical shocks are gas shocks in which the speed of the shock front is greater than the so-called Alfvén characteristic speed behind the shock. In terms of these building blocks the resolution of the shear flow discontinuity may be briefly described as follows: The fluid velocity is an odd function of x, and the magnetic field, the pressure and the density all are even functions of x. The initial discontinuity is resolved by two fast shocks moving away from the position of the initial discontinuity followed by two slow, centered, simple rarefaction waves. These rarefaction waves connect the constant state immediately behind the moving shock fronts either to the endpoints of an expanding zone in which the thermodynamic state is constant and the medium is motionless, or to the endpoints of a vacuum zone which expands with an appropriate longitudinal 'escape speed'. The latter alternative occurs whenever the initial discontinuity in the transverse velocity exceeds a certain minimum value, the 'cavitation value' say, which depends upon the state of the undisturbed medium. In this case the fluid velocity has in addition to the longitudinal escape speed a non-vanishing transverse component at the 'tails' of the rarefaction waves.

It will be shown that a complete quantitative description of the motion may be obtained from the knowledge of how two pressure ratios $p_1/p_o$ and $p_3/p_1$ depend on the magnitude of the initial discontinuity and on the remaining state variables in the undisturbed medium. Here $p_o$ and $p_1$ are the pressures in front of and behind the shocks and $p_3$ is the pressure at the 'tails' of the simple waves. The dependence of $p_1/p_o$ and $p_3/p_1$ on the parameters in question is established by employing the condition that the fluid velocity vanishes in the expanding zone between the rarefaction waves whenever the value of the initial discontinuity in the transverse velocity is less than the cavitation value mentioned above, or the condition that the electric field vanishes at the tails of the rarefaction waves whenever the initial discontinuity in the transverse velocity is greater than the cavitation value. The first condition is simply a consequence of the fact that the fluid velocity is an odd function of x; the second condition will be shown to follow from the quasistatic approximation to Maxwell's equations in the vacuum zone and the hydromagnetic analog of the Rankine-Hugoniot conditions at the boundary of a perfectly conducting compressible medium which expands into a vacuum. In general, it might be expected that these pressure ratios depend on $u_{y,0}$, $\rho_o$, $p_o$ and $H_x$, where $2u_{y,0}$ is the magnitude of the initial discontinuity and $\rho_o$, $p_o$, $H_x$ are, in the order given, the density, pressure and longitudinal magnetic field in the undisturbed medium. We shall show, however, that $p_1/p_o$ and $p_3/p_1$ depend only on the ratios $s_o = a_o^2/b_o^2$ and $u_{y,0}/a_o$ or alternatively $u_{y,0}/b_o$. Here $b_o = (\mu H_x^2 \rho_o^{-1})^{1/2}$ is the Alfvén speed* in the undisturbed medium and $s_o$ is the square ratio of the sound speed $a_o = (\gamma p_o \rho_o^{-1})^{1/2}$ and the Alfvén speed in the undisturbed medium. The constant $\gamma$ is the exponent of the density in the adiabatic equation of state of the medium. Plots of $p_1/p_o$ versus $u_{y,0}/a_o$ and $p_3/p_1$ versus $u_{y,0}/b_o$ are given in Figures 15 and 16.*

---

* The quantity $\mu$ is the magnetic specific inductive capacity of free space. The Giorgi mks system of units is employed throughout this report.

As already indicated, a complete description of the solution in the various flow regions may be obtained from this basic information. Of particular interest is the fact that in the region behind the rarefaction waves a transverse component of the magnetic field, $H_{y,3}$, is created even though such a component was nowhere present initially. In particular it can be shown that

$$H_{y,3} \sim (\rho_o/\mu)^{1/2}\, u_{y,0} \tag{1.1}$$

[cf. (5.50), (5.65), or (6.10), (6.10')] when $u_{y,0}$ is sufficiently small and that

$$H_{y,3} \sim \left[(1+\gamma)\, \rho_o/\mu\right]^{1/4} (H_x u_{y,0})^{1/2} \tag{1.2}$$

[cf. (5.37), or (6.11), (6.11')] when $u_{y,0}$ is sufficiently large. As already mentioned, $\rho_o$ is the density in the undisturbed medium, $H_x$ the longitudinal magnetic field**, $\mu$ the magnetic specific inductive capacity of free space, $\gamma$ the adiabatic exponent, and $u_{y,0}$ half the initial discontinuity in the transverse velocity. Thus, even when $H_x$ is very small, a large transverse magnetic field is created in the region between the rarefaction waves when $u_{y,0}$ is large enough. Associated with this result is the fact that the motion of the medium differs radically from the steady state gas dynamical shear flow even when $H_x$ is small, provided $u_{y,0}$ is large enough. In fact cavitation will result when $u_{y,0}$ is greater than the cavitation value noted above. The detailed nature of the dependence of $H_{y,3}$ on $u_{y,0}$ is given in Figure 17a where we have plotted $H_{y,3}/H_x$ versus $u_{y,0}/a_o$ and in Figure 17b where we have plotted $H_{y,3}/H_x$ versus $u_{y,0}/b_o$. In addition, we have plotted $(u_{x,3})_{esc}/b_o$, $u_{y,3}/b_o$ and $p_3/p_o$ versus $u_{y,0}/b_o$ [see Figures 18 and 19]. Here, $(u_{x,3})_{esc}$ is the longitudinal escape speed and $u_{y,3}$ the transverse fluid speed at the tail of the rarefaction wave in the region $x > 0$. The interpretation of these graphical results is deferred to Section 6.

---

* In all of the graphs appearing in this report the value of the adiabatic exponent $\gamma$ is assumed to be 5/3. The equation of state of the medium is therefore the same as that of an ideal monotonic gas.

** In one-dimensional hydromagnetic flow, the longitudinal component of the magnetic field $H_x$ can be shown to be independent of both the space variable x, and the time variable t.

Hydromagnetic shocks have been treated by De Hoffman and Teller (1950)[2], by Helfer (1952)[3] and Lüst in (1953)[4]-(a) and in (1955)[4]-(b). A detailed treatment of gas dynamical shocks may be found in the text of Courant and Friedrichs[5]. A theory of shocks and simple waves for general systems of hyperbolic partial differential equations of the type considered in this report has been given by Lax (1954)[6]. The problem of the resolution of a shear flow discontinuity was first formulated by Friedrichs (1954)[7]. This formulation was based on a new survey of hydromagnetic shocks in which, among other results, the inadmissibility of a shear flow discontinuity in the presence of a longitudinal magnetic field was noted and in which some properties of switch-on shocks were given. Friedrichs also discussed simple wave solutions of the one-dimensional system of hydromagnetic equations treated here. Of particular interest is the fact that he succeeded in reducing the problem of obtaining explicit slow and fast simple wave solutions in media governed by the adiabatic equation of state to essentially that of solving a single linear ordinary differential equation. The present work takes as a point of departure the formulation and results of Friedrichs just noted. In addition to giving a detailed treatment of the shear flow problem we extend slightly that part of Friedrich's results on switch-on shocks and simple waves which serves as a basis for this problem.

The shear flow problem treated here is perhaps the simplest hydromagnetic problem with discontinuous initial values that can be formulated. This simplicity is clearly bought at the expense of physical content. The loss of physical content, however, is partly compensated by the fact that a rigorous solution of a nonlinear problem is obtained. In addition, one may hope that, as in gas dynamics, a familiarity with the properties of this and similar one-dimensional solutions may lead to an increased understanding of more significant hydromagnetic phenomena.

In Section 2 we give a brief survey of pertinent facts about one-dimensional hydromagnetic flow and then formulate the problem in detail. Sections 3 and 4 are devoted to a discussion of the basic building blocks from which the solution is constructed; in Section 3 we discuss switch-on shocks and fast gas shocks, and in Section 4, slow simple waves. These basic motions are combined in Section 5 to form the solution. In this section we also sketch our procedure for obtaining the graphical results noted above. A survey, based on the results of Section 5, of some qualitative features of the motion is given in Section 6.

The reader who desires to obtain an overall view of our procedure and results without entering into all the detailed calculations is advised to read Section 2, subsections 3.1, 4.1, 5.1, and Section 6.

## 2. Survey of known results. Formulation of the problem

### 2.1 The equations of one-dimensional hydromagnetic motion

In order to introduce notations and terminology employed throughout this report, to motivate properly the formulation of the problem and the choice of building blocks entering into the solution, and to prepare for the considerations of subsequent sections, we shall first summarize some pertinent information concerning one-dimensional hydromagnetic motion. Explicitly, we shall give a brief survey of the possible types of hydromagnetic shocks and simple waves and recall some properties of these motions. We shall then discuss in detail the formulation of the problem. The following exposition is based on the work of Friedrichs[7].

We begin with a system of partial differential equations governing the motion of a perfectly conducting, neutral, non-viscous, compressible fluid. This system, which is essentially a one-dimensional version of that employed by Lundquist[5], is:

$$
\begin{array}{ll}
A_0 & H_x = \text{const (independent of } x \text{ and } t) \\[2ex]
A_1 & \dfrac{\partial \bar{H}_{tr}}{\partial t} + u_x \dfrac{\partial \bar{H}_{tr}}{\partial x} - H_x \dfrac{\partial \bar{u}_{tr}}{\partial x} + \bar{H}_{tr} \dfrac{\partial u_x}{\partial x} = 0 \\[2ex]
A_{2,x} & \rho \dfrac{\partial u_x}{\partial t} + \rho u_x \dfrac{\partial u_x}{\partial x} + \dfrac{\partial}{\partial x} \left\{ p + \mu(\bar{H}_{tr})^2/2 \right\} = 0 \\[2ex]
A_{2,tr} & \rho \dfrac{\partial \bar{u}_{tr}}{\partial t} + \rho u_x \dfrac{\partial \bar{u}_{tr}}{\partial x} - \mu H_x \dfrac{\partial \bar{H}_{tr}}{\partial x} = 0 \\[2ex]
A_3 & \dfrac{\partial \rho}{\partial t} + \dfrac{\partial}{\partial x} (\rho u_x) = 0 \\[2ex]
A_4 & \dfrac{\partial}{\partial t} \left[ \left( \dfrac{1}{2} \rho \bar{u}^2 + \rho e + \dfrac{1}{2} \mu \bar{H}^2 \right) \right] + \dfrac{\partial}{\partial x} \left[ u_x \left( \dfrac{1}{2} \rho \bar{u}^2 + \rho e + p + \mu \bar{H}^2 \right) \right] \\[2ex]
 & \qquad\qquad\qquad - \mu H_x^2 \dfrac{\partial}{\partial x} (\bar{H} \cdot \bar{u}) = 0 \\[2ex]
A_5 & \rho \dfrac{\partial S}{\partial t} + \rho u_x \dfrac{\partial S}{\partial x} = 0 \\[2ex]
A_6 & e = e(\rho, S), \qquad de = T dS + p d(\rho^{-1}).
\end{array}
\tag{2.1}
$$

All quantities appearing above are assumed to be functions of the time, t, and the single space variable, x. $\bar{H}$ is the magnetic intensity, $\bar{u}$ the velocity of the fluid particle; $H_x$ and $u_x$ are the components of these quantities in the positive x-direction while $\bar{H}_{tr}$ and $\bar{u}_{tr}$ are the components of these quantities in the plane transverse to the x-axis. The quantity $\mu$ is the magnetic inductive capacity, $\rho$ the density, p the pressure, T the temperature, e the specific internal energy (that is, internal energy per unit mass), and S the specific entropy. Equation $A_6$ is simply a statement of the first law of thermodynamics for a fluid particle. $A_5$ establishes the adiabatic character of the flow. Equations $A_3$ and $A_5$ are statements of the conservation of mass and energy, respectively. $A_{2,x}$ and $A_{2,tr}$ assert the conservation of momentum in the longitudinal and transverse directions. They are the component equations of

$$\rho \frac{\partial \bar{u}}{\partial t} + \rho(\bar{u} \cdot \nabla)\bar{u} + \nabla p + \mu\bar{H}x(\nabla \times \bar{H}) = 0.$$

The term $\mu\bar{H}x(\nabla \times \bar{H})$ in this equation is the force exerted on the current $\bar{J} = \nabla \times \bar{H}$ by the magnetic field $\mu\bar{H}$. Equations $A_o$ and $A_1$ are consequences of the relations

$$\nabla \cdot \bar{H} = 0$$

$$\frac{\partial \bar{H}}{\partial t} + \nabla \text{ x } (\bar{H}\text{x}\bar{u}) = 0 \quad ,$$

the first of which asserts the irrotational character of the magnetic field. The second equation relates the time rate of change of the magnetic induction $\mu\bar{H}$ and the curl of the electric field

$$(2.2) \qquad \bar{E} = \mu\bar{H} \text{ x } \bar{u}$$

in the perfectly conducting medium. The fact that $H_x$ is independent of x and t is a special feature of one-dimensional hydromagnetic motion.

It is assumed, here and in what follows, that the fluid obeys the equation of state for a polytropic ideal gas. It then follows from the adiabatic character of the flow $A_5$ and the first law of thermodynamics $A_6$ that

$$
\begin{aligned}
p &= K \rho^{\gamma} \\
e &= p \rho^{-1} / (\gamma - 1)
\end{aligned}
\tag{2.3}
$$

where $\gamma$ is the adiabatic exponent of the medium and K is an arbitrary function of the entropy S.

### 2.2 Hydromagnetic shocks

In a region in which the flow is continuous, equations $A_2$, $A_3$, $A_5$, and $A_6$ imply $A_4$. In this case equation $A_4$ may be discarded. However, when a region of flow is divided by a surface of discontinuity, $L = L(t)$, $A_4$ must be retained and together $A_0 - A_4$ lead to the hydromagnetic analog of the Rankine-Hugoniot conditions across L:*

$$
\begin{aligned}
&B_0 \qquad [H_n] = 0 \\
&B_1 \qquad \left[m\bar{H}\tau - H_n \bar{u}\right] = 0 \\
&B_2 \qquad \left[m\bar{u} + (p + \tfrac{1}{2}\mu \bar{H}^2)\,\bar{n} + \mu H_n \bar{H}\right] = 0 \\
&B_3 \qquad m\,[\tau] - [u_n] = 0, \qquad \text{or equivalently } [m] = 0 \\
&B_4 \qquad \left[m(\tfrac{1}{2}\bar{u}^2 + e + \tfrac{1}{2}\mu H^2 \tau) + u_n(p + \tfrac{1}{2}\mu H^2) - \mu H_n(\bar{H}\cdot\bar{u})\right] = 0.
\end{aligned}
\tag{2.4}
$$

---

* Equation $A_5$ must be replaced by the condition, $m[S] \geq 0$. This implies that the entropy 'behind' a shock is not less than that 'in front' of the shock (see next page).

Here $H_n$, $u_n$ are $\bar{H} \cdot \bar{n}$ and $\bar{u} \cdot \bar{n}$ respectively, where the vector $\bar{n}$ denotes the normal vector at any point of the discontinuity surface, L, and

$$(2.5) \qquad [Q] = Q_1 - Q_0,$$

the jump in any quantity Q across L, $Q_1$ being the value of Q on the side into which $\bar{n}$ points. In addition we have set

$$(2.6) \qquad \tau = \rho^{-1}$$

and

$$(2.7) \qquad m = \rho(u_n - U_n)$$

where $u_n$ and $U_n$ are the fluid and shock velocities in the normal direction. Note that the flux through the surface, m, is continuous across L [cf. $B_3$ above]. Depending upon whether $m \neq 0$ or $m = 0$ we speak of a shock or of a contact discontinuity. Since we are dealing exclusively with one-dimensional hydromagnetic flow depending on the space variable x it is clear that $\bar{n}$ is directed along either the positive or negative x-axis. In what follows, when the discontinuity is a shock we shall employ the convention that $\bar{n}$ points in the direction in which the fluid crosses the surface. Under these circumstances m is positive*. The region into which $\bar{n}$ points will be referred to as the region behind the shock; the remaining region will be called the region ahead of the shock. Fluid therefore crosses the shock wave from the region ahead of the shock to the region behind the shock. A shock is said to be forward facing or backward facing according as $\bar{n}$ is directed along the negative or positive x-directions. For a forward-facing shock the region ahead of the shock lies to the right of the region behind the shock, whereas for a backward-facing shock the region ahead of the shock lies to the left of the region behind the shock.

---

* When $m = 0$ we assume that $\bar{n}$ is directed along the positive x-axis.

Employing the identity

$$[PQ] = \tilde{P}\,[Q] + [P]\,\tilde{Q}, \tag{2.8}$$

where

$$\tilde{Q} = \frac{1}{2}(Q_o + Q_1) \tag{2.9}$$

is the mean value of any quantity having the value $Q_1$ behind and $Q_o$ ahead of the shock, we may write equations $B_1 - B_3$ as follows:

$$\begin{aligned} &C_1 \qquad m\tilde{\tau}\,[\bar{H}] + \tilde{\bar{H}}[u_n] - H_n[\bar{u}] = 0 \\ (2.10)\quad &C_2 \qquad m\,[\bar{u}] + [p]\,\bar{n} + \mu\bar{n}\,\tilde{\bar{H}}\cdot[\bar{H}] - \mu H_n[\bar{H}] = 0 \\ &C_3 \qquad m\,[\tau] - [u_n] = 0. \end{aligned}$$

These equations in conjunction with the similarly expanded form of $B_4$ may be regarded as a system of seven linear homogeneous equations in the seven unknowns $[p]$, $[\tau]$, $[\bar{u}]$ and the jumps in the transverse components of $\bar{H}$. Whenever non-trivial solutions of this system exist the determinant, det(C), must vanish. It can be shown that

$$\begin{aligned} \det(C) = m(m^2\tilde{\tau} - \mu H_x^2)\Big[&(m^2\tilde{\tau} - \mu H_x^2)\Big\{m^2\,\alpha\tilde{\tau} - (1+\alpha)\tilde{p} - \mu\big(\widetilde{\bar{H}}\big)^2 + \mu\big(\tilde{\bar{H}}\big)^2\Big\} \\ &- m^2\alpha\tilde{\tau}\,\mu\Big\{\big(\tilde{\bar{H}}\big)^2 - H_x^2\Big\}\Big] \end{aligned} \tag{2.11}$$

where $\alpha = (\gamma-1)^{-1}$. As long as $H_x$ is different from zero, m is a simple zero of det(C). The solution corresponding to such an m is a contact discontinuity. The nature of this solution will be discussed later in subsection 2.4. The solutions corresponding to the zeros of the factor $(m^2\tilde{\tau} - \mu H_x^2)$ are called transverse shocks*, and the solutions corresponding to the larger and smaller zeros of the remaining factor, assuming $(\tilde{H})^2 - H_x^2$ does not vanish, are called fast and slow shocks respectively. Among the various properties of these shocks the following are useful for our purposes. First, fast and slow shocks are compressive, that is, the density and pressure behind the shock exceed the corresponding quantities ahead of the shock, while in a transverse shock only the transverse magnetic field and transverse velocity suffer a discontinuity. Second, the magnetic field strength $|\bar{H}_{tr}|$ rises across a fast shock, drops across a slow shock, and remains constant across a transverse shock*. Third, under certain circumstances switch-on shocks exist. Switch-on shocks are shocks having a vanishing transverse magnetic field component in front but nevertheless a non-vanishing transverse magnetic field component behind the shock. Clearly switch-on shocks must be fast shocks. In Section 3, where we shall treat switch-on shocks in greater detail, we shall prove that the normal flow velocity, $u_n - U_n$, is equal to the so-called Alfvén speed $b = (\mu H_x^2 \rho^{-1})^{1/2}$ behind the shock. It should be mentioned, in this connection, that when the transverse magnetic field vanishes both in front and behind, the discontinuity surface the relations $B_1 - B_4$ reduce to the well-known Rankine-Hugoniot relations for gas dynamical flow with a constant transverse flow. The velocity of the gas shock in this system is in no way related to the Alfvén speed behind the shock. It is nevertheless useful to divide gas shocks into two classes according as the normal flow velocity $(u_{n,1} - U_n)$ behind these shocks is equal to or greater than the Alfvén speed behind the shock, or less than this speed. In the former case the gas shocks are called fast gas shocks; in the latter case they are called the slow gas shocks.

---

* de Hoffman and Teller call such shocks symmetrical shocks.

### 2.3 Hydromagnetic simple waves

In a given flow region R of the (x,t)-plane, simple wave solutions of equation (2.1) are continuous, continuously differentiable solutions of a special type. They may be characterized by the requirement that $H$, $\bar{u}$, $\rho$, $p$, and $S$ be constant on a one-parameter family of lines which cover R. This family of lines may be written in the form

---

* Since $\bar{H}_{tr}$ is discontinuous across a transverse shock it follows that the direction of $\bar{H}_{tr}$ must change.

$$x = Ut + \xi, \qquad U = U(\xi),$$

if not all the lines pass through the origin of the $(x,t)$-plane, or in the form

$$x = Ut \quad , \qquad U = U(\xi)$$

if they do. A simple wave whose flow region is covered by the latter family are referred to as *centered* simple waves. In a centered simple wave $\bar{H}$, $\bar{u}$, $p$, $\rho$ and $S$ are necessarily functions of $U(= x/t)$ alone; otherwise these quantities are necessarily functions of the parameter $\xi(= x-Ut)$. It can be shown that a *flow region adjacent to a region of constant state* is always a simple wave and that the transition from a simple wave region to a region of constant state takes place across a line of the type discussed above.* It is for these reasons that simple waves are useful building blocks in constructing solutions to flow problems.

For solutions of simple wave type, (2.1) reduces, on setting

$$(2.12) \qquad U = u_x \pm c,$$

to the following system of ordinary differential equations:

$$(2.13) \qquad \begin{array}{ll}
D_{1,y} & \mp c\, d\, H_y + H_y du_x - H_x du_y = 0 \\
D_{1,z} & \mp c\, d\, H_z + H_z du_x - H_x du_z = 0 \\
D_{2,x} & \mp \rho c du_x + dp + \frac{1}{2}\mu d(\bar{H}^2) = 0 \\
D_{2,y} & \mp \rho c du_y - \mu H_x\, dH_y = 0 \\
D_{2,z} & \mp \rho c du_z - \mu H_x dH_z = 0 \\
D_3 & \mp c d\rho + \rho du_x = 0 \\
D_4 & \mp c dS = 0,
\end{array}$$

---

*A state of flow is referred to as constant in a region of the $(x,t)$-plane if all quantities, $\rho$, $p$, $\bar{H}$, $\bar{u}$, $S$ are constant throughout the region.

where the differentials involving the parameter $\xi$ have been multiplied out. For non-trivial solutions the quantity c must be chosen in such a manner that the determinant of the system

$$(2.14) \qquad \det(D) = \pm \rho c^2(\rho c^2 - \mu H_x^2)\left[(\rho c^2 - \mu H_x^2)(c^2 - a^2) - c^2\mu(H_y^2 + H_z^2)\right]$$

vanishes. Here, $a = (\gamma p \rho^{-1})^{1/2}$ is the sound speed. The zeros of this determinantal expression are referred to as the characteristic disturbance speeds. The zero $c = (\mu H_x^2 \rho^{-1})^{1/2} = b$ is called the Alfvén, or the transverse disturbance speed, the smaller zero, $c_s$, of the factor in brackets is called the slow disturbance speed, and the larger zero, $c_f$, the fast disturbance speed. The velocities $U = u_x \pm b$ are accordingly called Alfvén (or transverse) characteristic velocities, and $U = u_x \pm c_s$, $U = u_x \pm c_f$ are called the slow and fast characteristic velocities. According to which speed c enters into the solution of (2.13), the simple wave is transverse, slow or fast. The wave corresponding to $c = 0$ is called a contact layer.

A solution of the system (2.13) corresponding to the upper (or lower) sign and hence to $U_x + c$ (or $U_x - c$) is referred to as a forward-facing (backward-facing) simple wave. As is the case with forward-facing (backward-facing) shocks, fluid particles enter the simple wave region from the right (left) if the simple wave is forward-facing (backward-facing). This remark is a consequence of the fact that $u_x + c$ (or $u_x - c$) is larger (smaller) than $u_x$, the longitudinal velocity of the fluid.

In the following survey of the properties of the various simple wave solutions it will be assumed that $H_x \neq 0$. Across a contact layer only $\rho$ and S may vary, the other quantities being necessarily constant. Across a transverse wave, $\rho$, p, S, and $u_x$ are constant. The transverse component of the magnetic field remains constant in magnitude but may change its direction arbitrarily but continuously with x; the transverse component of the velocity $\bar{u}_{tr}$ is given simply by $\bar{u}_{tr} = \bar{\alpha} \pm cH_x^{-1}\bar{H}_{tr}$, where $\bar{\alpha}$ is a constant transverse vector. Across a fast or slow simple wave S is constant; the magnitude of all other quantities may vary. A detailed description of these waves will be given in Section 4. It is, however, worthwhile noting here that the direction of $\bar{H}_{tr}$ remains constant across fast and slow simple waves and that $d\bar{u}_{tr}$ is parallel to $\bar{H}_{tr}$, i.e., $d\bar{u}_{tr} \times \bar{H}_{tr}$ vanishes. The fact that $d\bar{u}_{tr} \times \bar{H}_{tr}$ vanishes is a consequence of $D_{2,y}$ and $D_{2,z}$. The validity of the first statement is indicated by the following: Multiply equation $D_{1,y}$ by $H_z$ and equation $D_{2,z}$ by $H_y$ and subtract the former equation from the latter. Then eliminate $du_y$ and $du_z$ from the result by means of $D_{2,y}$ and $D_{2,z}$. We then have

$$(c - \mu H_x^2(\rho c)^{-1})\ (H_z dH_y - H_y dH_z) = 0.$$

Since it can be shown [see Section 4] that the first factor vanishes at only one point of a slow or fast simple wave, we conclude that the $H_y = \text{const}\cdot H_z$. It is assumed here that neither $H_y$ nor $H_z$ vanish identically in the fast or slow simple wave region under consideration. Corresponding relations exist for shock waves. In fact it is easily verified that the direction of $\bar{H}_{tr}$ behind a shock is collinear with that ahead provided $|\bar{H}_{tr}|$ does not vanish ahead of the shock [cf. (3.1)]. Moreover, since the transverse part of $C_2$ is

$$m[\bar{u}_{tr}] - \mu H_n\ [\bar{H}_{tr}] = 0$$

it follows that $[\bar{u}_{tr}] \times [\bar{H}_{tr}]$ vanishes. In particular, independently of whether $\bar{H}_{tr}$ vanishes ahead of the shock or not, if the transverse magnetic field is assumed to be parallel to the y-axis we may conclude that $u_z$ is constant across a shock. Similarly, if $\bar{H}_{tr}$ is parallel to the y-axis then $u_z$ is constant across fast and slow simple waves.

## 2.4 Formulation of the problem

We turn now to the formulation of the problem. In the following it will be assumed that $H_x > 0$, unless otherwise indicated. Since we are dealing with one-dimensional motion, discontinuity surfaces are necessarily planes normal to the x-axis. Let L be an initially stationary discontinuity surface located at $x = 0$ across which there exists at time $t = 0$ a shear flow discontinuity. By a shear flow discontinuity we mean one in which the transverse component of the velocity $\bar{u}_{tr}$ jumps without changing direction, the variables $u_x$, $\bar{H}$, $p$, $\rho$, $S$ remaining continuous and constant for all x. In particular it is assumed that at time $t = 0$

$$\begin{gathered} u_y = u_{y,0} > 0, \qquad x > 0; \qquad u_y = -u_{y,0}, \qquad x < 0, \\ p = p_0, \quad \rho = \rho_0, \quad u_x = u_z = 0, \quad \bar{H}_{tr} = 0, \quad S = S_0 \end{gathered} \tag{2.15}$$

[see Figure 1]. It should be observed that there is no loss in generality in assuming that $u_x$ and $u_z$ vanish and that the transverse speeds on either side of the discontinuity surface are equal, since a more general prescription of the initial motion may be reduced to this case by means of a galilean transformation; it is easily verified that the equations of motion (A) and the shock conditions (B) are invariant under such transformations.

Since the normal flow velocity $u_x$ vanishes initially and since L is assumed to be stationary initially, it follows that the flux through L, m, vanishes. The shear flow discontinuity therefore appears to be some form of hydromagnetic contact discontinuity. It will now be shown that such is not the case - more explicitly, that a shear flow discontinuity is not an admissible hydromagnetic motion if the longitudinal magnetic field $H_x$ is different from zero. To this end let us set m equal to zero in the Rankine-Hugoniot conditions, (2.4). Equations (2.4)-$B_0$ and $B_3$ and the entropy condition then yield the following relations:

(2.16) $\quad [H_n] = 0, \quad [u_n] = 0, \quad [\rho] \geq 0, \quad [S] \geq 0.$

These relations in conjunction with (2.4)-$B_2$ and $B_4$ then imply

(2.17) $\quad [p] = 0, \quad [\bar{H}_{tr}] = 0.$

Finally, the fact that $[\bar{H}_{tr}]$ and $[H_n]$ vanish implies, in virtue of (2.4)-$B_1$, that

(2.18) $\quad H_n [\bar{u}_{tr}] = 0 ,$

where $\bar{u}_{tr}$ is the transverse component of the fluid velocity $\bar{u}$.

Now the shear flow discontinuity (2.15) clearly satisfies the conditions listed in (2.16) and (2.17). Equation (2.18) is, however, not satisfied since we have assumed that $H_n = H_x > 0$. The shear flow discontinuity in question is therefore not an admissible hydromagnetic motion.

Note that when $H_x$ is permitted to vanish $\bar{u}_{tr}$ may be discontinuous across L; in this case the problem reduces to the one-dimensional gas dynamical problem of a shear flow discontinuity in a homogeneous medium. A shear flow discontinuity is, under these circumstances, an admissible gas dynamical motion and may persist for all time. On the other hand, when $H_x \neq 0$ the initial discontinuity must be resolved by a suitable motion of the medium.

To gain some insight into the cause of the motion consider instead of a discontinuity a thin shear flow layer across which the transverse component of velocity, $u_y$ say, varies smoothly from its value $u_y = -u_{y,0}$ on the left-hand side of the layer to the value $u_y = u_{y,0}$ on the right-hand side. To simplify matters assume that $u_z$ vanishes everywhere. In addition assume that $H_y = H_z = 0$ initially, and $H_x > 0$. For the sake of concreteness let us suppose that $u_y$ is an odd function of x throughout the layer which we shall assume to be symmetrically disposed with respect to the (y,z)-plane. From (2.2) we conclude that the electric field*, $E = E_z \bar{z}_o = -(\mu u_y H_x)\bar{z}_o$, is an odd function of x which varies smoothly from $(\mu u_{y,0} H_x)\bar{z}_o$ on the left face of the slab to $(-\mu u_{y,0} H_x)\bar{z}_o$ on the right face of the slab. The existence of this initial electric field results in the growth of a transverse component of the magnetic field in the layer. For t sufficiently small this transverse magnetic field, $\bar{H}_{tr}$, is given by [see (2.1)-$A_1$]

$$\bar{H}_{tr} = H_x \frac{\partial u_y}{\partial x} t \, \bar{y}_o .$$

Thus $\bar{H}_{tr}$ is directed only along the positive y-axis and is an even function of x, since $u_y$ is odd. The current

$$\bar{J} = \nabla \times \bar{H}_{tr} = \frac{\partial H_y}{\partial x} \bar{z}_o = (H_x \frac{\partial^2 u}{\partial x^2} t)\bar{z}_o$$

is then an odd function of x which is negative when $x > 0$ and is directed along the z-axis. The force per unit volume, $\bar{f}$, is then given by the expression

$$\bar{f} = \mu \bar{J} \times \bar{H} = -(\mu H_x^2 \frac{\partial u_y}{\partial x} \frac{\partial^2 u_y}{\partial x^2} t^2) \, \bar{x}_o .$$

This force is directed along the positive x-axis when $x > 0$ and along the negative x-axis when $x < 0$; thus it tends to produce separation. Note that we could have assumed that the longitudinal magnetic field was directed along the negative x-axis or that the initial transverse velocity was $u_y(-x)$ without changing the character of $\bar{f}$.

One can readily infer from the above discussion that the greater $u_{y,0}$, ($H_x$ remaining fixed) the greater the force tending to produce separation. If $u_{y,0}$ is made large enough one might expect the layers to separate altogether, leaving a vacuum in between. That this situation may actually arise will be seen later.

In determining the motion which resolves the initial discontinuity we admit solutions of the following type. First, we admit only those solutions which may be constructed from combinations of shocks, simple waves and constant states.

---

* The vectors $\bar{x}_o$, $\bar{y}_o$ and $\bar{z}_o$ constitute the unit orthogonal triad.

Second, admissible solutions are required to depend continuously on the parameters $u_{y,0}$, $H_x$, $p_0$ and $\rho_0$ - that is, on the parameters which characterize the initial state. Third, we require that the fluid velocity, $\bar{u}$, be an odd function of x while $\bar{H}$, $\rho$ and p are even functions of x. Fourth, we shall from the outset limit the class of solutions to those for which the transverse component of velocity is parallel to the y-axis, i.e., to those for which

$$(2.19) \qquad u_z = 0, \quad -\infty < x < \infty, \quad t > 0.$$

As already mentioned in the introductory section, the resolution of the initial discontinuity may be effected by two fast shocks (switch-on or fast gas shocks depending on the thermodynamic state of the undisturbed medium and the magnitude of the initial discontinuity) followed by slow centered simple waves. That the shocks in the resolution must be switch-on or pure gas shocks follows from the fact that the transverse magnetic field is zero initially and hence is absent in front of the advancing shocks. The choice of slow simple waves is related to the requirement that the shocks be switch-on or fast gas dynamical shocks. It will be recalled that the speed $|U_n|$ of both types of shocks are at least equal to the Alfvén characteristic speeds $|u_x \pm b|$ behind the shocks [see the end of subsection 2.2]. In slow (or fast) simple waves the characteristic speeds $|u_x \pm c|$ are at most (or at least) equal to the corresponding Alfvén characteristic speeds, as we shall show in Section 4. Of the two types of simple waves, clearly only the slow simple waves " follow" switch-on or fast gas shocks.

The third and fourth requirements on our class of solutions are easily seen to be compatible with the initial conditions, the continuum equations and the shock conditions. Moreover, they are consistent with the heuristic results obtained in our analysis of the shear flow layer. Note that the vanishing of $u_z$ everywhere implies that

$$(2.20) \qquad H_z = 0, \quad -\infty < x < \infty, \quad t > 0$$

in the fast shock slow simple wave resolution. This assertion follows from the relation, $d\bar{u}_{tr} \times \bar{H}_{tr} = 0$, which holds in slow and fast simple waves and from the relation, $[u_{tr}] \times [H_{tr}] = 0$, which holds across any admissible discontinuity. The converse is also true since $u_z$, by hypothesis, vanishes in front of the advancing shocks. Thus, under the present circumstances, the vanishing of $H_z$ everywhere is equivalent to the vanishing of $u_z$ everywhere. It should be recalled here that the direction of $\bar{H}_{tr}$ in slow (and fast) simple waves is constant across the wave. The requirement that $\bar{H}_{tr}$ be parallel to the y-axis in such a wave is therefore not a very severe restriction.

Consider now the region between the slow simple waves in the resolution of the shear flow discontinuity discussed above. This region, being bordered by simple wave regions, is clearly one of constant state. Since $\bar{u}$ is odd we must have

$$u_x = 0, \qquad u_y = 0, \qquad t > 0 \tag{2.21}$$

unless $\rho$ vanishes throughout the region. One must admit the alternative $\rho = 0$ in order to take into account the possibility of cavitation. As indicated above, the likelihood that cavitation occurs increases with the magnitude of the initial discontinuity, assuming the remaining parameters in the undisturbed medium are fixed. When cavitation occurs it is necessary to replace conditions (2.21) by the conditions

$$\left.\begin{array}{l} \rho = 0 \\ u_y H_x - u_x H_y = 0 \end{array}\right] \quad \text{at the endpoints of the vacuum zone.} \tag{2.22}$$

The second equation simply states that the electric field,

$$\bar{E} = \mu\bar{H} \times \bar{u} = \mu\left[u_y H_x - u_x H_y\right] \bar{z}_o , \tag{2.23}$$

vanishes at the endpoints of the vacuum zone. This result is a consequence of the fact that E vanishes throughout the vacuum zone, as we shall now show.

Maxwell's equations in the vacuum zone are

$$(2.24) \qquad \bar{x}_o \times \frac{\partial E_{tr}(x,t)}{\partial x} + \mu \frac{\partial \bar{H}(x,t)}{\partial t} = 0, \qquad \frac{\partial E_x(x,t)}{\partial x} = 0,$$

$$(2.25) \qquad \bar{x}_o \times \frac{\partial H_{tr}(x,t)}{\partial x} = 0 , \qquad \frac{\partial H_x}{\partial x} = 0,$$

where as usual we have assumed that the displacement current may be neglected and that all variable quantities depend on x and t alone. In accordance with our previous notation, $\bar{E}_{tr}$ and $\bar{H}_{tr}$ are the transverse electric and magnetic field components, $E_x$ and $H_x$ the longitudinal components of the electric and magnetic field, $\bar{H}$ the total magnetic field, and $\bar{x}_o$ the unit vector directed along the positive x-axis.

The two equations in (2.25) imply that $H_x$ is independent of x and t and that $\bar{H}_{tr}$ is independent of x. From (2.24) we then conclude that

$$(2.26) \qquad E_x = k_1 ,$$

$$(2.27) \qquad \bar{E}_{tr} = \mu \, \bar{x}_o \times \frac{\partial \bar{H}_{tr}}{\partial t} x + \bar{k}_2 ,$$

where $k_1$ is a scalar quantity and $\bar{k}_2$ a transverse vector quantity which depend on t alone. Now it can be shown [see Appendix I] that the Rankine-Hugoniot conditions at the boundary of a perfectly conducting, electrically neutral, compressible fluid which expands into a vacuum under action of magnetic and pressure forces are; assuming $\bar{H} \cdot \bar{n} \neq 0$,

$$(2.28) \qquad [\rho] = 0, \quad [\bar{H}] = 0, \quad [\bar{E}] = 0 .$$

The above relations imply that the density is continuous at this boundary and vanishes there and that surface current layers and charge layers (single or double) are absent. We observe, at this point, the fact that the boundary of a simple wave region consists of linear characteristics; in the present case, since the slow simple waves are centered, these linear characteristics pass through the origin of the (x,t)-plane. In addition, we recall that the state variables, and $\bar{H}_{tr}$ in particular, are constant along such characteristics. Thus the direction and magnitude of $\bar{H}_{tr}$ are constant at the moving boundary of the simple waves. Since $\bar{H}_{tr}$ is continuous at the boundaries separating the vacuum zone from the simple wave zone we conclude that $\bar{H}_{tr}$, in addition to being independent of x in the vacuum zone, is also independent of t. It follows immediately from (2.27) that

$$\bar{E}_{tr} = \bar{k}_2 \tag{2.29}$$

But $\bar{u}$ is odd and $\bar{H}$ is even. Therefore if $\bar{E} = \mu\bar{H}\times\bar{u}$ is the electric field at one endpoint of the vacuum zone, $\bar{E}' = -\mu\bar{H}\times\bar{u}$ is the electric field at the other. Employing this fact, the fact that $[\bar{E}]$ vanishes at the boundaries of the vacuum zone, and (2.29), we conclude that

$$\bar{E}_{tr} = 0. \tag{2.30}$$

In addition, we note that the electric field in the simple wave region is entirely transverse since both $\bar{u}$ and $\bar{H}$ lie in the (x,y)-plane. It follows from (2.26) that $E_x$ vanishes. Thus we have shown that the electric field vanishes throughout the vacuum zone.

It should be observed that the condition $u_y = 0$ imposed by Friedrichs [see [7] pp. 48-49] on the transverse component of the fluid velocity at the linear characteristics which bound the vacuum zone - that is, at the so-called "tails" of the simple waves - is incorrect and must be replaced by the less restrictive condition given in (2.27). This change affects the qualitative picture of the motion given by Friedrichs only when the initial discontinuity $2u_{y,0}$ is large enough to produce cavitation, and then only in the following manner. The fluid velocity at the tails of the simple waves has transverse components in addition to the escape velocities in the longitudinal direction. At each boundary the second equation of (2.22) governs the relation of the transverse velocity components to the longitudinal escape velocities.

It should be pointed out that this change also affects the relation between the transverse magnetic field developed behind the waves and the magnitude of the initial discontinuity, $2u_{y,0}$, when $u_{y,0}$ is large. Equations (13.5) and (13.7) of [7] must be replaced by (1.2) of the present report (see also (5.37)).

Some remarks are in order here regarding the choice of pairs of waves in the resolution of the initial discontinuity. The choice of pairs of waves is motivated by the following considerations. One expects shock waves to be completely determined by the prescription of one quantity, the pressure say, behind the wave, provided the state in front of the wave is known. The same may be said of simple waves. One may therefore hope to be able to prescribe a pair of such quantities behind a combination of a simple wave and a shock. In particular, one may hope to adjust these parameters in such a way that (2.21) or (2.22) is satisfied. This procedure is carried out in detail in Section 5 where the dependence of these parameters on the initial discontinuity, $2u_{y,0}$, and on the thermodynamic state is determined.

It should be understood from the outset that no claims are made with regard to the uniqueness of our solution. The solution does, however, appear to be the only one satisfying the initial conditions if we limit the class of admissible solutions to that discussed above and, moreover, impose the additional requirement that we employ at most two pairs of shocks or simple waves or a pair of shocks and a pair of simple waves. The validity of this statement may be tested by attempting to construct from the basic solutions discussed in subsections 2.2 and 2.3 an alternative solution satisfying all the necessary requirements.

## 3. Switch-on and fast gas dynamical shocks

### 3.1 Introductory remarks

As already mentioned, switch-on and pure gas dynamical shocks play a role in the resolution of the initial shear flow discontinuity. Switch-on shocks, it will be recalled, are fast shocks which have a non-vanishing transverse component of the magnetic field behind the shock in spite of the absence of such a component in front of the shock. Fast gas shocks are pure gas dynamical shocks satisfying the condition that the normal flow velocity behind the shock $(u_{n,1} - U_n)$ is greater or equal to the Alfvén disturbance speed, $b_1 = (\mu H_x^2 \rho_1^{-1})^{1/2}$, behind the shock. This section is devoted to discussing the properties of these shocks. We shall show that switch-on shocks exist provided $s_o$ ( $= \gamma p_o/H_x^2$), the square ratio of the sound speed $a_o \left[= (\gamma p_o \rho_o^{-1})^{1/2}\right]$ and the Alfvén disturbance speed $b_o \left[= (\mu H_x^2 \rho_o^{-1})^{1/2}\right]$ in front of the shocks, is less than unity and provided the shock strength, measured in terms of the pressure ratio, is below a certain critical value. When these conditions are satisfied it will be shown that the state behind the switch-on shock is known once the state in front, the direction of the transverse magnetic field, and the pressure ratio is prescribed. That the state behind a gas shock is determined by the state in front and the pressure ratio is a well-known fact; we shall therefore merely quote the results in a form suitable for subsequent purposes. When $s_o < 1$ we shall prove that the gas shock is fast if and only if the pressure ratio is above the critical value alluded to above. In addition, we shall show that as the pressure ratio passes through the critical value, the state behind a switch-on shock having a given state in front passes continuously into that of the fast gas shock having the same state in front.

It might be worthwhile adding here that only after these shocks are combined with the appropriate simple waves in forming the solution of the shear flow problem is it possible to fix the direction of the transverse magnetic field behind the switch-on shocks and to relate the shock strength to the strength $2u_{y,0}$ of the initial discontinuity.

## 3.2 Switch-on shocks

The analysis of switch-on shocks is based on the following jump relations:

$$(3.1)\qquad \left[(m^2\tau - \mu H_n^2)\,\bar{H}_{tr}\right] = 0, \qquad m \neq 0$$

$$(3.2)\qquad m^2 + \left[p + \frac{\mu}{2}(\bar{H}_{tr})^2\right][\tau]^{-1} = 0$$

$$(3.3)\qquad (m^2\tilde{\tau} - \mu H_n^2)\left\{\frac{m^2}{\gamma-1}\tilde{\tau} - \frac{\gamma}{\gamma-1}\tilde{p} - \mu\widetilde{(\bar{H})}^2 + \mu(\tilde{\bar{H}})^2\right\}$$

$$- \frac{m^2}{\gamma-1}\tilde{\tau}\;\mu\left\{(\tilde{\bar{H}})^2 - H_n^2\right\} = 0.$$

The first relation is obtained from the transverse part of $B_1$, namely

$$(3.4)\qquad \left[m\tau\,\bar{H}_{tr} - H_n\,\bar{u}_{tr}\right] = 0,$$

on substituting for $[\bar{u}_{tr}]$ from the transverse part of the momentum-conservation shock condition $B_2$, that is,

$$(3.5)\qquad \left[(m\,\bar{u}_{tr} - \mu H_n\,\bar{H}_{tr})\right] = 0.$$

Equation (3.2) follows from the longitudinal part of $B_2$ and the flux-conservation jump condition, $B_3$. The last relation, is the equation which results from equating the last factor in the right-hand side of (2.11) to zero. In accordance with the conventions of the previous section $Q_o$ and $Q_1$ are the values of any quantity Q ahead of and behind the switch-on shock $\tilde{Q} = (Q_1 + Q_2)/2$ and $[Q] = Q_1 - Q_o$. Since $\bar{H}_{tr,0}$ vanishes in front of a switch-on shock we have from (3.1)

$$(3.6)\qquad (m^2\tau_1 - \mu H_n^2)\,\bar{H}_{tr,1} = 0.$$

A necessary condition for the existence of a switch-on shock is therefore

$$m^2 \tau_1 - \mu H_n^2 = 0. \tag{3.7}$$

Eliminating $m^2$ from (3.2) by means of this relation we have

$$\frac{\mu}{2} (\bar{H}_{tr,1})^2 = -[p] - \mu H_n^2 \rho_1 [\tau]. \tag{3.8}$$

Since for switch-on shocks

$$\widetilde{\left(\bar{H}^2_{tr}\right)} = \frac{1}{2} \bar{H}^2_{tr,1}, \qquad \left(\widetilde{\bar{H}_{tr}}\right)^2 = \frac{\bar{H}^2_{tr,1}}{4}$$

$$\left[(\bar{H}_{tr})^2\right] = \left[\bar{H}_{tr}\right]^2 = (\bar{H}_{tr,1})^2, \tag{3.9}$$

then on eliminating $(\bar{H}_{tr,1})^2$ from (3.3) by means of (3.8) we obtain, employing (3.7), an equation involving only $\rho_o$, $p_o$ and the ratios $(\rho_1-\rho_o)/\rho_o$, $(p_1-p_o)/p_o$. This equation when solved for the ratio $(p_1-p_o)/p_o$ yields

$$\frac{p_1-p_o}{p_o} = \gamma\left(\frac{\rho_1-\rho_o}{\rho_o}\right)\left\{1 + \left(\frac{\gamma-1}{2}\right)\left(\frac{\rho_1-\rho_o}{\rho_o}\right)\frac{\mu H_n^2}{\gamma p_o}\right\}, \tag{3.10}$$

or alternatively, when solved for the ratio $(\rho_1-\rho_o)/\rho_o$,

$$\frac{\rho_1-\rho_o}{\rho_o} = \frac{1}{\gamma-1}\left(\frac{\gamma p_o}{\mu H_x^2}\right)\left\{-1 + \left(1 + \frac{2(\gamma-1)}{\gamma}\left(\frac{p_1-p_o}{p_o}\right)\frac{\mu H_x^2}{\gamma p_o}\right)^{\frac{1}{2}}\right\}. \tag{3.11}$$

It is apparent from the fact that $(p_1-p_o)/p_o$ is quadratic in $(\rho_1-\rho_o)/\rho_o$ that the sign before the square root term in (3.10) could also be negative. However, such a choice of sign would lead to negative values for the ratio $(p_1-p_o)/p_o$, that is, to switch-on shocks which are not compressive. Since all shocks, with the exception of transverse shocks are compressive, the choice of the positive sign is required.

Substituting the expression for [p] in (3.10) into (3.8) we find

(3.12) $$(H_{tr,1}/H_x)^2 = 2\,\frac{(\rho_1-\rho_0)}{\rho_0}\left\{1 - \left[\left(\frac{\gamma-1}{2}\right)\left(\frac{\rho_1-\rho_0}{\rho_0}\right) + \frac{\gamma p_0}{\mu H_x^2}\right]\right\} .$$

The fact that the right-hand side of this equation is positive for a switch-on shock results in the following restriction on the range of variation of the ratio $(\rho_1-\rho_0)/\rho_0$:

(3.13) $$0 < \frac{\rho_1-\rho_0}{\rho_0} < \frac{2}{\gamma-1}\left[1 - (\gamma p_0 / \mu H_x^2)\right] .$$

This relation, in turn, implies, in virtue of (3.10)

(3.14) $$0 < \frac{p_1-p_0}{p_0} < \frac{2\gamma}{\gamma-1}\left(\frac{\mu H_x^2}{\gamma p_0}\right)\left[1 - (\gamma p_0 / \mu H_x^2)\right] .$$

Within this range, the quantity $(H_{tr}/H_x)^2$ increases from zero to the maximum

(3.15) $$(H_{tr,1}/H_x)^2_{max} = \frac{1}{\gamma-1}\left[1 - (\gamma p_0 / \mu H_x^2)\right]^2$$

which occurs when

(3.16) $$\left(\frac{\rho_1-\rho_0}{\rho_0}\right) = \frac{1}{\gamma-1}\left[1 - (\gamma p_0 / \mu H_x^2)\right]$$

and then decreases to zero as the critical value of the excess pressure ratio

(3.17) $$\left(\frac{p_1-p_0}{p_0}\right)_{crit} = \frac{2\gamma}{\gamma-1}\,\frac{\mu H_x^2}{\gamma p_0}\left[1 - (\gamma p_0 / \mu H_x^2)\right]$$

is approached [cf. (3.14)] .

We have thus far shown that the relations (3.6) and (3.13) or (3.14) are necessary conditions for the existence of switch-on shocks. In addition to these conditions we note that the braced term in (3.13) or (3.14) is positive and that hence

$$\frac{\gamma p_o}{\mu H_x^2} < 1. \tag{3.18}$$

Conversely, if a shock has a vanishing transverse magnetic field ahead and is such that the relations (3.7),(3.13) or (3.14) and (3.18) are satisfied, then a non-vanishing transverse magnetic field exists behind the shocks.

Consider now the problem of determining the relationship between the state (1) behind a switch-on shock and the state (0) in front. Thus far, states have been described by the variables $\rho$, p, $\bar{u}$ and $\bar{H}_{tr}$, it being assumed that $H_x$ has been specified once and for all. By way of preparation for subsequent considerations, however, it is convenient to introduce the alternative set $\rho$, s, b, $\bar{u}$ and $\bar{H}_{tr}$, where,

$$s = \frac{\gamma p}{\mu H_x^2}, \qquad b = (\mu H_x^2 / \rho)^{1/2} . \tag{3.19}$$

Described in physical terms b is the Alfvén speed and s is the square ratio of the sound speed $\sqrt{\gamma p \rho^{-1}}$ and the Alfvén speed.

In the following it will be assumed that we know which region in the (x,t)-plane is the region behind the shock* and employ the ratio $(s_1-s_o)/s_o$ ($= (p_1-p_o/p_o)$) as a measure of the shock strength. It will be recalled [cf. Section 2.2] that the normal to the shock front, $\bar{n}$, is directed into the region behind the shock; $\bar{n}$ is therefore directed along the negative or positive x-axis according as the shock is forward or backward facing.

It will now be shown that both the state (1) behind the shock and the velocity $U_n$ of the shock front are completely determined whenever the state (0) ahead of the shock, the shock strength $(s_1-s_o)/s_o$, and the direction of the transverse magnetic field are specified. The necessity for prescribing the direction of the magnetic field is indicated by the following argument. Consider first the general situation where the transverse magnetic field does not vanish in front of the shock. The hydromagnetic Rankine-Hugoniot conditions $B_1, \ldots, B_4$ represent seven conditions on the fifteen variables $\rho_1$, $p_1$, $\bar{H}_{tr,1}$, $\bar{u}_{tr,1}$, $u_{x,1}$, $\rho_0$, $p_0$, $\bar{H}_{tr,0}$, $\bar{u}_{tr,0}$, $u_{x,0}$, $U_n$. When the state in front is prescribed, the total number of conditions is fourteen; these conditions yield, in general, a one-parameter family of states behind the shock. Assume now that the shock is a switch-on shock. In this case the four Rankine-Hugoniot conditions, $B_1$ and the transverse part of $B_2$ [cf. (3.4) and (3.5)], degenerate into three conditions, namely those given by the relations (3.5) and (3.7). If we prescribe the state in front we obtain thirteen conditions on the fifteen variables mentioned above. To determine the state behind the shock it is necessary to specify, in addition to the shock strength, another parameter. We may choose this parameter to be the direction of the transverse magnetic field behind the shock.

---

* Since switch-on shocks are compressive it is only necessary to specify which region of the (x,t)-plane is the region of higher pressure.

Without loss of generality we may assume that $\bar{H}_{tr}$ is parallel to the y-axis. The state (1) and the velocity of the shock front $U_n$ are then given by the following relations:

(3.20)

$$E_1 \qquad \frac{\rho_1-\rho_0}{\rho_0} = \frac{s_0}{\gamma-1}\left\{-1+\left[1+\frac{2(\gamma-1)}{\gamma}\left(\frac{s_1-s_0}{s_0}\right)\frac{1}{s_0}\right]^{1/2}\right\}$$

$$E_2 \qquad (H_{y,1}/H_x)^2 = \frac{2(\rho_1-\rho_0)}{\rho_0}\left\{1-\left[\left(\frac{\gamma-1}{2}\right)\left(\frac{\rho_1-\rho_0}{\rho_0}\right)+s_0\right]\right\}$$

$$E_{3,n} \qquad u_{n,1} = u_{n,0} - b_0\left\{(\rho_1/\rho_0)^{1/2}-(\rho_0/\rho_1)^{1/2}\right\}$$

$$E_{3,y} \qquad u_{y,1} = u_{y,0} + \text{sign}\,(H_{y,1})\,b_0(\rho_0/\rho_1)^{1/2}\,\frac{|H_{y,1}|}{H_n}$$

$$E_{3,z} \qquad u_{z,1} = u_{z,0}$$

$$E_4 \qquad U_n = u_{n,0} + b_0\,(\rho_1/\rho_0)^{1/2}$$

whenever

$$(3.21) \qquad 0 \leq \frac{s_1-s_o}{s_o} < \frac{2\gamma}{\gamma-1}\left[\frac{1}{s_o}-1\right], \quad s_o < 1.$$

The relations $E_1$ and $E_2$ are simply the results of substituting $p = \gamma^{-1}\mu H_x^2 s$ [cf. (3.18)] into (3.11) and (3.12). The relation $E_{3,n}$ is an immediate consequence of the longitudinal part of the flux conservation shock condition, $B_3$, and (3.7). $E_{3,y}$ and $E_{3,z}$ follow from (3.5) and (3.7). In deriving all the $E_3$-relations we have used the fact that m is positive in accordance with the convention established in subsection 2.1. The ratio $|H_{y,1} / H_x|$ appearing in the last term of $E_{3,y}$ is determined from $E_2$; sign $(H_y)$ appearing before this term is known since it has been assumed that the direction of this transverse magnetic field is specified. If it is assumed from the outset that $\bar{H}_{tr}$ is parallel to the y-axis it is only necessary to specify sign $(H_y)$ in addition to $(s_1-s_o)/s_o$.

In Figures 4 and 5 we have plotted $(\rho_1-\rho_o)/\rho_o$ and $(H_y/H_x)^2$ respectively, versus $s_1$, $0 < s_1 \leq 5 - 4s_o$ [cf. (3.20), the constant $\gamma$ is assumed to be $5/3$] for several values of $s_o$. These graphs will be useful in Section 5 where a numerical analysis of the resolution of the initial discontinuity is given.

### 3.3 Fast gas dynamical shocks

If we set $\bar{H}_{tr,1}$ and $\bar{H}_{tr,0}$ equal to zero in Eqs. (2.10) the system reduces to the system of shock relations of one-dimensional gas dynamics having a uniform flow transverse to the x-axis. Assuming that $(s_1-s_o)/s_o$ and the state $(\rho_o, b_o, s_o, \bar{u}_o)$ in front of the shock is prescribed, we have from the well-known results of gas dynamics [see Courant and Friedrichs[5], Chapt. 3]:

$$F_1 \qquad \left(\frac{\rho_1-\rho_o}{\rho_o}\right) = \frac{1-\mu^2}{1+\mu^2(s_1/s_o)}\left(\frac{s_1-s_o}{s_o}\right), \qquad \frac{\tau_o-\tau_1}{\tau_o} = \frac{1-\mu^2}{\mu^2+(s_1/s_o)}\left(\frac{s_1-s_o}{s_o}\right)$$

(3.22)

$$F_2 \qquad H_{tr,1} = H_{tr,0} = 0$$

$$
\begin{aligned}
&F_{3,x} && u_{n,1} = u_{n,0} - b_o\left(\frac{s_1-s_o}{s_o}\right)\left[\frac{(1-\mu^2)s_o}{\gamma(\mu^2+(s_1/s_o))}\right]^{1/2}\\
(3.22)\\
&F_{3,tr} && \bar{u}_{tr,1} = \bar{u}_{tr,0}\\
&F_4 && U_n = u_{n,0} - b_o\left[\left(\frac{\mu^2+(s_1/s_o)}{1-\mu^2}\right)\frac{s_o}{\gamma}\right]^{1/2} ,
\end{aligned}
$$

where

$$\mu^2 = (\gamma-1)\Big/(\gamma+1) .$$

The fast gas shock by definition satisfies the relation

$$u_{n,1} - U_n \geq b_1 = (\mu H_x^2\,\rho_1^{-1})^{1/2} = (\rho_o/\rho_1)^{1/2}\,b_o . \tag{3.23}$$

Now from (2.7) and $F_4$ and $F_1$

$$u_{n,1} - U_n = \frac{\rho_o}{\rho_1}(u_{n,0}-U_n) = b_1\left[\frac{1+\mu^2(s_1/s_o)}{\gamma(1-\mu^2)}\;s_o\right]^{1/2} . \tag{3.24}$$

The pure gas shock is therefore fast only for those values of $(s_1/s_o)$ for which

$$\left[\frac{1+\mu^2(s_1/s_o)}{\gamma(1-\mu^2)}\;s_o\right] \geq 1 , \tag{3.25}$$

that is, only for those values of $s_1/s_o$ for which

$$\frac{s_1-s_o}{s_o} \geq \frac{2\gamma}{\gamma-1}\left[\frac{1}{s_o} - 1\right] . \tag{3.26}$$

When $s_o \geq 1$, this relation is valid for all positive values of $(s_1-s_o)/s_o$. When $s_o < 1$, the expression on the right hand side of (3.26) is the minimum value that $(s_1-s_o)/s_o$ may have in a fast gas shock. This minimum value is clearly identical with the critical value of $(s_1-s_o)/s_o$ in the switch-on shock.

At this critical value it is easily verified that the values of $(\rho_1-\rho_o)/\rho_o$, $(H_{y,1}/H_x)^2$, $u_{n,1}$, $\bar{u}_{tr,1}$ and $U_n$ are the same whether computed in accordance with (3.20) or (3.22). It follows that as the excess pressure ratio passes through the critical value, the state behind a switch-on shock having a given state in front passes continuously into the state behind a fast gas shock with the same state in front.

## 4. Slow and fast simple waves

### 4.1 Preliminary comments - Terminology

Certain features of fast and slow simple waves have already been discussed in Section 2. In the present section, slow and fast simple waves will be treated in greater detail. Since the resolution of the initial discontinuity involves only slow simple waves, our attention will be directed, in the main, toward ascertaining the properties of such waves.

As already mentioned, the flow adjacent to a region of constant state is always a simple wave and the transition from a zone of constant state to that of a simple wave takes place across a linear characteristic [cf. subsection 2.3]. This characteristic is called the head of the simple wave if the fluid particles enter across it, the tail of the simple wave if the fluid particles leave across it. If the characteristics in the simple wave region of the (x,t)-plane diverge with increasing time the simple wave is said to be a rarefaction wave; otherwise the wave is said to be a compression wave. Since the resolution of the initial discontinuity involves centered simple waves, and since such waves are manifestly rarefaction waves we shall be concerned here exclusively with rarefaction waves.

In subsection 4.2 we shall prove that in slow simple rarefaction waves the characteristics speeds $|u_x \pm c|$ are at most equal to the corresponding Alfvén characteristic speeds $|u_x \pm b|$, while the opposite relation holds for these characteristic speeds in a fast rarefaction wave. Furthermore, we shall show that centered rarefaction waves are, in general, completely determined by prescribing the state at the head, and the pressure ratio at the tail. At the head of a slow centered simple wave the transverse magnetic field may vanish. Under these circumstances it is necessary to prescribe, in addition to the state at the head and the pressure ratio at the tail, the direction of the transverse magnetic field;

we have already established in subsection 2.3 the fact that the direction of the transverse magnetic field is constant across slow (and fast) simple waves. If, as we may suppose, the transverse magnetic field is parallel to the y-axis, it is only necessary to prescribe the sign of this quantity. Assuming the z-component of the particle velocity vanishes at the head of the rarefaction wave, we shall show that the transverse velocity $u_y$ decreases or increases as we proceed across the simple wave from head to tail according as the sign of the transverse magnetic field is positive or negative. This fact plays a role in determining the sign of $H_y$ in the rarefaction waves which serve as building blocks in the resolution of the initial discontinuity. In order later to be in a position to satisfy the condition that $u_y$ vanish at the tails of the rarefaction waves [cf. (2.21)], we shall find it necessary to choose $H_y$ to be positive.

The slow and fast simple wave solutions discussed in this section were first given by K. O. Friedrichs in [7], (1954). In this work, as already mentioned in Section 1, he reduced the problem of obtaining slow and fast simple wave solutions in media governed by the adiabatic equation of state to essentially that of solving a single linear* ordinary differential equation [see (4.8)]. It will be shown that closed form solutions of this equation exist for values of the adiabatic exponent, $\gamma$, for which $\theta = \gamma/(2-\gamma)$ is a positive integer. In particular, a closed form solution may be obtained when $\gamma = 5/3$ -- i.e., when the equation of state for the medium is that of an ideal monotonic gas. The expressions for the longitudinal and transverse velocity of a slow (or fast) simple wave involve integrals which cannot be evaluated in closed form even for the special values of the parameter $\gamma$ noted above. Subsection 4.3 is devoted to developing suitable approximate expressions for these quantities.

---

* In a recent work[9] Owens has obtained, it appears, slow and fast simple wave solutions by employing a procedure which differs somewhat from that of Friedrichs. His procedure is based on integrating a single non-linear ordinary differential equation.

The numerical results of the present section are summarized graphically in Figures 6 through 12. Here, as in the previous and succeeding sections, all computations are based on the choice $\gamma = 5/3$ for the adiabatic exponent.

### 4.2 Slow and fast simple rarefaction waves

Slow and fast simple waves, by definition, correspond to the smaller and larger roots, $c_s$ and $c_f$, respectively, of the equation

$$\mu(\bar{H}_{tr})^2 = c^{-2}(c^2 - a^2)(\rho c^2 - \mu H_x^2); \tag{4.1}$$

(4.1) is the result of setting the last factor of (2.14) equal to zero. For our present purposes it is convenient, following Friedrichs[7], to introduce the dimensionless quantities

$$\begin{aligned} q &= (c/a)^2 \\ s &= (\rho a^2) / (\mu H_x^2) . \end{aligned} \tag{4.2}$$

The quantity q is the square ratio of the disturbance and sound speeds c and a respectively; s is the square ratio of the sound speed and the Alfvén speed,

$$b = (\mu H_x^2 \rho^{-1})^{1/2} .$$

Since we are dealing with a polytropic gas undergoing an adiabatic process, the square of the sound speed $a^2$ is $\gamma p \rho^{-1}$. Hence we have

$$s = (\gamma p / \mu H_x^2). \tag{4.3}$$

In terms of s and q (4.1) becomes

$$(4.4) \qquad (\bar{H}_{tr})^2 = (q-1)(s-q^{-1})H_x^2 \,.$$

Because the left-hand side of this equation is non-negative, the first two factors on the right-hand side must have the same sign. It follows immediately that

$$(4.5) \qquad \begin{array}{lll} q < 1, & s \leq \frac{1}{q} & \text{in a slow simple wave} \\ q > 1, & s \geq \frac{1}{q} & \text{in a fast simple wave} \end{array}$$

unless $(\bar{H}_{tr})^2$ vanishes everywhere in the simple wave region, in which case

$$(4.6) \qquad q = 1.$$

Under these circumstances, as may be verified from an inspection of (2.13) (the D relations), the hydromagnetic simple wave reduces to a one-dimensional gas dynamical simple wave in which the transverse velocity $\bar{u}_{tr}$ is constant. Assuming that $(\bar{H}_{tr})^2$ does not vanish identically we have from (4.2) and (4.5)

$$(4.7) \qquad \begin{array}{ll} c_s \leq b < a & \text{in a slow simple wave} \\ a < b \leq c_f & \text{in a fast simple wave.} \end{array}$$

It follows immediately from these relations that the characteristic speeds $|u_x \pm c_s|$ in a slow simple wave are less than or equal to the corresponding Alfvén characteristic speeds $|u_x \pm b|$, while in a fast simple wave the characteristic speeds $|u_x \pm c_f|$ are greater than or equal to the corresponding Alfvén characteristic speeds.

From (4.4) and the relations $D_{2,x}$ and $D_3$ of (2.13) we obtain the following linear differential equation [cf. [7] p. 40] for s as a function of q:

(4.8)
$$\frac{ds}{dq} + \frac{\theta s}{1-q} = \frac{\theta}{q^2(1-q)} ,$$

where

(4.9)
$$\theta = \gamma/(2-\gamma) \qquad 1 < \gamma < 2.$$

Now from (4.5) it is clear that in a slow simple wave q and s are confined to the region in the first quadrant of the (q,s)-plane bounded on the right by $q = 1$ and above by the arc $s = q^{-1}$, $0 \leq q \leq 1$ [see Fig. 6]. Let $(q_{tr}, s_{tr})$ be a point on the hyperbolic arc, i.e., let*

(4.10)
$$q_{tr} = \frac{1}{s_{tr}} , \qquad 0 < q_{tr} < 1.$$

Then, integrating from q to $q_{tr}$ we have from (4.8)

(4.11)
$$s = s(q, q_{tr}; \theta) = \frac{1}{q_{tr}} \left(\frac{1-q}{1-q_{tr}}\right)^{\theta} - \theta(1-q)^{\theta} \int_{q}^{q_{tr}} \omega^{-2}(1-\omega)^{-(\theta+1)} d\omega.$$

We do not give the corresponding expression for the fast waves since it will not be required in subsequent sections.

It will be assumed here and hereafter that θ is a non-negative integer. Several values of the adiabatic exponent γ, $1 < \gamma < 2$, for which θ is integral are given in the following table:

(4.12)

| γ | 4/3 | 3/2 | 8/5 | 5/3 |
|---|---|---|---|---|
| θ | 2 | 3 | 4 | 5 |

---

* When $q_{tr} = s_{tr}^{-1}$, then $c = b = (\mu H_x^2 \rho^{-1})^{1/2}$; that is, c equals the disturbance speed of transverse simple waves [see subsection 2.3].

Note that when the equation of state for the medium is that of a polytropic monatomic gas, then $\gamma = 5/3$ and $\theta = 5$.

Expanding the integrand in the last term of (4.11) in partial fractions we get

$$\frac{1}{\omega^2(1-\omega)^{\theta+1}} = (\theta+1)\left(\frac{1}{\omega} + \frac{1}{1-\omega}\right) + \frac{1}{\omega^2} + \sum_{k=1}^{\theta} \frac{(\theta+1-k)}{(1-\omega)^{k+1}} .$$

After inserting this expression for the integrand into (4.11) we get, after performing the indicated integration,

$$\begin{aligned} s = {} & \frac{1}{q_{tr}}\left(\frac{1-q}{1-q_{tr}}\right)^{\theta} - \theta(1-q)^{\theta}\left[(\theta+1)\log\left(\frac{q_{tr}(1-q)}{q(1-q_{tr})}\right) + \left(\frac{1}{q} - \frac{1}{q_{tr}}\right)\right. \\ & \left. + \sum_{k=1}^{\theta}\left(\frac{\theta+1-k}{k}\right)\left\{\frac{1}{(1-q_{tr})^k} - \frac{1}{(1-q)^k}\right\}\right] , \\ & q_{cav} \le q \le q_{tr} = s_{tr}^{-1} , \end{aligned} \tag{4.13}$$

where $q_{cav}$ is that value of the square ratio, $c^2/a^2$, of the disturbance speed to the sound speed at which cavitation occurs; i.e., at which $s = 0$.

Let $\rho_1$, $b_1$, $s_1 > 0$, $H_{y,1}$, $u_{x,1}$ and $u_{y,1}$ describe the physical state of the medium at a given point of the slow simple wave. Solving for $q$ in (4.4) and setting $s = s_1$, $H_{tr}^2 = H_{y,1}^2$, we have*

$$q_1 = \frac{1+s_1 + (H_{y,1}/H_x)^2 - \sqrt{\left[1 + s_1 + (H_{y,1}/H_x)^2\right]^2 - 4s_1}}{2s_1} . \tag{4.14}$$

Since $(q_1, s_1)$ is necessarily a point on one of the curves of the family $s = s(q, q_{tr}; \theta)$, where the function $s(q, q_{tr}; \theta)$ is given explicitly in (4.13), we arrive at the rather complicated equation $s_1 = s(q_1, q_{tr}; \theta)$ relating $q_{tr}$ to the quantities $q_1$ and $s_1$. This equation may be solved for $q_{tr}$, graphically or employing appropriate numerical methods. Thus the knowledge of $|H_{y,1}|$ and $s_1$ of a point of a slow simple wave determines $q_{tr}$ and consequently which of the $s = s(q, q_{tr}, \theta)$ - relations governs the dependence of s and q throughout the simple wave.

---

*As already mentioned, the direction of $\bar{H}_{tr}$ is constant across slow and fast simple waves. In the discussion which follows we may therefore set $H_z = 0$ without loss of generality.

Now, employing the equation of state $(p/p_1) = (\rho/\rho_1)^{\gamma}$, we obtain the following expressions for the density, sound speed, and disturbance speed:

$$
\begin{aligned}
&\rho = \rho_1 \, (s/s_1)^{1/\gamma} \\
(4.15) \qquad &a = a_1 (s/s_1)^{(\gamma-1)/2\gamma} = s_1^{1/2} \, b_1 (s/s_1)^{(\gamma-1)/2\gamma} \\
&c = a q^{1/2} = (s_1/s_{tr})^{1/2} \, b_1 (q/q_{tr})^{1/2} \, (s/s_1)^{(\gamma-1)/2\gamma} .
\end{aligned}
$$

From these relations together with $F_{2,x}$, $F_{2,y}$, $F_{2,z}$ [cf. (2.13)] and (4.4), we have

$$
\begin{aligned}
&du_x = \pm \frac{\sqrt{s_1} \, b_1}{\gamma} \, q^{1/2} (s/s_1)^{-(\gamma+1)/2\gamma} \, d(s/s_1), \\
(4.16) \qquad &du_y = \text{sign}\,(H_{y,1}) \left[ \frac{(1-q)}{(1-qs)q} \right]^{1/2} du_x, \\
&u_z = u_{z,1} .
\end{aligned}
$$

The factor* sign $(H_{y,1})$ arises from the necessity of extracting the square root of the expression $(H_{y,1}/H_x)^2 = (q^{-1}-1)(1-qs)$. If we now regard q as the function of s obtained by solving for q in (4.13), $q = q(s, s_{tr}; \theta)$, say, and if we introduce the variable of integration

$$(4.17) \qquad \sigma = s/s_{tr} ,$$

we have on integrating from $s/s_{tr}$ to $s_1/s_{tr}$, $0 \leq s < s_1 < s_{tr}$,

---

*It will be recalled that the direction of $H_y$ is constant across slow and fast simple waves. Sign $(H_y)$ is therefore constant across such waves.

$$\begin{aligned} u_x &= u_{x,1} \mp \frac{b_1}{\gamma}\left(\frac{s_1}{s_{tr}}\right) \mathcal{K}(s,s_1;s_{tr}) , && 0 \le s < s_1 < s_{tr}, \\ u_y &= u_{y,1} \mp \operatorname{sign}(H_{y,1}) \frac{b_1}{\gamma} \left[s_1(1-q_{cav})\right]^{\frac{1}{2}} \lambda(s,s_1,s_{tr}), && 0 \le s < s_1 < s_{tr}, \end{aligned} \tag{4.18}$$

where

$$\begin{aligned} \mathcal{K}(s,s_1;s_{tr}) &= \left(\frac{s_{tr}}{s_1}\right)^{\frac{\gamma-1}{2\gamma}} \int_{s/s_{tr}}^{s_1/s_{tr}} (q/q_{tr})^{\frac{1}{2}} \sigma^{-\frac{\gamma+1}{2\gamma}} \, d\sigma , \qquad 0 \le s \le s_1 \le s_{tr} , \\ \lambda(s,s_1;s_{tr}) &= \left(\frac{s_{tr}}{s_1}\right)^{\frac{\gamma-1}{2\gamma}} \int_{s/s_{tr}}^{s_1/s_{tr}} \left[\frac{(1-q)/(1-q_{cav})}{1-(q/q_{tr})\,\sigma}\right]^{\frac{1}{2}} \sigma^{-\frac{\gamma+1}{2\gamma}} \, d\sigma, \quad 0 \le s \le s_1 \le s_{tr} . \end{aligned} \tag{4.19}$$

Now, as is easily verified,

$$\begin{aligned} \mathcal{K}(s,s_1;s_{tr}) &= \left(\frac{s_{tr}}{s_1}\right)^{\frac{\gamma-1}{2\gamma}} \left[\mathcal{K}(s/s_{tr};s_{tr}) - \mathcal{K}(s_1/s_{tr};s_{tr})\right] \\ \lambda(s,s_1;s_{tr}) &= \left(\frac{s_{tr}}{s_1}\right)^{\frac{\gamma-1}{2\gamma}} \left[\lambda(s/s_{tr};s_{tr}) - \lambda(s_1/s_{tr};s_{tr})\right] , \end{aligned} \tag{4.20}$$

where by definition

$$\begin{aligned} \mathcal{K}(s/s_{tr};s_{tr}) &\equiv \mathcal{K}(s,s_{tr};s_{tr}) \\ \lambda(s/s_{tr};s_{tr}) &\equiv \lambda(s,s_{tr};s_{tr}). \end{aligned} \tag{4.21}$$

We conclude, therefore, that it is only necessary to determine the dependence of $\mathcal{K}(s/s_{tr};s_{tr})$ and $\lambda(s/s_{tr};s_{tr})$ on the variable $s/s_{tr}$ and the parameter $s_{tr}$ in order to obtain the corresponding information about $\mathcal{K}(s,s_1;s_{tr})$ and $\lambda(s,s_1;s_{tr})$. Assuming this information to be available we have shown that the specification of the quantities, $\rho$, $b$, $H_y/H_x$, $u_x$ and $u_y$ at one point of the simple wave fixes the dependence of these variables on $s/s_{tr}$ at all points of the the simple wave, in accordance with (4.4), (4.13), (4.14), (4.15), (4.18) and

(4.19). We have thus far implicitly assumed that $H_y \neq 0$ in specifying the state at one point. Now in a slow simple wave, $H_y$ vanishes when the disturbance speed c equals the Alfvén speed $b = (\mu H_x^2 \rho^{-1})^{1/2}$, that is, when $q_{tr} = s_{tr}^{-1}$. Under these circumstances in addition to specifying the state (1) and $s/s_{tr}$ it is necessary to specify the sign of the magnetic field.

Before discussing the solution quantitatively, it is worthwhile at this point to note certain qualitative features of slow and fast simple wave motion which may be deduced without the aid of a detailed numerical analysis. In what follows it is assumed that the simple waves under discussion are rarefaction waves. We shall show that in slow or fast simple waves the density ρ, the sound speed a, and the disturbance speed c vary in the same sense as the pressure, while the magnitude of the transverse magnetic field $|H_y|$ varies in the opposite sense. Moreover, in forward-facing slow or fast simple waves, the longitudinal velocity $u_x$ and the characteristic velocity $u_x + c$ vary in the same sense as the pressure while in backward-facing slow or fast simple waves, $u_x$, $u_x + c$ and the pressure vary in opposite senses. Finally, we shall show that in slow and fast forward-facing simple waves the transverse velocity, $u_y$, varies in the same sense as or in the opposite sense to the pressure according as sign $(H_y)$ is positive or negative, while in backward-facing slow or fast simple waves $u_y$ varies in the same sense as or the opposite sense to the pressure according as sign $(H_y)$ is negative or positive.

To prove the first statement let us rewrite (4.8) in the following form:

$$\frac{ds}{dq} = \theta\, q^{-2}(1-q)^{-1}(1-q^2 s).$$

Because of the relations (4.5) the right-hand side of this equation is positive. Thus in slow or fast simple waves q varies in the same sense as s. Since s is proportional to the pressure [cf. (4.3)], it follows that q varies in the same sense as p. From (4.14) we may then conclude that in a slow or fast simple wave, the density, the sound speed and the disturbance speed vary in the same sense as the pressure.

To determine how $|H_y|$ varies with p, we write (4.4) in the form

$$H_y^2 = (q^{-1}-1)\,(1-sq)H_x^2 \,.$$

Because of the relations (4.3) the signs of the factors $(q^{-1}-1)$ and $1-sq$ are the same. Moreover, the absolute value of these factors and s vary in opposite senses. It follows that $|H_y|$ and p vary in opposite senses across fast and slow simple waves.

The statement concerning the longitudinal, transverse and characteristic velocities follows from (4.15) and (4.18) and the corresponding relations for fast simple waves.

### 4.3 Approximate expressions for $\kappa(s/s_{tr};s_{tr})$ and $\lambda(s/s_{tr};s_{tr})$

We turn now to the detailed examination of the simple wave solution. In Figure 6 we have plotted* $s = s(q,q_{tr};\theta)$ [see (4.13)] against q, $q_{cav} \leq q \leq q_{tr}$, for several values of $q_{tr}$. The dependence of $|H_y/H_x|$ (which, from (4.4), equals $\sqrt{(q^{-1}-1)(1-qs)}$ ) on $s/s_{tr}$, $0 \leq s/s_{tr} \leq 1$, along each of these curves is depicted in Figure 7. To obtain similar information about $u_x$ and $u_y$ it is clear, in virtue of relation (4.20), that it is only necessary to determine the dependence of $\kappa(s/s_{tr};s_{tr})$ and $\lambda(s/s_{tr};s_{tr})$ on the variable $(s/s_{tr})$, $0 \leq s/s_{tr} \leq 1$, for the values of $s_{tr}$ $(= q_{tr}^{-1})$ which correspond to the values of $q_{tr}$ employed above. As mentioned earlier, the complicated nature of the relation between s and q makes it necessary to evaluate the integral expressions for $\kappa(s/s_{tr};s_{tr})$ and $\lambda(s/s_{tr};s_{tr})$ by means of an approximation procedure.

---

* In all graphs appearing in this and in the remaining sections θ is taken to be 5 (see (4.9)). The equation of state of the medium is therefore that of a polytropic, monatomic gas.

Let us represent the equation for the portion of the $s(q,q_{tr};\theta)$-curve through the points $(q_{cav},0)$ and $(q_{tr},s_{tr})$ in the following manner:

$$(4.22)\qquad (s/s_{tr})\left[1+\varepsilon(s,s_{tr})\right] = (q-q_{cav}), \qquad q_{cav} \le q \le q_{tr} \, .$$

The quantity $\varepsilon(s,s_{tr})$ measures, for each q in the specified range, the deviation of the $s(q,q_{tr};\theta)$-curve from the straight line segment

$$(4.23)\qquad (s/s_{tr}) = (q-q_{cav}) / (q_{tr}-q_{cav}), \qquad q_{cav} \le q \le q_{tr} \, .$$

Now the $s(q,q_{tr};\theta)$-curves [see Figure 6] are almost linear; we may therefore neglect $\varepsilon(s,s_{tr})$ without incurring too great a loss in accuracy. In the analysis which follows (4.23) will be employed in lieu of (4.22).

It will now be shown that

$$(4.24)\qquad \begin{aligned} K(s/s_{tr};s_{tr}) = 5(q_{cav}/q_{tr})^{\frac{1}{2}} \Bigg[\left\{1-(s/s_{tr})^{\frac{1}{5}}\right\} + \frac{\alpha}{12}\left\{1-(s/s_{tr})^{\frac{6}{5}}\right\} \\ - \frac{\alpha^2}{88}\left\{1-(s/s_{tr})^{\frac{11}{5}}\right\} + \dots\Bigg], \quad 0 \le s/s_{tr} \le 1, \end{aligned}$$

$$(4.25)\qquad \begin{aligned} \lambda(s/s_{tr};s_{tr}) = \Bigg[B\left(\frac{1}{5}, \frac{1}{2}; \frac{s}{s_{tr}}\right) - \frac{\delta+\beta}{2} B\left(\frac{6}{5}, \frac{1}{2}; \frac{s}{s_{tr}}\right) + \frac{3\delta^2+2\delta\beta-\beta^2}{8} B\left(\frac{11}{5}, \frac{1}{2}, \frac{s}{s_{tr}}\right) \\ + \frac{\beta^2\delta-\beta^3-3\beta\delta^2-5\delta^3}{16} B\left(\frac{16}{5}, \frac{1}{2}; s_{tr}\right) + \dots\Bigg], \quad 0 \le s/s_{tr} \le 1. \end{aligned}$$

Here

$$(4.26)\qquad B(p,q;s/s_{tr}) = \int_{s/s_{tr}}^{1} \sigma^{p-1}(1-\sigma)^{q-1}\, d\sigma, \, ^{*}$$

and the quantities, $\alpha$, $\beta$ and $\delta$ are defined as follows:

---

[*] The quantities p and q employed here are in no way related to the pressure and the square ratio $q = c^2/a^2$ .

$$\alpha = (q_{tr}-q_{cav}) \,/\, q_{cav}$$

$$(4.27) \qquad \beta = (q_{tr}-q_{cav}) \,/\, (1-q_{cav})$$

$$\delta = (q_{tr}-q_{cav}) \,/\, q_{tr} \;.$$

To obtain the above expression for $K(s/s_{tr};s_{tr})$ from the integral expression for this quantity [cf. (4.19)] we expand $(q)^{1/2}$ in powers of $(q-q_{cav})/q_{cav}$, substitute for $q-q_{cav}$ from (4.23); then we multiply through by $\sigma^{-4/5}$ and integrate from $s/s_{tr}$ to unity. To obtain the corresponding expression for $\lambda(s/s_{tr};s_{tr})$ [cf. (4.19)] we first substitute for q in $(1-qs)^{-1/2}$ from (4.23) to get

$$\left[1-(s/s_{tr})\right]^{-1/2} \left[1-\delta(s/s_{tr})\right]^{-1/2}$$

and expand the last factor in powers of $\delta(s/s_{tr})$. Then we expand $(1-q)^{1/2}$ in powers of $(q-q_{cav})/(1-q_{cav})$ and express $q-q_{cav}$ in terms of $s/s_{tr}$ by means of (4.23). The resulting power series is then multiplied by

$$\sigma^{-4/5}\left[1-(s/s_{tr})\right]^{-1/2}$$

and by the power series expression for $\left[1-\beta(s/s_{tr})\right]^{-1/2}$ and then integrated termwise from $(s/s_{tr})$ to unity.

In Figures 8 and 9 we have plotted α, δ and β versus $q_{tr}$, $0 \leq q_{tr} \leq 1$. The limiting values of these ratios near $q_{tr} = 0$ are obtained from the fact that*

$$(4.28) \qquad q_{cav} \sim \frac{\theta}{\theta+1}\, q_{tr} \qquad q_{tr} \to 0$$

and

$$(4.29) \qquad 1-q_{cav} \sim \left(\frac{2}{3}\right)^{\frac{1}{5}} (1-q_{tr})^{\frac{4}{5}}, \quad q_{tr} \to 1.$$

---

* See Appendix II.

It should be observed that $\alpha$ and $\delta$ are less than .2 in the range $0 \leq q_{tr} \leq 1$ while $\beta$ is less than .5 for $0 \leq q_{tr} \leq .975$ but increases rapidly to unity when $.975 \leq q_{tr} \leq 1$. The series expression in the right-hand side of (4.23) therefore converges rapidly for all $q_{tr}$, $0 \leq q_{tr} \leq 1$; the same is true of the right-hand side of (4.24) over the smaller $q_{tr}$-interval $0 \leq q_{tr} \leq .975$.

It is desirable to rewrite the expression for $\lambda(s/s_{tr};s_{tr})$ somewhat, in order to put in evidence the relative contributions of the individual terms of the sum and to have an expression better suited for computational purposes. To this end let us write $B(p,q;x)$ in the form

$$B(p,q;x) = B(p,q;0)\left[1 - I_x(p,q)\right] , \qquad 0 \leq x \leq 1 , \tag{4.30}$$

where

$$I_x(p,q) = \frac{\int_0^x \sigma^{p-1}(1-\sigma)^{q-1}d\sigma}{B(p,q;0)} . \tag{4.31}$$

Note that

$$0 \leq I_x(p,q) \leq 1, \qquad 0 \leq x \leq 1 , \tag{4.32}$$

and that

$$B(p,q;0) = \int_0^1 \sigma^{p-1}(1-\sigma)^{q-1}d\sigma = \frac{\Gamma(p)\Gamma(q)}{\Gamma(p+q)} , \tag{4.33}$$

the last equation being a statement of the well-known relation between the gamma function and the beta function. Substituting for $B(p,q;x)$ in (4.24) and making use of the fact that

$$\begin{aligned} B(6/5,\ 1/2;\ 0) &= (2/7)\ B(1/5,\ 1/2;\ 0) \\ B(11/5,\ 1/2;0) &= (2/7)(12/7)\ B(1/5,\ 1/2;0) \\ B(16/5,\ 1/2;0) &= (2/7)(12/17)(22/27)B(1/5,\ 1/2;0) \end{aligned} \tag{4.32}$$

we have finally

$$\begin{aligned}\lambda(s/s_{tr};s_{tr}) = B(1/5,1/2;0)\Bigg[&\left\{1-I_x(\tfrac{1}{5},\tfrac{1}{2})\right\} - \frac{\delta+\beta}{2}\left(\frac{2}{7}\right)\left(\frac{12}{17}\right)\left\{1-I_x(\tfrac{6}{5},\tfrac{1}{2})\right\} \\ &+ \frac{3\delta^2+2\delta\beta-\beta^2}{8}\left(\frac{2}{7}\right)\left(\frac{12}{17}\right)\left\{1-I_x(\tfrac{11}{5},\tfrac{1}{2})\right\} \\ &+ \frac{(\delta\beta^2-\beta^3-3\beta\delta^2-5\delta^3)(\frac{2}{7})(\frac{12}{17})(\frac{22}{27})}{16}\left\{1-I_x(\tfrac{16}{5},\tfrac{1}{2})\right\} \\ &+ \cdots\Bigg],\end{aligned} \tag{4.35}$$

where

$$B(\tfrac{6}{5},\tfrac{1}{2};0) = \frac{\Gamma(1/5)\Gamma(1/2)}{\Gamma(7/10)} = 6.286. \tag{4.36}$$

When $p \geq 6/5$, numerical values of $I_x(p,1/2)$ for values of $x$ in the interval $0 \leq x \leq 1$ may be obtained from K. Pearson's tables of the incomplete beta functions[9] by interpolating between the tabulated values of $p$. The first term

$$B(1/5,1/2;x) = B(p,q;0)\left[1 - I_x(p,q)\right]$$

may be obtained directly, for example, by expanding the terms $(1-\sigma)^{-1/2}$ as a power series in $\sigma$ and integrating termwise.

The dependence of $\kappa(s/s_{tr};s_{tr})$ and $\lambda(s/s_{tr};s_{tr})$ on $s/s_{tr}$, $0 \leq s/s_{tr} \leq 1$, for $q_{tr} = s_{tr}^{-1} = 0.05$ and $q_{tr} = 0.975$ is depicted in Figures 10 and 11. The curves corresponding to $q_{tr}$ lying between these values are not shown. Figure 12 is added in order to facilitate interpolation between these curves; in it we have plotted $\kappa(0;s_{tr})$ and $\lambda(0;s_{tr})$ versus $q_{tr}$, $0 \leq q_{tr} \leq 1$. This information is useful for interpolation since it is found that

$$\frac{\mathcal{K}\left[s/s_{tr};s_{tr}\right] - \mathcal{K}\left[s/s_{tr};(.05)^{-1}\right]}{\mathcal{K}\left[s/s_{tr};(.975)^{-1}\right] - \mathcal{K}\left[s/s_{tr};s_{tr}\right]} \cong \frac{\mathcal{K}\left[0;s_{tr}\right] - \mathcal{K}\left[0;(.05)^{-1}\right]}{\mathcal{K}\left[0;(.975)^{-1}\right] - \mathcal{K}\left[0;s_{tr}\right]}$$

(4.37)

$$\frac{\lambda\left[s/s_{tr};s_{tr}\right] - \lambda\left[s/s_{tr};(.05)^{-1}\right]}{\lambda\left[s/s_{tr};(.975)^{-1}\right] - \lambda\left[s/s_{tr};s_{tr}\right]} \cong \frac{\lambda\left[0,s_{tr}\right] - \lambda\left[0;(.05)^{-1}\right]}{\lambda\left[0;(.975)^{-1}\right] - \lambda\left[0;s_{tr}\right]} ,$$

to a sufficient degree of accuracy.

From the integral expressions for $\mathcal{K}(s/s_{tr};s_{tr})$ and $\lambda(s/s_{tr};s_{tr})$ it is easily verified that

$$\mathcal{K}(s/s_{tr};s_{tr}) \cong \mathcal{K}(0;s_{tr}) - 5\sqrt{\frac{q_{cav}}{q_{tr}}}\,(s/s_{tr})^{1/5}, \quad (s/s_{tr}) \to 0$$

(4.38)

$$\lambda(s/s_{tr};s_{tr}) \cong \lambda(0;s_{tr}) - 5\,(s/s_{tr})^{1/5}, \quad (s/s_{tr}) \to 0.$$

These asymptotic results are independent of the linear approximation employed in deriving the series expression for $\mathcal{K}(s/s_{tr};s_{tr})$ and $\lambda(s/s_{tr};s_{tr})$.

To prepare for the analysis of the next section it will be useful to obtain the corresponding asymptotic relations for $\lambda(s/s_{tr};s_{tr})$ and $\mathcal{K}(s/s_{tr};s_{tr})$ as $s/s_{tr}$ approaches unity. In the neighborhood of $s/s_{tr} = 1$ the $s(q,q_{tr},\theta)$-curve may be approximated by the straight line,

$$q \cong q_{tr} + \left.\frac{dq}{ds}\right|_{q=q_{tr}} (s-s_{tr}).$$

Employing (4.31) we have, since $q_{tr} = s_{tr}^{-1}$,

$$q \cong q_{tr} - \frac{q_{tr}}{\theta}\left[1 - (s/s_{tr})\right].$$

It follows that

$$1-qs \cong \frac{\theta+1}{\theta}\left[1 - (s/s_{tr})\right]\left\{1 - \frac{1}{\theta+1}\left[1 - (s/s_{tr})\right]\right\}.$$

Thus, retaining only first order terms, we get

$$(4.39)\qquad 1 - qs \cong \frac{\theta+1}{\theta}\left[1 - (s/s_{tr})\right] .$$

Similarly, neglecting higher-order terms, we have

$$1 - q \cong 1 - q_{tr} .$$

Employing these approximations in the expression for $\lambda(s/s_{tr};s_{tr})$ we have

$$\lambda(s/s_{tr};s_{tr}) = (1-q_{cav})^{-1/2} \int_{s/s_{tr}}^{1} \left[\frac{1-q}{1-qs}\right]^{\frac{1}{2}} \sigma^{-\frac{\gamma+1}{2\gamma}}\, d\sigma$$

$$= \left[\frac{1-q_{tr}}{1-q_{cav}}\;\frac{\theta}{\theta+1}\right]^{\frac{1}{2}} \int_{s/s_{tr}}^{1} \frac{\sigma^{-\frac{\gamma+1}{2\gamma}}}{\left[1-\sigma\right]^{1/2}}\, d\sigma .$$

Integrating and retaining only higher-order terms, we get finally, since $\theta/\theta+1 = \gamma/2$ [cf. (4.9)],

$$(4.40)\qquad \lambda(s/s_{tr};s_{tr}) \cong \left[2\gamma\left(\frac{1-q_{tr}}{1-q_{cav}}\right)\right]^{\frac{1}{2}} \left[1 - (s/s_{tr})\right]^{\frac{1}{2}}, \qquad s/s_{tr} \to 1.$$

The corresponding expression for $K(s/s_{tr};s_{tr})$,

$$(4.41)\qquad K(s/s_{tr};s_{tr}) \cong \left[1 - (s/s_{tr})\right] ,$$

follows immediately from the definition of $K(s/s_{tr};s_{tr})$.

## 5. Resolution of the shear flow discontinuity

### 5.1 Preliminary considerations; notation

As indicated in Section 1, the resolution of the initial discontinuity may be effected by two fast shocks of equal strength moving away from the initial discontinuity with equal but opposite speeds, followed by two slow centered rarefaction waves. These slow centered rarefaction waves are, like the shocks, symmetrically disposed with respect to the origin at each instant, and connect the constant states behind the shocks to an expanding zone of constant state between the simple waves or to a vacuum zone which expands with an appropriate " escape speed" according as cavitation does or does not occur. It will be recalled that the fast shocks could either be fast pure gas dynamical shocks or switch-on shocks, and that the choice of these waves was dictated by the absence of a transverse magnetic field in front of the shocks. In light of the analysis of Section 3 we now know that the resolution of the initial discontinuity is effected by fast gas shocks unless $s_o$, the square ratio of the sound speed and the Alfvén speed in the undisturbed medium, is less than unity and the shock strength, measured in terms of the pressure ratio, is below a certain critical value, in which case the resolution is effected by switch-on shocks.

In further specifying the nature of the resolution it is assumed [see subsection 2.4] that (i) the transverse component of the particle velocity is parallel to the y-axis and that (ii) the pressure, density, and transverse magnetic field components are even functions of x, while the velocity components are odd functions of x. Assumption (i) implies that the transverse component of the magnetic field is parallel to the y-axis [see subsection 2.4]. Assumption (ii) implies the vanishing of the transverse and longitudinal velocities in the zone of constant state behind the rarefaction waves, assuming, of course, that cavitation has not been produced. In case the magnitude of the initial shear flow discontinuity is large enough to produce cavitation, the vanishing of the velocity behind the rarefaction waves must be replaced by the condition that the electric field vanishes at the tails of the rarefaction waves [see subsection 2.4, equations (2.22)-(2.30)]. Under these circumstances the tails of the rarefaction waves are allowed to move in the y-direction with equal and opposite transverse speeds and in the longitudinal direction with equal and opposite "escape speeds".

The object of this section is to prove that this motion is indeed a solution of the initial-value problem formulated in Section 1 and to provide the basis for a complete description of the motion. Before doing this, however, it will be convenient to establish here the notation to be employed and to describe briefly the procedure to be followed in subsequent subsections.

Because of the symmetry, it is clear we need only consider the motion in the region $x > 0$. In Figure 3a we have depicted the basic flow regions in the positive half of the $(x,t)$-plane. These basic flow regions are:

Region (0) : The region of constant state in front of the forward-facing shock;

Region (1) : The region of constant state behind the shock;

Region (2) : The flow region of the slow, centered, simple forward-facing rarefaction wave;

Region (3) : The region of constant state following the tail of the forward-facing simple wave.

Similar quantities in the various regions will be distinguished by appending appropriate subscripts. The state at a point in region j, $j = 0, 1, 2, 3$, will be characterized by the values $\rho_j$, $p_j$, $H_{y,j}$, $H_x$, $u_{x,j}$, $u_{y,j}$ or alternatively by the values

$$s_j(= \gamma p_j/\mu H_x^2),\ b_j(= \sqrt{\mu H_x^2 \rho_j^{-1}}\ ),\ (H_{y,j}/H_x),\ (u_{x,j}/b_j) \text{ and } (u_{y,j}/b_j) \text{ or } (u_{y,j}/a_j).$$

It will be recalled, that $p_j$ is the pressure, $\rho_j$ the density, $H_x$ the fixed longitudinal magnetic field component, $H_{y,j}$ the transverse magnetic field component, $b_j$ the Alfvén speed, $a_j$ the sound speed, in Region j, $j = 0, 1,2,3$ and $s_j(=(a_j/b_j)^2)$ the square ratio of the sound speed to the Alfvén speed in Region j, $j = 0,1,2,3$.

The complete description of the motion entails the knowledge of how the physical state in regions (0)-(3), the velocity of the shock front, and the head and the tail of the simple wave depend upon the thermodynamic state in front of the shock, on $H_x$, and on the magnitude of the initial discontinuity in velocity $2u_{y,0}$. To establish this dependence we recall that the state behind a fast shock and the state at the tail of the rarefaction wave depends only on the pressure ratios $p_1/p_o$ ($= s_1/s_o$) and $p_3/p_1$ ($= s_3/s_1$) respectively, assuming the state in front is specified [see Sections 3 and 4]*. Since the state (1) behind the shock is the state in front of the rarefaction wave it follows that state (3) at the tail of the rarefaction wave depends upon the two parameters $p_1/p_o$ and $p_3/p_1$ in addition to the state in front of the shock. If cavitation has not been reached, then $p_3 = s_3 \neq 0$. From the expressions for $u_x$ and $u_y$ [cf. (4.18)-(4.19)] in the simple wave region we obtain, after setting $u_y = u_x = 0$ at the tail, two relations of the form

$$R_i \left[(s_3/s_1),\ (s_1/s_o);\ (u_{y,0}/b_o), s_o\right] = 0, \qquad i = 1,\ 2.$$

By a combination of the graphical and numerical methods we then obtain the dependence of $s_3/s_1$ and $s_1/s_o$ on $u_{y,0}/b_o$ for several values of the parameter $s_o$.

It can be shown that cavitation is produced when the ratio $u_{y,0}/b_o$ exceeds a certain minimum value depending on the parameter $s_o$. In this case $s_3$ ($= \gamma p_3/\mu H_x^2$) vanishes at the tail of the rarefaction wave. This condition in conjunction with the second condition of (2.22) leads to a relation of the form

$$S\left[s_1/s_o;(u_{y,0}/b_o),\ s_o\right] = 0$$

from which, again by numerical and graphical means, the dependence of the ratio $s_1/s_o$ on the ratio $u_{y,0}/b_o$ and on $s_o$ is established. It should be observed that the state in front of the advancing shocks is characterized by the values $\rho_o$, $u_{y,0}/b_o$, $s_o$, $b_o$. It is therefore fortunate that the relations $R_i = 0$, $i = 1,2$, and $S = 0$ do not depend on $\rho_o$ and $b_o$ explicitly.

---

* We leave open for the moment questions involving the direction of the transverse magnetic field. See, however, subsections 4.1, 5.21, and 5.31.

In subsection 5.2 we summarize the formulas giving the state behind the fast shocks in terms of the pressure ratio $p_1/p_0 = s_1/s_0$ and the state in front. In subsection 5.3 the corresponding expressions characterizing the states in the simple wave region are given in terms of the ratio $p_2/p_1 = s_2/s_1$ and the one-parameter family of states in Region (1) at the head of the rarefaction wave. The program for establishing the dependence of $s_1/s_0$ and $s_3/s_1$ on $u_{y,0}/b_0$ for various values of $s_0$ is outlined in subsection 5.4. The results are summarized in the Figures 15c and 16. In expressing the dependence of $s_1/s_0$ on the state in the undisturbed medium it is also useful, for reasons which will be apparent later, to plot $s_1/s_0$ versus $u_{y,0}/a_0$, where $a_0$ $\left[= b_0 \sqrt{s_0}\right]$ is the speed of sound in the undisturbed medium. The curves corresponding to $s_0 \geq 1$ are shown in Figure 15a, those corresponding to $s_0 < 1$ in 15b. The limiting forms of the dependence of $s_1/s_0$, $s_3/s_1$ $(H_{y,3}/H_x)$ and other quantities of interest on $u_{y,0}/b_0$ corresponding to small and large values of $u_{y,0}/b_0$ are discussed in subsection 5.5. On the basis of the results of this and the preceding subsection it is a routine matter to plot the remaining state variables in regions (1) - (3) versus $u_{y,0}/b_0$ or any related quantity. For the sake of brevity, however, we shall merely plot the ratio $(H_{y,3}/H_x)$ versus $(u_{y,0}/a_0)$ and $(u_{y,0}/b_0)$ and, in addition, $(u_{x,3})_{esc}/b_0$ and $(u_{y,3}/b_0)$ versus $u_{y,0}/b_0$. Here, $(u_{x,3})_{esc}$ is the longitudinal " escape speed" and $u_{y,3}$ the transverse velocity at the tail of the rarefaction wave when $(u_{y,0}/b_0)$ is large enough to produce cavitation.

### 5.2 The state behind the fast shocks assuming the pressure ratio and state in front is prescribed

5.21 The switch-on shock. Let

$$\eta = \frac{p_1}{p_0} = \frac{s_1}{s_0}. \tag{5.1}$$

From (3.20) we have, on taking into account the conditions in front of the switch-on shock and the fact that the shock is forward-facing,

$$
(5.2)\quad
\begin{aligned}
&S_1 && \frac{\rho_1-\rho_0}{\rho_0} = \frac{s_0}{\gamma-1}\left[-1+\left\{1+\frac{2(\gamma-1)}{\gamma}\left(\frac{\eta-1}{s_0}\right)\right\}^{1/2}\right] \\
&S_2 && \left(\frac{H_{y,1}}{H_x}\right)^2 = 2\left(\frac{\rho_1-\rho_0}{\rho_0}\right)\left[1-\left\{\left(\frac{\gamma-1}{2}\left(\frac{\rho_1-\rho_0}{\rho_0}\right)+s_0\right\}\right] \\
&S_{3,x} && u_{x,1} = b_0\left[\sqrt{\frac{\rho_1}{\rho_0}}-\sqrt{\frac{\rho_0}{\rho_1}}\right] \\
&S_{3,y} && u_{y,1} = u_{y,0} - \left|\frac{H_{y,1}}{H_x}\right|\sqrt{\frac{\rho_0}{\rho_1}}\, b_0 \\
&S_4 && U_x = b_0\sqrt{\frac{\rho_0}{\rho_1}} = b_1
\end{aligned}
$$

whenever

$$
(5.3)\qquad \eta - 1 \leq \frac{2\gamma}{\gamma-1}\left[\frac{1}{s_0}-1\right], \quad s_0 < 1.
$$

Note that

$$
(5.4)\qquad u_{x,1} + b_1 = U_x ,
$$

that is, the characteristic Alfvén speed behind the shock is equal to the shock speed

It should be observed that the negative sign has been employed in front of the term involving the transverse magnetic field [cf. $E_{3,y}$, (3.20)]. In making this choice of sign we are anticipating the fact that the switch-on shock is followed by a rarefaction wave of the type discussed later in subsection 5.31. It will be seen that $H_y$ is positive in this rarefaction wave. In order to make a continuous connection at the head of the rarefaction wave with the state in front, $H_{y,1}$ must also be chosen positive. Equation $S_{3,y}$ is a consequence of this requirement and the fact that the shock is forward-facing.

5.22 The fast gas shock. From (3.22) we have, on taking into account the conditions in front of the shock and the fact that the fast shock is forward-facing,

(5.5)

$G_1$ $$\frac{\rho_1-\rho_0}{\rho_0} = \frac{1-\mu^2}{1+\mu^2\eta}(\eta-1); \quad \frac{\tau_0-\tau_1}{\tau_0} = \frac{1-\mu^2}{\mu^2+\eta}(\eta-1), \quad \tau = \rho^{-1}$$

$G_2$ $$H_{y,1} = H_{y,0} = 0$$

$G_{3,x}$ $$u_{x,1} = b_0(\eta-1)\left[\frac{(1-\mu^2)s_0}{\gamma(\mu^2+\eta)}\right]^{\frac{1}{2}}$$

$G_{3,y}$ $$u_{y,1} = u_{y,0}$$

$G_4$ $$U_x = b_0\left[\frac{(\mu^2+\eta)s_0}{\gamma(1-\mu^2)}\right]^{\frac{1}{2}}$$

whenever

(5.6) $$s_0 \geq 1$$

or whenever

(5.7) $$s_0 < 1 \text{ but } \eta - 1 \geq \frac{2\gamma}{\gamma-1}(s_0^{-1}-1).$$

Here

(5.8) $$\mu^2 = \frac{\gamma-1}{\gamma+1} .$$

From (3.23) we have

(5.9) $$u_{x,1} + b_1 < U_x ;$$

i.e., the Alfvén characteristic velocity behind the shock is less than the velocity of the shock front.

In the resolution of the initial discontinuity, gas shocks will be employed when $s_o \geq 1$. When $s_o < 1$, switch-on shocks or gas shocks will be employed according as $\eta - 1$ is less than or greater than the critical value $\left[2\gamma/(\gamma-1)\right](s_o^{-1}-1)$. As shown in Section 3 the state behind the switch-on shock is identical with that behind the pure gas shock when $\eta - 1 = \left[(2\gamma)/(\gamma-1)\right](s_o^{-1}-1)$, so that as $\eta - 1$ increases through the critical value the switch-on shock changes continuously into a fast pure gas shock.

### 5.3 The state in the simple wave region (Region (2)) behind the shock

5.31 The RS combination* $\left[s_o < 1;\ \eta - 1 < \left\{\frac{2\gamma}{\gamma-1}(s_o^{-1}-1)\right\}\right]$. Since the state in front of the rarefaction wave is the state behind the switch-on shock and since the rarefaction wave is forward-facing in the region $x > 0$ we have from (4.15), (4.18) and (5.2)

$$\text{RS}_1 \qquad \frac{\rho_3}{\rho_o} = \frac{\rho_1}{\rho_o}\left(\frac{s_2}{s_1}\right)^{\frac{1}{\gamma}}, \qquad 0 \leq s_2/s_1 \leq 1$$

$$\text{RS}_2 \qquad (H_{y,2}/H_x)^2 = (q_2^{-1}-1)(1-q_2 s_2), \qquad H_{y,2} \geq 0$$

$$\text{RS}_{3,x} \qquad \frac{u_{x,2}}{b_o} = \left[(\rho_1/\rho_o)^{\frac{1}{2}} - (\rho_o/\rho_1)^{\frac{1}{2}}\right] - \frac{1}{\gamma}(\rho_o/\rho_1)^{\frac{1}{2}}(s_1/s_{tr})^{\frac{1}{2}}\mathcal{K}(s_2,s_1;s_{tr})$$

$$(5.10) \qquad \text{RS}_{3,y} \qquad \frac{u_{y,2}}{b_o} = \frac{u_{y,0}}{b_o} - (\rho_o/\rho_1)^{\frac{1}{2}}\left|\frac{H_{y,1}}{H_x}\right| - \frac{(\rho_o/\rho_1)^{\frac{1}{2}}}{\gamma}\left[s_1(1-q_{cav})\right]^{\frac{1}{2}}\lambda(s_2,s_1;s_{tr})$$

$$\text{RS}_4 \qquad c_2 = b_1\left(\frac{s_1}{s_{tr}}\right)^{\frac{1}{2}}\left(\frac{q_2}{q_{tr}}\right)^{\frac{1}{2}}\left(\frac{s_2}{s_1}\right)^{\frac{\gamma-1}{2\gamma}} = b_o\left(\frac{\rho_o}{\rho_1}\right)^{\frac{1}{2}}\left(\frac{s_1}{s_{tr}}\right)^{\frac{1}{2}}\left(\frac{q_2}{q_{tr}}\right)^{\frac{1}{2}}\left(\frac{s_2}{s_1}\right)^{\frac{\gamma-1}{2\gamma}},$$

where exact and approximate expressions for $\mathcal{K}(s_2,s_1;s_{tr})$ and $\lambda(s_2,s_1;s_{tr})$ are given in Section 4 [cf. (4.19), (4.20), (4.24) and (4.35)] and where

---

* The expression " the RS-combination" should be read as " the rarefaction wave-switch-on shock combination" .

$$(5.11) \qquad \frac{\rho_1-\rho_0}{\rho_0} = \frac{s_0}{\gamma-1}\left[-1+\left\{1+\frac{2(\gamma-1)}{\gamma}\,\frac{(\eta-1)}{s_0}\right\}^{\frac{1}{2}}\right]$$

[cf. equation $S_1$, (5.2)].

At the as yet undetermined head of the simple wave, $s_2 = s_1$, $q_2 = q_1$, and

$$(5.12) \qquad (H_{y,2}/H_x)^2 = (H_{y,1}/H_x)^2 = 2\left(\frac{\rho_1-\rho_0}{\rho_0}\right)\left[(1-s_0) - \frac{\gamma-1}{2}\left(\frac{\rho_1-\rho_0}{\rho_0}\right)\right]$$

[cf. $S_2$, (5.2)]. Solving for $q_1$ in $RS_1$, (5.10), we get

$$(5.13) \qquad q_1 = \frac{(1+s_1)+(H_{y,1}/H_x)^2 - \sqrt{\left[1+s_1+(H_{y,1}/H_x)^2\right]^2 - 4s_1}}{2s_1}$$

where [see (5.1)]

$$(5.14) \qquad s_1 = \eta s_0 .$$

Assuming for the moment that $s_0$ is fixed we may regard (5.13) and (5.14) as the parametric representation of a curve in the $(q,s)$-plane, $\eta$ serving as the parameter. In Figure 13 we have plotted $s_1$ versus $q_1$ for several values of $s_0$. The points on these curves lie below the hyperbolic arc $s = q^{-1}$, $.2 \leq q \leq 1$. Only at the critical value $\eta = 1 + \frac{2\gamma}{\gamma-1}(s_0^{-1}-1)$ is $(q_1,s_1)$ a point on this arc, and by definition $\eta$ is less than this value in a switch-on shock. We are therefore led to the relation

$$(5.15) \qquad 0 \leq s_1/s_{tr} < 1$$

which, in virtue of $RS_4$, implies that

$$(5.16) \qquad c_2 < b_1 ;$$

i.e., the disturbance speed in the simple-wave region is less than the Alfvén disturbance speed behind the switch-on shock. Combining this result with that stated in (5.4) we arrive at the following relation between the velocity, $U_x$, of the shock front and the characteristic speed, $u_{x,1} + c_1$, at the head of the rarefaction wave:

$$(5.17) \qquad u_{x,1} + c_1 < u_{x,1} + b_1 = U_x .$$

Thus the rarefaction wave " follows" the switch-on shock.

It should be observed that sign $(H_{y,1})$ has been chosen positive in passing from the expression for $u_y$ in (4.18) to that given in $RS_{3,y}$. This choice of sign is made to meet the requirement that $u_{y,3}$ vanish at the tail of the rarefaction wave for all values of $u_{y,0}$ which do not exceed the minimum value necessary to produce cavitation.

5.32 The RG combination* $\left[s_o \geq 1 \text{ or } s_o < 1 \text{ but } \eta - 1 \geq \frac{2\gamma}{\gamma-1}(s_o^{-1}-1)\right]$. At the head of the rarefaction wave in the RS combination we have $q_2 = q_1$ and $s_2 = s_1$. It will be shown below that

$$(5.18) \qquad q_1 = q_{tr}, \qquad s_1 = s_{tr} = q_{tr}^{-1} .$$

From (5.5), which expresses the state behind the fast shock in terms of the ratio $\eta = p_1/p_o$ and the state in front, and from (4.15) and (4.18), which expresses the state in the simple wave region in terms of the ratio $s_2/s_{tr}$ and the state at the head, we then have

$$(5.19) \qquad \begin{array}{lll} RG_1 & \dfrac{\rho_2}{\rho_o} = \left[\dfrac{\mu^2+\eta}{1+\mu^2\eta}\right]\left(\dfrac{s}{s_{tr}}\right)^{\frac{1}{\gamma}}, & 0 \leq s/s_{tr} \leq 1 \\ RG_2 & (H_{y,2}/H_x)^2 = (q_2^{-1}-1)(1-q_2 s_2) & \end{array}$$

---

* The expression " the RG combination" should be read as " the rarefaction wave-pure gas shock combination" .

$$\mathrm{RG}_{3,x} \qquad \frac{u_{y,2}}{b_o} = (\eta \; -1)\left[\frac{(1-\mu^2)s_o}{\gamma(\mu^2+\eta)}\right]^{\frac{1}{2}} - \frac{1}{\gamma}\left[\frac{1+\mu^2\eta}{\mu^2+\eta}\right]^{\frac{1}{2}} K(s_2/s_{tr};s_{tr})$$

(5.19 cont'd)

$$\mathrm{RG}_{3,y} \qquad \frac{u_{y,2}}{b_o} = \frac{u_{y,0}}{b_o} - \frac{\left[s_{tr}(1-q_{cav})\right]^{\frac{1}{2}}}{\gamma}\left[\frac{1+\mu^2\eta}{\mu^2+\eta}\right]^{\frac{1}{2}}\lambda(s_2/s_{tr};s_{tr})$$

$$\mathrm{RG}_4 \qquad c_2 = b_1\left(\frac{q}{q_{cav}}\right)^{1/2}\left(\frac{s}{s_{tr}}\right)^{\frac{\gamma-1}{2\gamma}} = b_o\left(\frac{\rho_o}{\rho_1}\right)^{1/2}\left(\frac{q}{q_{tr}}\right)\left(\frac{s}{s_{tr}}\right)^{\frac{\gamma-1}{2\gamma}} .$$

Exact integral expressions for $K(s_2/s_{tr},s_{tr})$ and $\lambda(s_2/s_{tr},s_{tr})$, $0 \leq s_2/s_{tr} \leq 1$, may be obtained from (4.19). Approximate series expressions for these functions are given in (4.24) and (4.35). Plots of $K$ and $\lambda$ versus $s_2/s_{tr}$, based on these approximate series are given in Figures 10 and 11.

That $q_2 = q_{tr}$ and $s_2 = q_{tr}^{-1}$ at the head of the rarefaction wave is a consequence of the fact that $H_{y,1}$ vanishes behind the gas shock [cf. equation $G_2$, (5.5)]. At the head of the rarefaction wave we then conclude from $RG_2$ that $q_2 = 1$ or $q_2 = s_2^{-1}$. It is easily verified that when $q_2 = 1$, the hydromagnetic simple wave reduces to a pure gas dynamical wave. Such a simple wave cannot be employed to effect the resolution of the initial discontinuity since $u_{y,2}$ ($= u_{y,C}$) remains constant across the wave. The remaining alternative is therefore $q_2 = q_{tr}$ and $s_2 = s_{tr} = q_{tr}^{-1}$ at the head of the rarefaction wave.

From $RG_4$ we conclude that $c_2 = b_1$ at the head of the simple wave. We have therefore verified the fact that the head of the simple wave follows the fast gas shock [see (5.9)].

Note that we have again chosen sign ($H_y$) to be positive in passing from the expression for $u_y$ in (4.18) to that given in $RG_{3,y}$, (5.19). As is the case with the RS combination this choice of sign is necessitated by the requirement that $u_{y,3}$ vanish at the tail of the rarefaction wave for values of $u_{y,0}$ below the minimum value required to produce cavitation.

### 5.4 Program for establishing the dependence of $\eta (= s_1/s_o)$ on $(u_{y,0}/b_o)$ for several values of $s_o$.

5.41 Preliminary remarks. Our objective is to obtain a solution satisfying the conditions

$$(5.20) \qquad u_{x,3} = 0, \qquad u_{y,3} = 0$$

in the region of constant state behind the simple wave unless cavitation occurs in which case (5.20) is replaced by

$$(5.20') \qquad \rho_3 = 0, \qquad u_{y,3}H_x - u_{x,3}H_{y,3} = 0$$

at the tail of the rarefaction wave. We then investigate the dependence of this solution on the initial state. This initial state will be characterized by the quantities $u_{y,0}/b_o$, $\rho_o$, $b_o$, $s_o$. As an inspection of (5.10) and (5.19) reveals that it suffices to know how $\eta$ and $s_3/s_1$ depend upon $(u_{y,0}/b_o)$ and on the initial thermodynamic state $(\rho_o,b_o,s_o)$. Actually, as will soon be apparent, $\eta$ and $s_3/s_1$ depend only on $(u_{y,0}/b_o)$ and $s_o$. Consequently the amount of computation that is necessary to establish the dependence of the solution on the thermodynamic state in front is materially reduced.

The procedure for establishing the dependence of $\eta$ and $s_3/s_1$ on $(u_{y,0}/b_o)$ and $s_o$ falls naturally into two parts according as cavitation has or has not occurred. Let us first prove that cavitation always occurs when $\eta$ is large enough. For fixed $\rho_o$, $s_o$, $b_o$ let $\eta_{cav}$ be the minimum value of the ratio $s_1/s_o$ $(= p_1/p_o)$ at which cavitation occurs. For this value of $\eta$, $u_{x,3}$ still vanishes at the tail of the simple wave. Solving $RG_{3,x}$, (5.19) for $\eta_{cav}$, after first setting the left-hand side of this equation equal to zero, we obtain*

$$(5.21) \qquad \eta_{cav} = \frac{(A+2) + \sqrt{(A+2)^2 + 4(4A-1)}}{2}, \quad A = \left[K(0,s_{tr})^2/5s_o\right],$$

---

* The quantity $\eta$ is at least unity; this fact requires the use of the positive sign before the radical in (5.21).

for all $s_o$ such that

$$(5.22) \qquad \eta_{cav} - 1 \geq \frac{2\gamma}{\gamma-1} (s_o^{-1}-1).$$

Note that $K(0;s_{tr})$ versus $q_{tr} = s_{tr}^{-1}$ has been plotted in Figure 12; it should be observed that $K(0;s_{tr})$ varies only slightly with $s_{tr}$. When $s_o$ is fixed, the right-hand side of (5.21) therefore varies only slightly with $s_{tr}$. The quantity $[(s_{tr})_{cav}/s_o] = \eta_{cav}$ may then be obtained by a rapidly convergent iteration procedure. In Figure 14 we have plotted $\eta_{cav}$ versus $s_o$. This curve is intersected by the curve $\eta -1 = \left[(2\gamma)/(\gamma-1)\right](s_o^{-1}-1)$ at $s_o \cong 0.05$. When $s_o$ is below this value the expression for $\eta_{cav}$ given in (5.21) must be replaced by a similar expression which results from $SG_{3,x}$, (5.10), after setting $u_{x,2} = 0$ and solving for $\eta_{cav}$. Since, however, values of $s_o$ below .0625 will not be employed in our computations it will not be necessary to present this result here. It is nevertheless worthwhile mentioning that in this case too $\eta_{cav}$ depends only on $s_o$. Summarizing, we have shown that cavitation occurs when $\eta$ is greater than a certain minimum value, $\eta_{cav}$, that this minimum value depends only on $s_o$, and that cavitation is produced in only the RG combination even when $s_o < 1$ provided, however, that $s_o > .05$.

In the following two subsections we sketch our program for obtaining the dependence of $\eta$, $s_3/s_1$, $(u_{x,3})_{esc}/b_o$ and $(H_{y,3}/H_x)$ on $(u_{y,0}/b_o)$ for various values of the parameter $s_o$. In subsection 5.42 it is assumed that $s_o \geq 1$ or that $s_o \leq 1$ but that $\eta - 1 \geq \left[(2\gamma)/(\gamma-1)\right](s_o^{-1}-1)$ (the RG combination); in subsection 5.43 it is assumed that $s_o < 1$ and that $\eta -1 < \left[(2\gamma)/(\gamma-1)\right](s_o^{-1}-1)$ (the RS combination). When $s_o < 1$, the dependence of $\eta$, $s_3/s_1$, $(u_{x,e})_{esc}/b_o$ and $(H_{y,3}/H_x)$ on $(u_{y,0}/b_o)$ for all $u_{y,0} > 0$ is obtained by combining the results of these subsections. The results are summarized in the graphs of Figures 15-18 where we have plotted $\eta$, $s_3/s_1$, $(u_{x,3})_{esc}/b_o$ and $(H_{y,3}/H_x)$ versus $u_{y,0}/b_o$ for $s_o = .0625$, .1250, .25, .5, 1, 5, 10.

5.42 The program for the RG combination $\left[s_o \geq 1 \text{ or } s_o < 1 \text{ but } \eta - 1 \geq \frac{2\gamma}{\gamma - 1}(s_o^{-1} - 1)\right]$.

Case I: $\eta < \eta_{cav}$.

From $RG_{3,x}$ and $RG_{3,y}$ of (5.19) we have, on setting $u_{x,2}$ and $u_{y,2}$ equal to zero and writing $s_3$ ($\neq 0$) for $s_2$

$$K(s_3/s_{tr};s_{tr}) = (\eta - 1)\left[\frac{\gamma(1-\mu^2)s_o}{1+\mu^2\eta}\right]^{\frac{1}{2}} \tag{5.23}$$

$$\frac{u_{y,0}}{b_o} = \frac{1}{\gamma}\left[\frac{s_{tr}(1-q_{cav})(1+\mu^2\eta)}{\mu^2+\eta}\right]^{\frac{1}{2}} \lambda(s_3/s_{tr};s_{tr}). \tag{5.24}$$

Recall that $s_{tr} = \eta s_o$ and that $q_{cav}$ is a function of $s_{tr}$. These two equations therefore lead to relations of the form

$$R_i\left[\eta, \frac{s_3}{s_1}, \frac{u_{y,0}}{b_o}, s_o\right], \qquad i = 1, 2,$$

which do not depend on $\rho_o$ and $b_o$ explicitly. Now we assume that $s_o$ is one of the values mentioned above; our program for establishing the dependence of $\eta$, $s_3/s_1$, $(u_{x,3})_{esc}/b_o$ and $(H_{y,3}/H_x)$ on $u_{y,0}/b_o$ is the following:

(I-1): Choose several values of $\eta < \eta_{cav}$ in such a manner that $(q_{tr}, s_{tr}) = \left[\eta s_o, (\eta s_o)^{-1}\right]$ is a point of $s = q^{-1}$ and at the same a point of the plotted $s(q,q_{tr};\theta)$-curves [see Figure 6].

(a) It may happen (when $s_o$ very large or near unity) that it is impossible to do this either because $s_{tr}$ is too large to be shown on the graph or because $s_{tr} < 1.0256 = (.975)^{-1}$, that is, smaller than the smallest value of $s_{tr}$ for which $s(q,q_{tr},5)$ is plotted on the graph. Under these circumstances we employ the linear approximation to $s(q,q_{tr};5)$ noted in Section 4 [cf. (4.23)] in the program which follows. The dependence of $q_{cav}$ on $q_{tr}$ may be obtained from Figure 8.

(I-2): Compute for each value of $\eta$ chosen in I-1 the value of the expression for $K(s_3/s_{tr};s_{tr})$ in the right-hand side of (5.23). Then determine the ratio $s_3/s_{tr}$ from the plot of $K(s/s_{tr};s_{tr})$ versus $s/s_{tr}$ (Figure 10). To obtain the desired accuracy in the neighborhood of $s_3/s_{tr} \sim 0$, it proves necessary to employ suitable approximate expressions for $K(s_3/s_{tr};s_{tr})$ [cf. (4.38)] or to employ a graph with a scales that are larger than those employed here. The same is true of $\lambda(s_3/s_{tr};s_{tr})$ in the neighborhood of $s_3/s_{tr} = 0$ [see Figure 11 and (4.38)].

(I-3): Determine from Figure 11 the value of $\lambda(s_3/s_{tr};s_{tr})$ corresponding to $s_3/s_{tr}$ obtained in I-2.

(I-4): Determine $\eta$ and $s_3/s_{tr}$ as functions of $u_{y,0}/b_o$. To obtain the dependence of $\eta$ on $u_{y,0}/b_o$ it is merely necessary to compute the right-hand side of (5.21) as a function of $\eta$. This dependence is illustrated in Figure 15c.

To determine the dependence of $s_3/s_{tr}$ on $u_{y,0}/b_o$ note first that the values of $\eta$ which correspond to $s_3/s_{tr}$ may be obtained from I-2. The dependence of $s_3/s_{tr}$ on $u_{y,0}/b_o$ then follows from the relation of $\eta$ to $u_{y,0}/b_o$ just established.

(I-5): Determine $(H_{y,3}/H_x)$ as a function of $u_{y,0}/b_o$. Note first that $(H_{y,3}/H_x) = [(q_3^{-1}-1)(1-q_3 s_3)]^{1/2}$ at the tail of the rarefaction wave and hence throughout Region (3). In Figure 7 we have plotted $(H_y/H_x) = [(q^{-1}-1)(1-q_3 s_3)]^{1/2}$ for various values of $q_{tr}$ $(= s_{tr}^{-1})$. Since $s_3/s_{tr}$ is known, $(H_{y,3}/H_x)$ may be obtained from this graph. When $s_{tr}$ is very large or close to unity, Figure 7 no longer supplies the necessary information. In this case we employ the linear approximation to $s(q,q_{tr};5)$ [see (4.23)] in conjunction with the formula for $(H_{y,3}/H_x)$ just mentioned and compute $(H_{y,3}/H_x)$. The results are summarized in the graphs of Figure 17b.

Case II: $\eta > \eta_{cav}$.

In this case we set $s_2$ equal to zero in (5.19) $RG_{3,x}$ and $RG_{3,y}$ and employ the second relation of (5.20') to get for $\eta > \eta_{cav}$:

$$(5.25) \qquad \frac{(u_{x,3})_{esc}}{b_o} = \left[(\eta - 1)\left\{\frac{(1-\mu^2)s_o}{\gamma(\mu^2+\eta)}\right\}^{1/2} - \frac{1}{\gamma}\left\{\frac{1+\mu^2\eta}{\mu^2+\eta}\right\}^{1/2} K(0,s_{tr})\right]$$

$$(5.26) \qquad \frac{u_{y,0}}{b_o} = \frac{1}{\gamma}\left\{\frac{s_{tr}(1-q_{cav})(1+\mu^2\eta)}{\mu^2+\eta}\right\}^{1/2} \lambda(0;s_{tr}) + \frac{H_{y,3}}{H_x}(u_{x,3})_{esc}$$

$$(5.26') \qquad \frac{u_{y,3}}{b_o} = \frac{u_{y,0}}{b_o} - \frac{1}{\gamma}\left\{\frac{s_{tr}(1-q_{cav})(1+\mu\eta)}{\mu^2+\eta}\right\}^{1/2} \lambda(0,s_{tr}).$$

Here the ratio $(H_{y,3}/H_x)$ at the tail of the rarefaction wave is given by the expression [see (5.19), $RG_2$; take $s_2 = 0$]

$$(5.27) \qquad H_{y,3}/H_x = \sqrt{q_3^{-1}(1-q_3)}\,, \qquad q_3 = q_{cav}\,.$$

Assuming $s_o$ is one of the values employed in Case I above we proceed in accordance with the following recipe:

(II-1): Obtain the value of $\lambda(C;s_{tr})$ for each $s_{tr} = q_{tr}^{-1} = \eta s_o$ from Figure 12 for several values of $\eta > \eta_{cav}$.

(II-2): Obtain for each $q_{tr} = s_{tr}^{-1}$ the corresponding $q_{cav} = q_3$ from Figure 8 and compute the ratio $(H_{y,3}/H_x)$ by means of (5.27).

(II-3): Obtain the value of $K(0;s_{tr})$ from Figure 12 for each $s_{tr} = \eta s_o$ and then compute the right-hand side of (5.25) for each $\eta$ employed above thereby determining the dependence of $(u_{x,3})_{esc}/b_o$ on $\eta$.

(II-4): Utilize the information in II-1 - II-3 and compute the right-hand side of (5.26) thereby determining the dependence of $\eta$ on $(u_{y,0}/b_o)$. Graphs of the relationship between $\eta$ and $(u_{y,o}/b_o)$ for several values of the parameter $s_o$ appear in Figure 15c.

(II-5): Determine the dependence of $(H_{y,3}/H_x)$ on $(u_{y,0}/b_o)$ by combining the results of II-4 and II-2. Graphs of the relationship between $(H_{y,3}/H_x)$ and $(u_{y,0}/b_o)$ for several values of the parameter $\varepsilon_o$ appear in Figure 17b.

(II-6): Determine the dependence of $(u_{x,3})_{esc}/b_o$ and $(u_{y,3}/b_o)$ on $(u_{y,0}/b_o)$. Employ the information obtained in II-3 and II-4. Graphs of $(u_{x,3})_{esc}/b_o$ and $(u_{y,3}/b_o)$ versus $u_{y,0}/b_o$ are given in Figure 18.

5.43 The program for the RS combination $\left[\eta < 1 + \frac{2\gamma}{\gamma-1}(s_o^{-1}-1);\ .0625 \leq s_o < 1\right]$. In the following it will be assumed that $1 > s_o \geq .0625$. Under these circumstances.

(5.28) $$\eta \leq 1 + \frac{2\gamma}{\gamma-1}(s_o^{-1}-1) < \eta_{cav},$$

(see subsection 5.41).

Now from $RS_{3,x}$ and $RS_{3,y}$ of (4.24) we have, on setting $u_{x,2}$ and $u_{y,2}$ equal to zero,

(5.29) $$K(s_3, s_{tr}; s_{tr}) = \gamma(s_{tr}/s_1)^{1/2}\left(\frac{\rho_1-\rho_o}{\rho_o}\right)$$

(5.30) $$\frac{u_{y,0}}{b_o} = \left(\frac{\rho_o}{\rho_1}\right)^{\frac{1}{2}}\left|\frac{H_{y,1}}{H_x}\right| + \frac{\sqrt{s_1}}{\gamma}\left(\frac{\rho_o}{\rho_1}\right)^{\frac{1}{2}}(1-q_{cav})^{\frac{1}{2}}\lambda(s_3/s_1; s_{tr}).$$

Assuming $s_o$ fixed*, we may establish the dependence of $\eta$, $(s_3/s_1)$ and $H_{y,3}/H_x$ on $(u_{y,0}/b_o)$ by proceeding in accordance with the following prescription.

(I-1): Choose $\eta$, $1 \leq \eta \leq 1 + \frac{2\gamma}{\gamma-1}(s_o^{-1}-1)$, such that the point $(q_1, s_1) = (q_1, \eta s_o)$ is a point of intersection of an $s(q, q_{tr}; 5)$-curve and the curve whose parametric equations are given in (5.13) and (5.14). Each such point may be obtained graphically from Figure 13 or an enlarged version of it.

---

* In our computations we chose $s_o$ to be .5, .250, .125 and .0625.

(I-2): Obtain $q_{tr}$ and $q_{csv}$ corresponding to $(q_1, s_1)$ from Figure 13.

(I-3): For each $s_1$ determine $(\rho_1-\rho_o)/\rho_o$ from Figure 4.

(I-4): Compute the right-hand side of (5.29) and then find $s_3/s_1$ from the plot of $\mathcal{K}(s_3/s_1;s_{tr})$ versus $s_3/s_1$. (These curves are not given here; they may be obtained from the $\mathcal{K}(s_3/s_1;s_{tr})$-curves of Figure 10 by making use of (4.20).)

(I-5): Determine the value of $\lambda(s_3,s_1;s_{tr})$ from the $\lambda(s_3,s_1;s_{tr})$ versus $s_3/s_1$-curves. (These curves are not given here; they may be obtained from the $\lambda(s_3/s_{tr};s_{tr})$-curves of Figure 11 by making use of (4.20).)

(I-6): For each $s_1$ $(= \eta\, s_o)$ determine $H_{y,1}/H_x$ from Figure 5.

(I-7): Compute the right-hand side of (5.30), for each value of $\eta$ employed in the previous steps and obtain in this manner the dependence of $\eta$ on $u_{y,0}/b_o$, $1 \leq \eta \leq \eta_{crit} = 1 + \frac{2\gamma}{\gamma-1}(s_o^{-1}-1)$. In order to keep the diagram uncluttered, the $\eta$-versus $(u_{y,0}/b_o)$-curves in this region have been omitted in Figure 15c. However, these curves may be obtained from Figure 15b, where we have plotted the corresponding $\eta$ versus $u_{y,0}/a_o = u_{y,0}/b_o\sqrt{s_o}$ -curves.

(I-8): Compute $H_{y,3}/H_x = \left[(q_3^{-1}-1)(1-q_3 s_3)\right]$. Note that the value of $s_3/s_1$ is known from I-4. Compute $s_3 = (s_3/s_1)s_1$ and determine $q_3$ from the appropriate $s(q,q_{tr};5)$-curve in Figure 13 [see I-2].

(I-9): Determine the dependence of $(s_3/s_1)$ on $(u_{y,0}/b_o)$ by plotting the values of $(s_3/s_1)$ obtained in I-4 versus the values $(u_{y,0}/b_o)$ obtained in I-7 [see Figure 16].

(I-10): Determine the dependence of $(H_{y,3}/H_x)$ on $u_{y,0}/b_o$, $0 \leq (u_{y,0}/b_o) \leq (u_{y,0})_{crit}/b_o$, by combining the results of I-8 and I-9 [see Figure 17b].

### 5.5 Approximate expressions for $\eta$, $s_3/s_1$ and $(H_{y,3}/H_x)$

5.51 Approximate expressions for $\eta$, $(H_{y,3}/H_x)$ when $(u_{y,0}/b_o)$ is very large. Let us choose $u_{y,0}/b_o$ so large that for the corresponding $\eta$ we have

$$\eta \gg \eta_{cav} > 1, \quad \text{whenever } s_o \geq .05 \tag{5.31}$$

or

$$\eta \gg \eta_{crit} = 1 + \frac{2\gamma}{\gamma-1}(s_o^{-1}-1) \geq \eta_{cav} > 1, \quad \text{whenever } s_o < .05. \tag{5.32}$$

In both cases, as we have shown in subsection 5.41, the resolution of the shear flow discontinuity is effected by an RG combination. For fixed $s_o$ we may assume, since $\eta$ is very large compared with unity, that

$$s_{tr} = \eta\, s_o \gg 1 \tag{5.33}$$

and consequently that [cf. (4.28)]

$$q_{cav} \cong \frac{\theta}{\theta+1}\, q_{tr} \cong \frac{\theta}{\theta+1}\, \frac{1}{s_{tr}} \cong 0 \quad . \tag{5.34}$$

Since $\eta$ exceeds $\eta_{cav}$, the quantity $s_3$ vanishes at the tail of the rarefaction wave and hence, as already noted in (5.27),

$$(H_{y,3}/H_x) = \left[(1-q_{cav})q_{cav}^{-1}\right]^{1/2} .$$

Employing (5.34) we then conclude that

$$(H_{y,3}/H_x) \cong \left(\frac{\theta+1}{\theta}\right)^{1/2} s_{tr}^{1/2} = \left(\frac{\theta+1}{\theta}\right)^{1/2} (\eta\, s_o)^{1/2} . \tag{5.35}$$

Neglecting lower order terms we have from (5.20), (5.21) and (5.35)

$$\frac{u_{y,0}}{b_o} \cong \frac{H_{y,3}}{H_x} (u_{x,3})_{esc}$$

$$\frac{(u_{x,3})_{esc}}{b_o} \cong \left\{ \frac{1-\mu^2}{\gamma} \right\}^{1/2} (\eta \ s_o)^{1/2} .$$

Consequently, we may conclude, since $\theta = \gamma/(2-\gamma)$, $\mu = (\gamma-1)/(\gamma+1)$, that

(5.36) $$\eta s_o \cong \frac{\gamma}{2} (1+\gamma)^{1/2} \left( \frac{u_{y,0}}{b_o} \right)$$

(5.37) $$\frac{H_{y,3}}{H_x} \cong (1+\gamma)^{1/4} \left( \frac{u_{y,0}}{b_o} \right)^{1/2}$$

(5.38) $$\frac{(u_{x,3})_{esc}}{b_o} \cong \frac{1}{(1+\gamma)^{1/4}} \left( \frac{u_{y,0}}{b_o} \right)^{1/2} .$$

Moreover, since

$$u_{y,3} = \frac{H_{y,3}}{H_x} (u_{x,3})_{esc}$$

at the tail of the rarefaction wave we have,

(5.38') $$\frac{u_{y,3}}{b_o} \cong \frac{u_{y,0}}{b_o} .$$

When the adiabatic exponent $\gamma$ is taken to be 5/3 we find

(5.36') $$\eta s_o \cong 1.36 \left( \frac{u_{y,0}}{b_o} \right),$$

(5.37') $$\frac{H_{y,3}}{H_x} \cong 1.27 \left( \frac{u_{y,0}}{b_o} \right)^{1/2} ,$$

(5.38') $$\frac{(u_{x,3})_{esc}}{b_o} \cong .787 \left( \frac{u_{y,0}}{b_o} \right)^{1/2} .$$

The relation (5.37') replaces the incorrect result for a monotonic gas given in [7], [see pp. 49-50].

### 5.52 Approximate expressions for $\eta$, $s_3/s_{tr}$ and $(H_{y,3}/H_x)$ when $(u_{y,0}/b_o)$ is small.

Case I: $s_o \geq 1$ (the RG combination)

When $s_o \geq 1$, the resolution of the initial discontinuity is effected by the RS combination. Assuming $\eta - 1$ is small we have from (5.23) and (5.24), on neglecting terms involving higher powers of $(\eta - 1)$,

$$K(s_3/s_{tr}; s_{tr}) \cong (\eta - 1)(s_o)^{1/2} \tag{5.39}$$

$$\frac{u_{y,0}}{b_o} \cong \frac{1}{\gamma}\left[s_o(1-q_{cav})\right]^{1/2} \lambda(s_3/s_{tr}; s_{tr}). \tag{5.40}$$

Since

$$s_3/s_{tr} \cong 1 \tag{5.41}$$

when $\eta - 1$ and $(u_{y,0}/b_o)$ are small [see Figures 15 and 16], the relations (5.39) and (5.40) become, in virtue of (4.40) and (4.41),

$$\left[1 - (s_3/s_{tr})\right] \cong (\eta - 1)(s_o)^{1/2} \tag{5.42}$$

$$\left(\frac{u_{y,0}}{b_o}\right) \cong \left[\frac{2s_o(1-q_{tr})}{\gamma}\right]^{1/2} \left[1-(s/s_{tr})\right]^{1/2} . \tag{5.43}$$

Now

$$1-q_{tr} \cong 1-(\eta s_o)^{-1}\left[(\eta - 1)s_o + (s_o - 1)\right] / s_o .$$

Consequently

$$\left(\frac{u_{y,0}}{b_o}\right) \cong \left[\frac{2\left\{(\eta - 1)s_o + (s_o - 1)\right\}}{\gamma}\right]^{1/2} \left[1-(s/s_{tr})\right]^{1/2} . \tag{5.43'}$$

Equations (5.42) and (5.43') when solved for $(\eta - 1)$ and $\left[1-(s_3/s_{tr})\right]$ yield the following results

$$(5.44) \qquad \eta - 1 \cong \frac{1}{2}\left(\frac{s_c - 1}{s_o}\right)\left[-1 + \left\{1 + \frac{2\gamma s_o^{1/2}}{(s_o-1)^2}\left(\frac{u_{y,0}}{b_o}\right)^2\right\}^{1/2}\right],$$

$$(5.45) \qquad \left[1-(s_3/s_{tr})\right] \cong \frac{1}{2}\left(\frac{s_o - 1}{s_o^{1/2}}\right)\left[-1 + \left\{1 + \frac{2\gamma s_o^{1/2}}{(s_o-1)^2}\left(\frac{u_{y,0}}{b_o}\right)^2\right\}^{1/2}\right].$$

When $s_o > 1$ and $(u_{y,0}/b_o)$ is sufficiently small we get

$$(5.46) \qquad \eta \cong 1 + \frac{\gamma}{2s_o^{1/2}(s_o-1)}\left(\frac{u_{y,0}}{b_o}\right)^2$$

$$(5.47) \qquad s_3/s_{tr} \cong 1 - \frac{\gamma}{2(s_o-1)}\left(\frac{u_{y,0}}{b_o}\right)^2, \qquad s_o > 1.$$

On the other hand, when $s_o$ is unity we have

$$(5.48) \qquad \eta \cong 1 + \left(\frac{\gamma}{2}\right)^{1/2}\left(\frac{u_{y,0}}{b_o}\right)$$

$$(5.49) \qquad s_3/s_{tr} \cong 1 - \left(\frac{\gamma}{2}\right)^{1/2}\left(\frac{u_{y,0}}{b_o}\right).$$

Now since $s_3 \sim s_{tr}$ we must have $q_3 \sim q_{tr}$. Employing this fact and (4.41), we obtain for $(H_{y,3}/H_x)$ [cf. $RG_2$, (5.19)]

$$(H_{y,3}/H_x) \cong \left[\frac{2}{\gamma}(s_{tr}-1)\right]^{1/2}\left[1-(s/s_{tr})\right]^{1/2}.$$

Comparing this expression with that for $(u_{y,0}/b_o)$ in (5.43) and noting that $s_o(1-q_{tr}) = \left[s_o(s_{tr}-1)/\eta\, s_o\right] \sim (s_{tr}-1)$, we have finally

$$(5.50) \qquad (H_{y,3}/H_x) \cong (u_{y,0}/b_o),$$

(cf. [7], p. 50).

Case II: $s_o < 1$ (the RS combination)

When $s_o < 1$, the resolution is effected by an RS combination. Now when $\eta - 1$ is sufficiently small $S_1$ and $S_2$ of (5.2) become

$$\frac{\rho_1 - \rho_o}{\rho_o} \cong \frac{\eta - 1}{\gamma}, \qquad \eta - 1 \cong 0 \tag{5.51}$$

$$\left(\frac{H_{y,1}}{H_x}\right)^2 \cong \frac{2(\rho_1 - \rho_o)}{\rho_o}(1 - s_o) = \frac{2(1 - s_o)}{\gamma}(\eta - 1), \quad \eta - 1 \cong 0. \tag{5.52}$$

Moreover, when

$$s_1 = \eta s_o < 1 \tag{5.53}$$

and

$$s \cong s_1 \tag{5.54}$$

the expressions for $K(s_3/s_1;s_{tr})$ and $\lambda(s_3/s_1;s_{tr})$ may be approximated as follows:

$$K(s_3,s_1;s_{tr}) = \int_s^{s_1} (q/q_{tr})^{1/2} \left(\frac{s}{s_1}\right)^{-\frac{4}{5}} d\left(\frac{s}{s_1}\right) \cong (q_1/q_{tr})^{1/2}\left[1 - (s_3/s_1)\right] \tag{5.55}$$

$$\begin{aligned} \lambda(s_3,s_1;s_{tr}) &= \int_s^{s_1} \left[\frac{(1-q)/(1-q_{cav})}{1 - qs}\right]^{\frac{1}{2}} \left(\frac{s}{s_1}\right)^{-\frac{4}{5}} d\left(\frac{s}{s_1}\right) \\ &\cong \left[\frac{(1-q_1)/(1-q_{cav})}{1-q_1 s_1}\right]^{\frac{1}{2}} \left[1 - (s_3/s_1)\right]. \end{aligned} \tag{5.56}$$

Therefore when $\eta - 1$ is sufficiently small we have from (5.29), (5.30) and (5.51), (5.52)

$$\left[1 - (s_3/s_1)\right] \cong (s_1 q_1)^{-1/2}(\eta - 1) \tag{5.57}$$

$$(5.58)\qquad \frac{u_{y,0}}{b_o} \cong \left[\frac{2(1-s_o)(\eta-1)}{\gamma}\right]^{\frac{1}{2}} - \frac{\sqrt{s_o}}{\gamma}\left[\frac{1-q_1}{1-q_1 s_1}\right]^{\frac{1}{2}}\left[1-(s_3/s_1)\right]$$

where [cf. (5.13)]

$$(5.59)\qquad q_1 = \frac{(1+s_1)+(H_{y,1}/H_x)^2 - \left[(1-s_1)^2+s(1+s_1)(H_{y,1}/H_x)^2 + O\left\{(H_{y,1}/H_x)^4\right\}\right]^{1/2}}{2} .$$

Neglecting the term $O\left\{(H_{y,1}/H_x)^4\right\}$ and assuming, in addition, that the ratio of the second and the first term in the braces is small compared with unity, we conclude that

$$(5.60)\qquad q_1 \cong \left[1 - \frac{2}{\gamma}(\eta - 1)\right], \qquad \eta - 1 \sim 0$$

or

$$(5.60')\qquad 1 - q_1 \cong \frac{2}{\gamma}(\eta - 1), \qquad \eta - 1 \sim 0.$$

Substituting this expression for $(1-q_1)$ and the expression for $\left[1-(s_3/s_1)\right]$ given in (5.57) into (5.58) we get

$$(5.61)\qquad \frac{u_{y,0}}{b_o} \cong \left[\frac{2(1-s_o)}{\gamma}\right](\eta-1)^{\frac{1}{2}} - \frac{1}{\gamma}\left[\frac{2}{\gamma(1-s_o)}\right]^{\frac{1}{2}}\left[(\eta-1)^{\frac{1}{2}}\right]^2 .$$

As a result we have, on solving for $(\eta-1)^{1/2}$,

$$(5.62)\qquad (\eta-1)^{\frac{1}{2}} \cong \frac{\gamma(1-s_o)}{2}\left[1 - \left\{1 - 4\left(\frac{\gamma}{2}\right)^{\frac{1}{2}}\frac{1}{\gamma(1-s_o)^{3/2}}\left(\frac{u_{y,0}}{b_o}\right)\right\}^{\frac{1}{2}}\right] .$$

Assuming, the second term in the brace is small compared with unity, we get

$$(5.63)\qquad \eta \cong 1 + \frac{\gamma}{2(1-s_o)}\left(\frac{u_{y,0}}{b_o}\right)^2, \qquad \frac{u_{y,0}}{b_o} \simeq 0$$

and, in addition,

(5.64) $$s_3/s_1 \cong 1 - \frac{\gamma}{2s_o^{1/2}(1-s_o)} \left(\frac{u_{y,0}}{b_o}\right)^2, \quad \frac{u_{y,0}}{b_o} \sim 0.$$

Now the ratio $(H_{y,3}/H_x) = \left[(q_3^{-1}-1)(1-q_3s_3)\right]^{1/2}$ at the tail of the rarefaction wave is effectively $(H_{y,1}/H_x)$, since $q_3 \cong q_1$ and $s_3 \cong s_1$. Consequently, we have from (5.63) and (5.52)

(5.65) $$\left(\frac{H_{y,3}}{H_x}\right) \cong \left(\frac{H_{y,1}}{H_x}\right) \simeq \frac{u_{y,0}}{b_o}$$

(see [7], p. 50).

## 6. Interpretation of the results

### 6.1 Introductory remarks

On the basis of the results of the preceding section we are in a position to obtain a complete description of the motion. More explicitly, by choosing successively greater values of time, t, we could obtain a picture of how the various disturbances propagate away from the initial discontinuity [see for example Figure 3], and by varying the parameters which characterize the state in front of the shocks we could establish quantitatively the dependence of the solution in each of the flow regions on the state of flow in the undisturbed medium. To carry out such a program adequately would, however, be beyond the scope of this report. We shall instead limit ourselves to discussing certain general features of the motion. Attention will be focused exclusively on the character of the motion in the region behind the shock and in the region at the tail of the simple wave.

Let us recall some of the notations and conventions employed in the preceding sections. First, in view of the symmetry of the motion, there is no loss in generality in limiting our considerations to the motion along the positive x-axis. In Figure 3a we have depicted the basic flow regions in the positive half of the (x,t)-plane. These basic flow regions are: Region (0), the region of constant state in front of the (forward-facing) shock; Region (1), the region of constant state behind the shock; Region (2), the flow region of the slow, centered, forward-facing rarefaction wave; Region (3), the region of constant state following the tail of the forward-facing simple wave. The state in Region j, $j = 0, 1, 2, 3$ is characterized by the quantities $\rho_j$, $b_j \left[= (\mu H_x^2 \rho_j^{-1})^{1/2}\right]$, $s_j \left[= (a_j/b_j)^2 = \gamma p_j/\mu H_x^2\right]$, $(H_{y,j}/H_x)$, $u_{x,j}/b_j$ (or $u_{x,j}/a_j$) and $u_{y,j}/b_j$ (or $u_{y,j}/a_j$). Here, in Region (j), $\rho_j$ is the density; $b_j$ the Alfvén disturbance speed; $s_j$ the square ratio of the sound speed $a_j$ to the Alfvén disturbance speed $b_j$; $H_{y,j}$ and $u_{y,j}$ the components of magnetic field and fluid velocity respectively, transverse to the x-axis; and $u_{x,j}$ the longitudinal component of the fluid velocity. In addition, $H_x$ is the fixed longitudinal magnetic field, $\mu$ the magnetic specific inductive capacity, and $\gamma$ the adiabatic exponent*. In terms of these notations our chief objective may be expressed as follows: To find in Regions (1) and (3) qualitative information about the dependence of the solution on (i) the ratio $u_{y,0}/a_o$ for fixed $s_o$, and on (ii) $s_o(= \gamma p_o/\mu H_x^2)$ for fixed $u_{y,0}/a_o$ or for fixed $u_{y,0}/b_o$, according as $s_o$ is made to vary by varying $H_x$ or $p_o$. It will be recalled that $u_{y,0}$ is half the magnitude of the initial discontinuity in the transverse velocity. It should be emphasized that the corresponding information could easily be obtained for the simple wave region, Region (2), but for the sake of brevity we shall not do so.

### 6.2 Some general features of the solution in Region (1), behind the shock

The dependence of the state in Region (1), behind the shock, on $s_o$ and $u_{y,0}/a_o$ or any equivalent set of parameters may be obtained, as we have already observed in Section 5, from the knowledge of how the shock strength $\eta = p_1/p_o$, that is, the ratio of the pressure $p_1$ behind to $p_o$ in front of the shock, depends on these parameters. As is perhaps to be expected, the dependence of $\eta$ on these parameters may differ according as the resolution is effected by a gas shock or a switch-on shock or, stated analytically, according as

(6.1) $$s_o \geq 1 \quad \text{or} \quad s_o < 1 \quad \text{but} \quad \eta \geq \eta_{crit}$$

or

(6.2) $$s_o < 1, \quad \text{but} \quad \eta < \eta_{crit} .$$

It will be recalled that

---

* It should be recalled that all graphical results are based on the choice of $\gamma = 5/3$ for the adiabatic exponent.

$$(6.3)\qquad \eta_{crit} = 1 + \frac{2\gamma}{\gamma-1}\,(s_o^{-1}-1), \qquad s_o < 1,$$

is that value of the shock strength above which the switch-on shock reduces to a pure gas shock. In the following we shall treat these two cases separately.

6.21 Some general features of the solution in Region (1) behind the pure gas shock. Here, in accordance with (6.1), we assume that $s_o \geq 1$ or $s_o < 1$ but $\eta \geq \eta_{crit}$. Consider Figure 15a, where we have plotted $p_1/p_o = \eta = \eta\,[u_{y,0}/a_o, s_o]$ versus $u_{y,0}/a_o$ for several values of the parameter $s_o$. For values of $s_o < 1$ we have plotted only those portions of the $\eta$ versus $u_{y,0}/a_o$-curves which correspond to values of $\eta$ which are greater than $\eta_{crit}$. From the figure we conclude that for fixed $s_o$ the shock strength $\eta$ increases monotonically with $u_{y,0}/a_o$. In addition, as we have shown in Section 5, (5.36), (5.46) and (5.63),

$$(6.4)\qquad \eta \cong 1 + \frac{\gamma s_o^{1/2}}{2(s_o-1)}\left(\frac{u_{y,0}}{a_o}\right)^2, \qquad \frac{u_{y,0}}{a_o} \to 0, \qquad s_o > 1$$

$$(6.4')\qquad \eta \cong 1 + \left(\frac{\gamma}{2}\right)^{1/2}\left(\frac{u_{y,0}}{a_o}\right), \qquad \frac{u_{y,0}}{a_o} \to 0, \qquad s_o = 1$$

$$(6.5)\qquad \eta \cong \frac{\gamma}{2}\left(\frac{1+\gamma}{s_o}\right)^{1/2}\frac{u_{y,0}}{a_o}, \qquad \frac{u_{y,0}}{a_o} \to \infty, \qquad s_o > 0.$$

Since $(\rho_1-\rho_o)/\rho_o$, $u_{x,1}/a_o$, and $U_x/a_o$ increase with increasing $\eta$ [cf. $G_1$, $G_3$, $G_4$, (5.5)] we may conclude, moreover, that these quantities increase with increasing $u_{y,0}/a_o$, assuming $s_o$ is fixed. Both $u_{x,1}/a_o$ and $U_x/a_o$ approach infinity with $u_{y,0}/a_o$ while $(\rho_1-\rho_o)/\rho_o$ approaches the constant value $(1-\mu^2)\mu^2 = 3$ (when $\gamma = 5/3$) as $u_{y,0}/a_o$ approaches infinity. The transverse velocity is continuous across a gas shock [see $G_{3,y}$, (5.5)] while the transverse magnetic field vanishes on both sides of the shock front.

Thus, if the values of the sound and the Alfvén disturbance speeds in front of the pure gas shock are held fixed, the values of the shock strength, the excess density ratio, the speed of the shock front, and of the components of fluid velocity behind the shock vary in the same sense as the magnitude $2u_{y,0}$ of the initial shear flow discontinuity.

Now let us fix $u_{y,0}$, the pressure $p_o$, and the sound speed in front of the gas shock and vary $H_x$. Assume, in particular, that

$$(6.6) \qquad \hat{H}_x > H_x .$$

Then the ratio $u_{y,0}/a_o$ is fixed but the quantity $s_o$ varies, i.e.,

$$(6.7) \qquad \hat{s}_o = \gamma p_o/\mu \hat{H}_x^2 < s_o = \gamma p_o/\mu H_x^2 .$$

If now $f = f\left[(u_{y,0}/a_o), s_o\right]$ is any function of $(u_{y,0}/a_o)$ and $s_o$, let $\hat{f}$ denote the value $f\left[(u_{y,0}/a_o), \hat{s}_o\right]$. Then from Figure 15a and from $G_1$, $G_3$ and $G_5$, (5.5) we conclude that*

$$(6.8) \qquad \begin{gathered} \hat{\eta} > \eta , \qquad \widehat{\left(\frac{\rho_1-\rho_o}{\rho_o}\right)} > \left(\frac{\rho_1-\rho_o}{\rho_o}\right) \\ \hat{u}_{x,1} > u_{x,1}, \qquad \hat{U}_{x,1} > U_{x,1} . \end{gathered}$$

Thus, if the magnitude of the initial shear flow discontinuity and the values of the pressure and the density in front of the gas shock are held fixed, then the values of the shock strength, the excess density ratio, the shock speed and the longitudinal component of particle velocity behind the shock vary in the same sense as the (fixed) longitudinal component $H_x$ of the magnetic field, and hence in the opposite sense to the square ratio $s_o$ of the sound speed to the Alfven disturbance speed in front of the shock.

In Figure 15c we have plotted $\eta = \eta\left[u_{y,0}/b_o, s_o\right]$ versus $u_{y,0}/b_o$ for several values of $s_o$. As in Figure 15a, the portions of the curves corresponding to $s_o < 1$ and lying below the critical value have been omitted. Employing this figure and $G_1$, (5.5) and proceeding in the above manner we conclude that if the magnitude of the initial shear flow discontinuity and the values of the longitudinal magnetic field and the density in front of the gas shock are held fixed, then the shock strength and the excess density ratio increase as the pressure in front of the shock decreases and hence as the square ratio $s_o$ of the sound speed to the Alfvén disturbance speed in front of the shock decreases.

---

* It is assumed, of course, that the $\hat{\eta} = \eta(\hat{s}_o)$ and $\eta = \eta(s_o)$ are both greater than critical values corresponding to $\hat{s}_o$ and $s_o$.

Unlike the previous case, the qualitative dependence of $u_{x,1}$ and $U_{x,1}$ on $p_o$ and $u_{y,0}/b_o$ is not immediately revealed by $G_{3,x}$ and $G_5$, (5.5). This dependence could of course be established graphically, but we shall not do so here.

It was stated in Section 1 that the motion of the medium differs radically from the corresponding steady-state gas dynamical shear flow motion even when $H_x$ is small, if the magnitude of the initial shear flow discontinuity is large enough. This statement follows from the fact that the value, $2(u_{y,0})_{cav}$, of the initial discontinuity at which cavitation occurs remains finite as $H_x$ approaches zero and hence as $s_o$ vanishes; all other parameters are assumed fixed. Actually, $(u_{y,0})_{cav}/a_o$ approaches the value 3.67 as $s_o$ approaches infinity, a fact which may be inferred from an inspection of Figure 15a. Clearly then, in contrast to the corresponding gas dynamical situation where the motion is steady and purely transverse, the resolution of the shear flow discontinuity involves a longitudinal motion which results in cavitation even for very small $H_x$ if $u_{y,0}/a_o$ is somewhat larger than the value 3.67.

The radical difference between the gas dynamical motion, which may be regarded as a hydromagnetic motion in the absence of magnetic fields, and the hydromagnetic motion considered here could perhaps have been anticipated from our discussion of the shear flow layer in subsection 2.4. We showed there that the force per unit volume $\bar{f}$, within the layer, is given by the expression $-\mu H_x^2\left(\frac{\partial u_y}{\partial x}\right)\left(\frac{\partial^2 u_y}{\partial x^2}\right) t^2 \bar{x}_o$, where t, the time, is sufficiently small. Clearly, no matter how small $H_x$ is taken, it is possible to make $\Gamma$ as large as one pleases by making the $\partial u_y/\partial x$ large enough. This may be accomplished by making the difference, $2u_{y,0}$, of $u_y$ at the right and the left side of the shear flow layer large enough. Thus, by making $u_{y,0}$ large enough one might expect to produce a large-scale longitudinal motion and perhaps even cavitation, as long as $H_x$ does not vanish altogether.

6.22 Some general features of the motion in Region (1) behind the switch-on shock. In accordance with (6.1) we assume here that $s_o < 1$ and $\eta \leq \eta_{crit}$. In Figure 15b we have plotted $\eta = \eta\left[(u_{y,0}/a_o), s_o\right]$ versus $(u_{y,0}/a_o)$ for several values of parameter $s_o$ less than unity and for $(u_{y,0}/a_o)$ in the range $0 \leq u_{y,0}/a_o \leq (u_{y,0})_{crit}/a_o$. Here, $(u_{y,0})_{crit}$ is, for fixed $s_o$, the value of $u_{y,0}$ when $\eta = \eta_{crit}$. When $u_{y,0}$ is small we have [cf. (5.63)]

$$\eta \cong 1 + \frac{\gamma s_o}{2(1-s_o)}\left(\frac{u_{y,0}}{a_o}\right)^2 . \tag{6.9}$$

From Figure 15b and $S_1$, $S_{3,x}$ and $S_4$, (5.2) we deduce the following facts. If the values of the sound and the Alfvén disturbance speeds in front of the switch-on shock are held fixed, then the shock strength, the excess density ratio, and the longitudinal component of the particle velocity behind the shock are monotonically increasing functions of the magnitude of the initial discontinuity in the transverse velocity, whereas the speed of the shock front decreases monotonically as this magnitude increases. Furthermore, if the magnitude of the initial discontinuity, $2u_{y,0}$, and the values of the pressure and the density in front of the switch-on shock are held fixed, then the shock strength, the excess density ratio*, the longitudinal component of fluid velocity behind the shock, and the speed of the shock front increase with decreasing $H_x$ and hence with increasing $s_o$.

It should be observed that in a pure gas shock the variation of $\eta$, $(\rho_1-\rho_o)/\rho_o$, $u_{x,1}$, and $U_x$ with $H_x$ for fixed $u_{y,0}$ and $a_o$ is opposite to the variation of the corresponding quantities in a switch-on shock [see subsection 6.21]. In addition, whereas $u_{y,1} = u_{y,0}$ and $H_{y,1} = 0$ behind the pure gas shock, in the present case $u_{y,1}$ and $H_{y,1}$ differ from the corresponding values in front of the shock and moreover depend on $H_x$. The nature of this dependence could be obtained from $S_2$ and $S_{3,y}$, (5.2), and Figures 4,5, and 15b; however we shall not include these considerations here.

---

* The dependence of $(\rho_1-\rho_o)/\rho_o$ on $s_o$ was established graphically.

If we were to superimpose Figures 15a and 15b, the family of curves corresponding to values of $s_o \geq 1$ would intersect those corresponding to values of $s_o < 1$. It is therefore not possible to make any general statement regarding the behavior of the entire family of curves which would be valid in the common range of $u_{y,0}/a_o$. It might appear strange that the pressure $p_1/p_o$ is smaller behind switch-on shocks than behind gas shocks when $u_{y,0}/a_o$ is sufficiently small. This fact could perhaps be explained by recalling that the total pressure behind a switch-on shock includes, in addition to the usual pressure term, a term involving the magnetic pressure, $\mu H_{y,1}^2/2$, and that the contribution of this term to the total pressure behind the shock is not taken into account in our definition of shock strength.

### 6.3 Some general features of the motion in Region (3) between the rarefaction waves.

Turning now to the discussion of the state between the tails of the simple waves, let us first consider Figure 19. Here, we have plotted* $p_3/p_o = s_3/s_o$ versus $u_{y,0}/b_o$ for several values of the parameter $s_o$. The curves of this figure may be obtained from those of Figure 16 by using the relation $p_3/p_o = \eta(p_3/p_1) = \eta(s_3/s_1)$. In contrast to the curves of Figure 16, however, the curves of Figure 19 corresponding to different values of $s_o$ do not intersect. It is easily shown that the $\rho_3/\rho_o$-versus $u_{y,0}/b_o$-curves enjoy the same property and moreover vary with $u_{y,0}/b_o$ in the same way as do the $p_3/p_o$-curves. We conclude therefore that if the magnitude of the shear flow discontinuity, $2u_{y,0}$, *and the values of the longitudinal magnetic field and the density in front of the shocks are held fixed, then the pressure* $p_o$ *in front of the shocks and the ratios* $p_3/p_o$, $\rho_3/\rho_o$ *vary in the same sense.* It will be recalled that $p_3$ and $\rho_3$ *are the pressure and density in the Region (3) behind the rarefaction waves while* $p_o$ *and* $\rho_o$ *are the corresponding quantities in the undisturbed region in front of the advancing shocks.*

---

* An approximate expression for $p_3/p_o$ when $u_{y,0}$ is small may be obtained from the results of subsections 5.51 and 5.52.

Similarly, from an inspection of Figures 17b and 19 we conclude that *if the magnitude of the shear flow discontinuity and the values of the longitudinal magnetic field and the density in front of the shocks are held fixed, then the pressure* $p_o$ *in front of shocks and the magnitude of the longitudinal "escape velocities" and of the transverse velocities at the tails of the simple waves vary in the opposite senses whereas the pressure in front of the shocks and the transverse component* $H_{y,3}$ *of the magnetic field in the region between the rarefaction waves vary in the same sense.*

From Figure 17a, where we have plotted $H_{y,3}/H_x$ versus $u_{y,0}/a_o$, it is an easy matter to deduce the following result. *If the magnitude of the initial discontinuity* $2u_{y,0}$ *and the values of the pressure and the density in front of the shock are held fixed, then the transverse magnetic field* $H_{y,3}$ *in the region between the rarefaction waves is a non-decreasing function of the (fixed) longitudinal magnetic field* $H_x$.

When $u_{y,0}$ is small we know from (5.50) and (5.65) that

$$(6.10) \qquad H_{y,3}/H_x \cong u_{y,0}/b_o \qquad u_{y,0} \to 0$$

or, equivalently, that

$$(6.10') \qquad H_{y,3} \cong (\rho_o/\mu)^{1/2} u_{y,0} \qquad u_{y,0} \to 0.$$

On the other hand when $u_{y,0}$ is large we know from (5.37) that

$$H_{y,3}/H_x \cong (1+\gamma)^{1/4}(u_{y,0}/b_o)^{1/2}, \qquad u_{y,0} \to \infty \tag{6.11}$$

or, equivalently, that

$$H_{y,3} \cong \left[(1+\gamma)\rho_o/\mu\right]^{1/4} (H_x u_{y,0})^{1/2}, \qquad u_{y,0} \to \infty. \tag{6.11'}$$

Thus, $H_{y,3}$ *is independent of* $H_x$ *when* $u_{y,0}$ *is small and increases as the square root of* $H_x$ *and the fourth root density when* $u_{y,0}$ *is large*.

It should be emphasized that care must be exercised in applying (6.11') to a given physical situation. The reason for this is the following: Equation (6.11') is valid only for sufficiently large values of $u_{y,0}$ and, in particular, only for those values of $u_{y,0}$ which greatly exceed the minimum value of this quantity necessary to produce cavitation. Even if it be granted that it makes sense to use the fluid dynamical notions of fluid velocity, density and the like, the objection to assuming that the conductivity of the fluid is infinite must be met.

As we have already emphasized in the introductory section of this work, (6.11') implies that arbitrarily large transverse magnetic fields may be created in the region behind the rarefaction waves, provided the fixed longitudinal magnetic field component does not vanish altogether and provided the magnitude of the initial shear flow discontinuity is made sufficiently large. Associated with this is the fact that the motion which resolves the initial discontinuity may, under the same circumstances, be made to differ radically from the corresponding gas dynamical motion. In fact shocks of arbitrarily large strength may be produced since [cf. (6.5)] the expression ratio $p_1/p_o$ of the pressure $p_1$ behind the (gas) shocks to the pressure $p_o$ in front is given by the following expression:

$$p_1/p_o = \frac{1}{2}\left(\frac{1+\gamma}{\gamma p_o}\,\mu\right)^{1/2}\left(\frac{H_x \rho_o u_{y,0}}{p_o}\right). \tag{6.12}$$

## Acknowledgments

The author would like to express his gratitude to Professor K. O. Friedrichs, for suggesting this problem and for his generous advice, and to both Professor K. O. Friedrichs and Professor J. B. Keller for criticizing parts of the manuscript.

Thanks are also due to the members of the computing staff, in particular to Mr. J. Lehnsen, and to Mr. O. Fleischman of the Magneto-hydrodynamics Research Group, for their help in carrying out the many laborious computations, and in addition to Miss L. Joyner and Mr. K. Bass for drawing the numerous figures.

See Fig. 3 on following page

FIG. 3. Waveforms of a resolution consisting of fast gas shocks followed by slow, centered rarefaction waves. The fast gas shocks must be replaced by switch-on shocks when the Alfvén disturbance speed is supersonic ahead of the shocks and the magnitude of the initial discontinuity, $2u_{y,0}$, is below a certain critical value which depends upon the ratio between the sound speed and Alfvén disturbance speed. In this case the ratio $(H_y/H_x)$ [see Figure (c)] of the transverse to the longitudinal component of the magnetic field is positive in the region behind the shocks. It is assumed in the above diagrams that the magnitude of the initial discontinuity is below the minimum value required to produce cavitation. When $2u_{y,0}$ exceeds this minimum value, $p_3$, the pressure in Region (3), vanishes. In addition, the longitudinal component, $u_x$, and the transverse component, $u_y$, of the particle velocity no longer vanish at the " tails" of the simple waves - that is, at the inner boundary lines of the simple waves [see Figures (c) and (e)]; both velocities are positive in the region $x > 0$ and negative in the region $x < 0$.

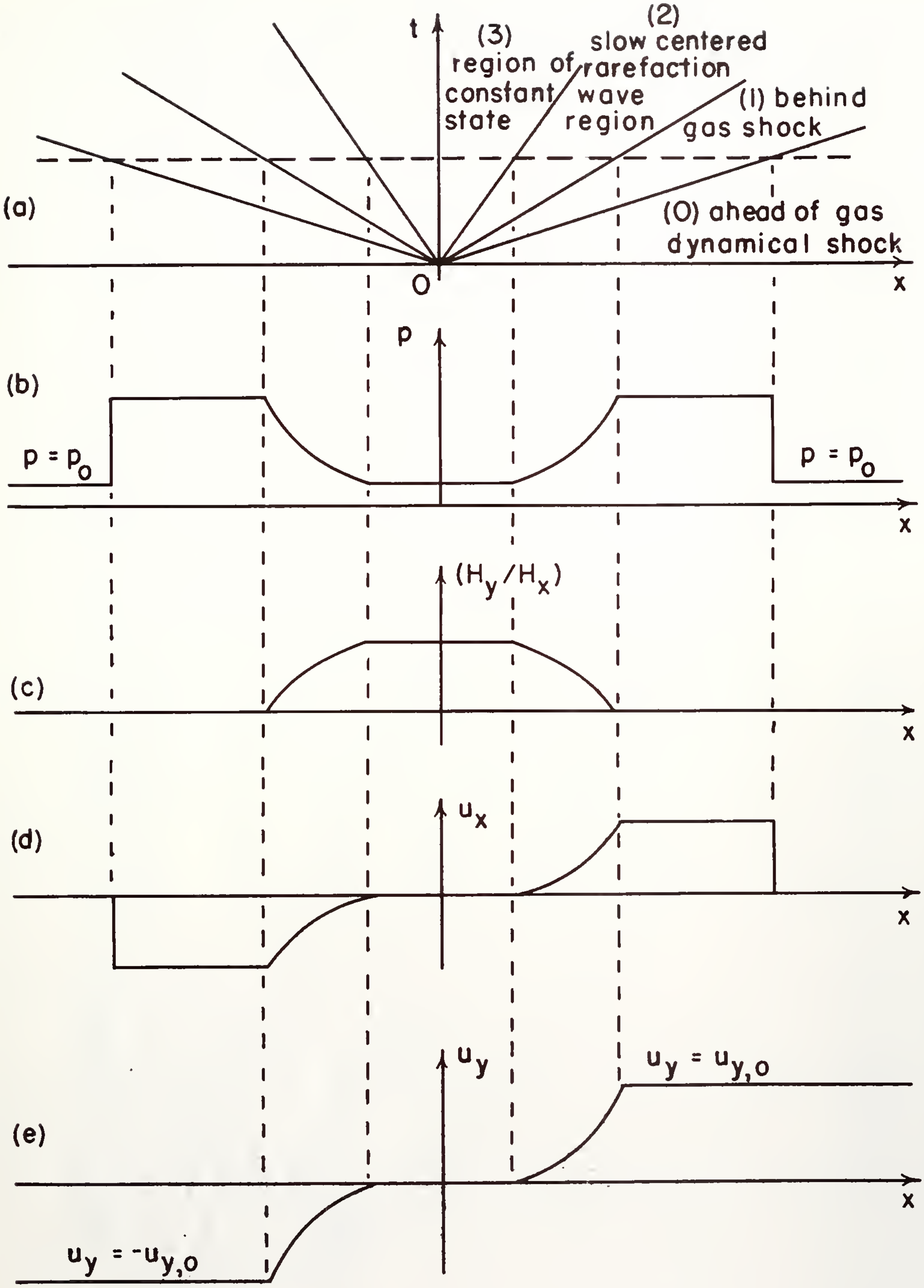
t
(3)
region of
constant
state
(2)
slow centered
rarefaction
wave
region
(1) behind
gas shock
(0) ahead of gas
dynamical shock
(a)
O
x
(b)
p
p = p_o
p = p_o
x
(c)
(H_y/H_x)
x
(d)
u_x
x
(e)
u_y
u_y = u_y,o
u_y = -u_y,o
x

FIG. 3

FIG. 4. Graph of the relationship between the excess density ratio, $(\rho_1-\rho_o)/\rho_o$, in switch-on shocks and the product, $s_1$, of the pressure ratio $(p_1/p_o)$ and $s_o$ [see (3.20), $E_2$]. Here, $\rho_1$ and $p_1$ are the density and pressure behind the switch-on shock; $\rho_o$ and $p_o$ the corresponding quantities in front. The parameter $s_o$ is the square ratio of the sound to the Alfvén disturbance speed in front of the shock. Switch-on shocks exists only when $s_o$ is less than unity - that is, when the Alfvén speed is supersonic in front of the shocks, and then only if $s_1 \leq 5-4s_o \equiv (s_1)_{crit}$. The pure gas shock expression [see $F_1$, (3.22)] for the excess density ratio applies when $s_1$ exceeds $(s_1)_{crit}$ and is employed to continue the curves in the figure to the right of the dashed line.

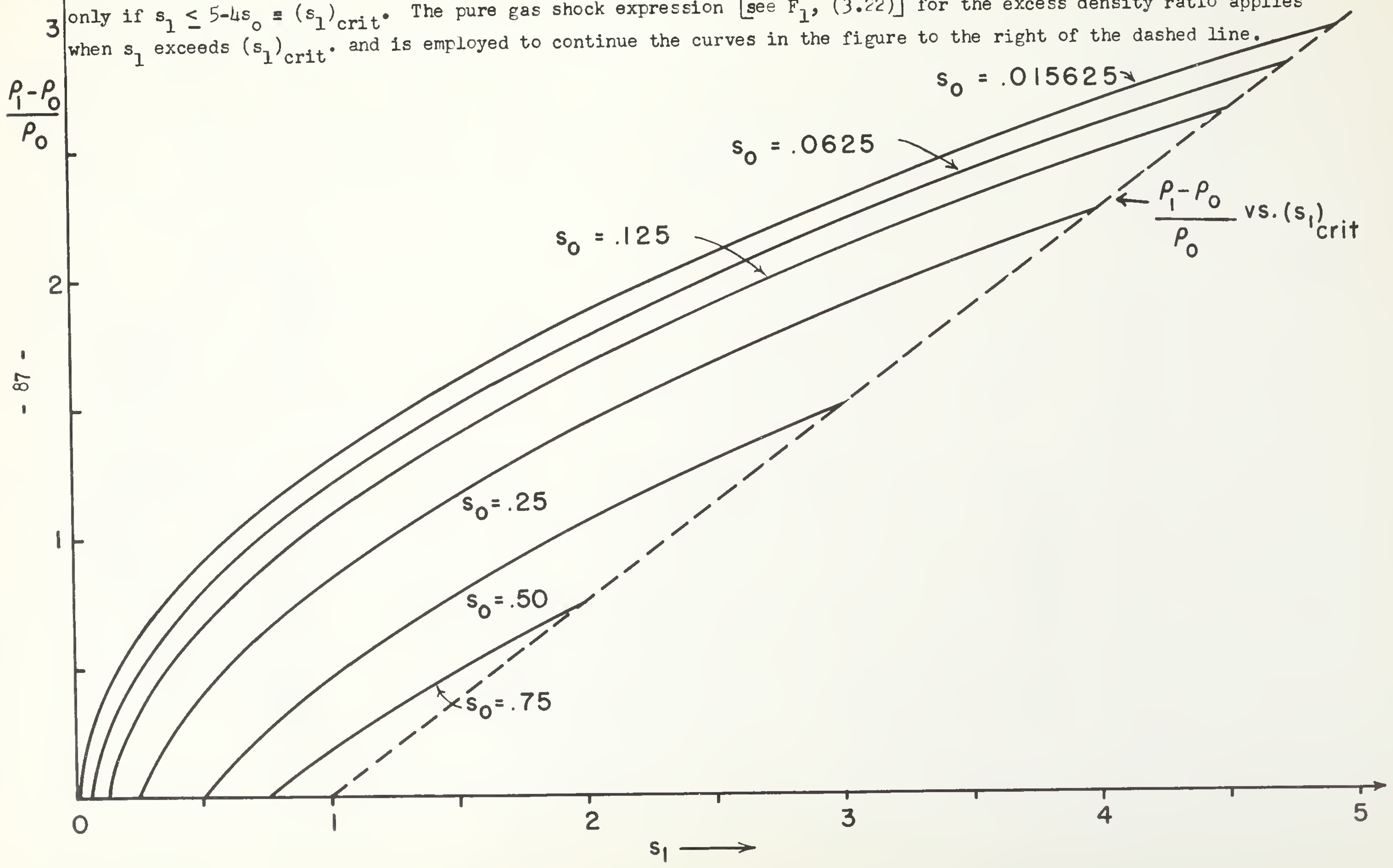

FIG. 5. Graph of the relationship between the absolute value of the ratio $H_{y,1}/H_x$, where $H_{y,1}$ is the transverse component of the magnetic field behind a switch-on shock and $H_x$ is the fixed longitudinal component, and $s_1$, the product of the pressure ratio $p_1/p_o$ and $s_o$, [see (3.20), $E_2$]. For an explanation of the notation see the caption of Figure 4. For each value of $s_o$ the quantity $|H_{y,1}/H_x|$ increases from zero to the maximum $\sqrt{1.5(1-s_o)}$ as $s_1$ varies from zero to $s_1 = s_o[1+(5/4)(1-s_o^2)/s_o]$ and then decreases to zero as $s_1$ approaches $(s_1)_{crit} = 5-4s_o$.

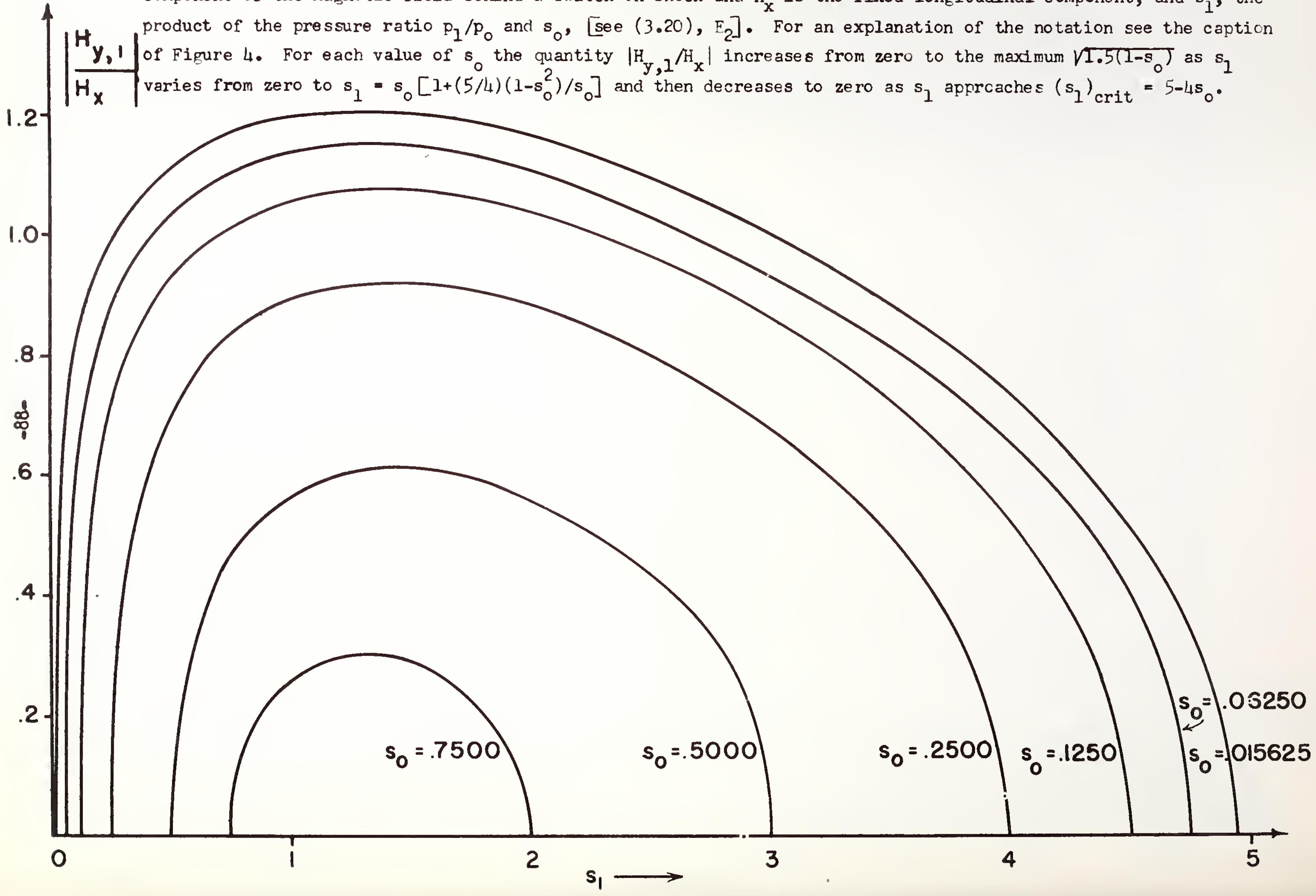

FIG. 6. Graph of the relationship between $s = s(q,q_{tr};5)$ and $q$ in a slow simple wave. The ordinate, $s$, is the square ratio of the sound speed to the Alfvén disturbance speed, while the abscissa, $q$, is the square ratio of the slow simple wave disturbance speed and the sound speed. The function $s(q,q_{tr};5)$ is, for each $q_{tr}$, the solution of the basic ordinary linear differential equation (4.8). [As usual it is assumed that $\gamma$, the adiabatic exponent, is 5/3; hence $\theta = 5$.] After integration (4.8) leads to the expression given in (4.13). Note that when $q = q_{tr}$, then $s = s_{tr} = q_{tr}^{-1}$. Thus, $(q_{tr},s_{tr})$ is a point of the arc $s = q^{-1}$. The various s-versus-q-curves correspond to the following choices for the value of the parameter $q_{tr}$: $q_{tr}$ = .975, .95, .925, .9, ..., .2, .14286, .1, .05.

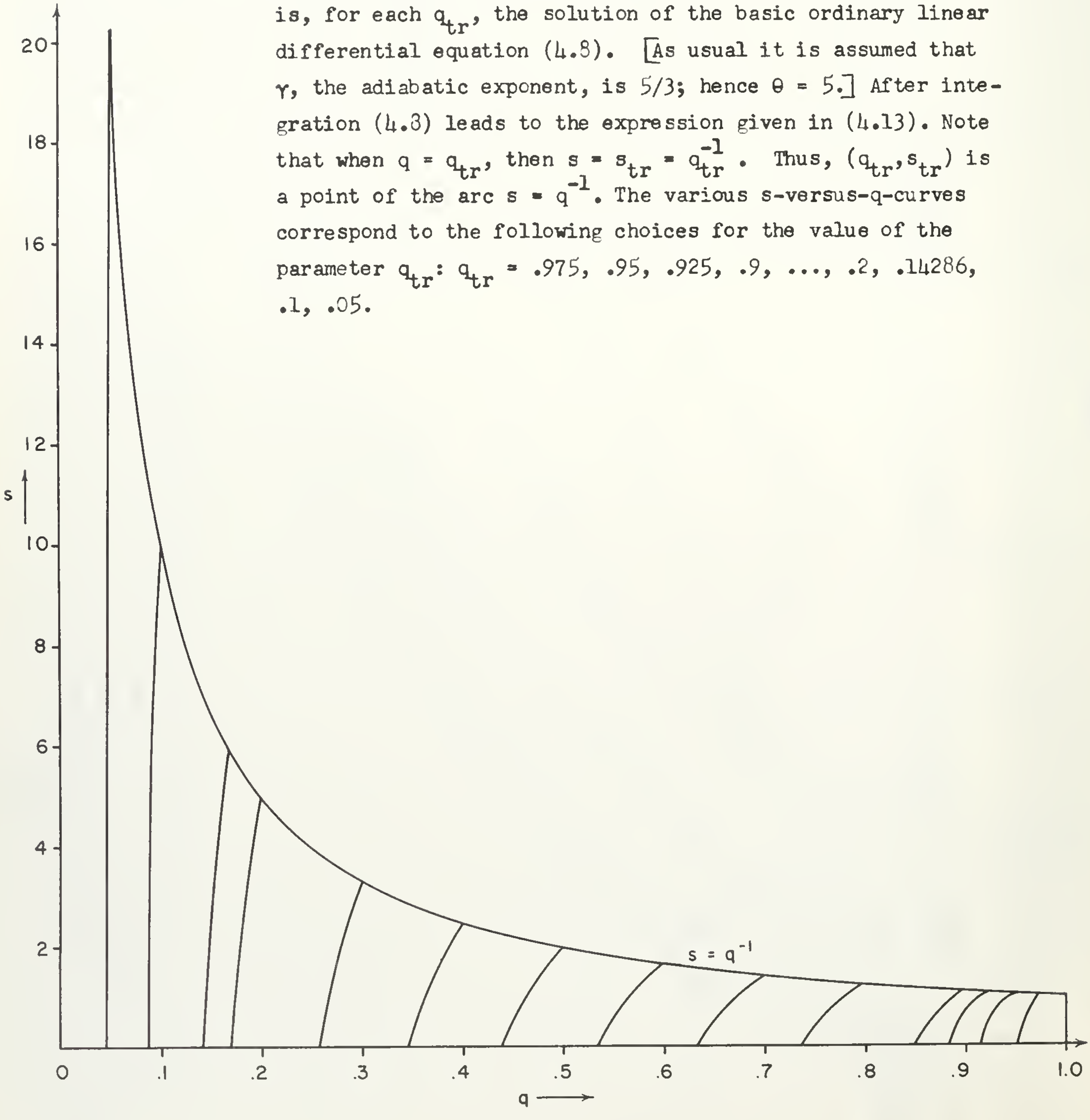

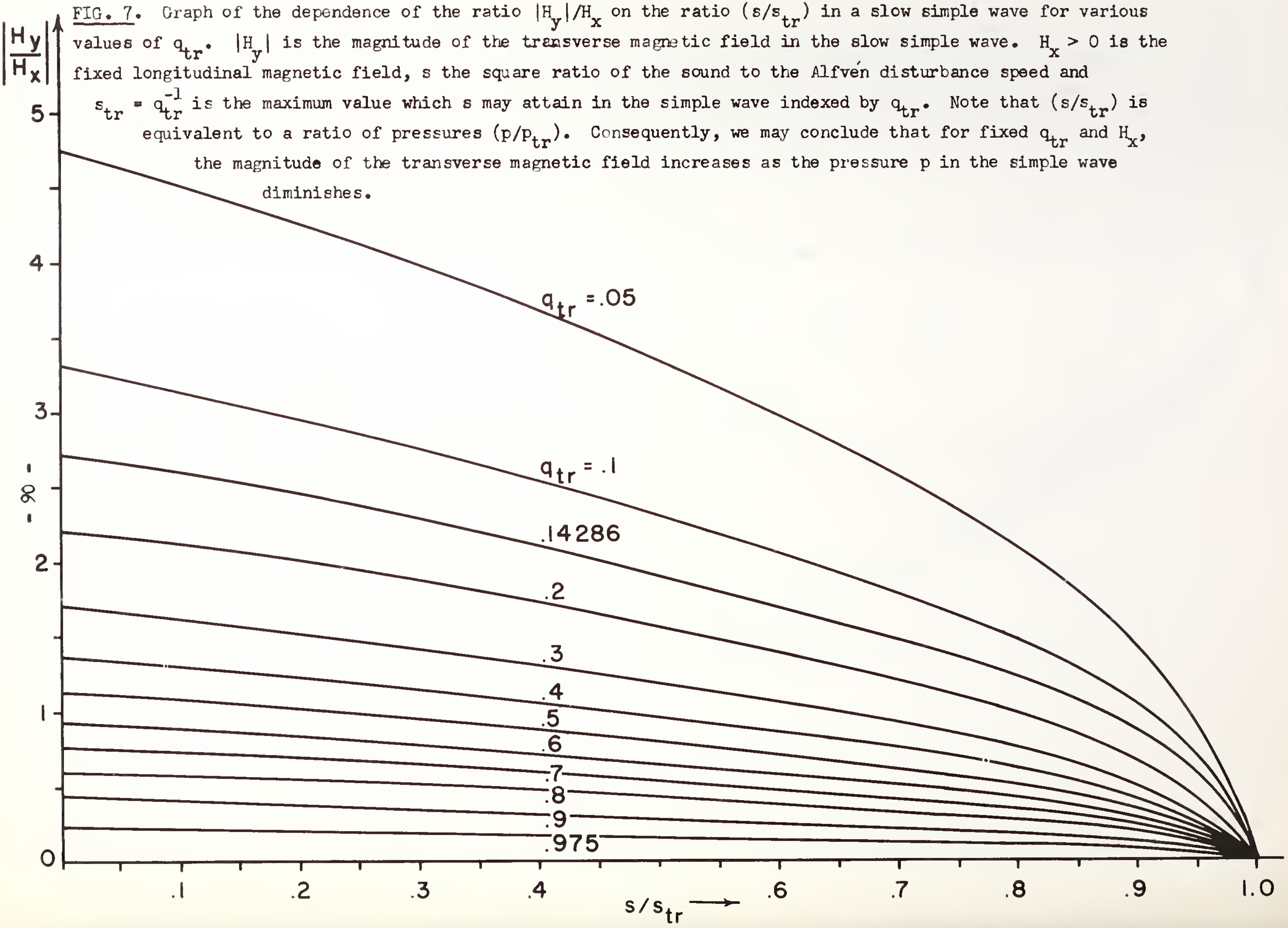

FIG. 7. Graph of the dependence of the ratio $|H_y|/H_x$ on the ratio $(s/s_{tr})$ in a slow simple wave for various values of $q_{tr}$. $|H_y|$ is the magnitude of the transverse magnetic field in the slow simple wave. $H_x > 0$ is the fixed longitudinal magnetic field, s the square ratio of the sound to the Alfvén disturbance speed and $s_{tr} = q_{tr}^{-1}$ is the maximum value which s may attain in the simple wave indexed by $q_{tr}$. Note that $(s/s_{tr})$ is equivalent to a ratio of pressures $(p/p_{tr})$. Consequently, we may conclude that for fixed $q_{tr}$ and $H_x$, the magnitude of the transverse magnetic field increases as the pressure p in the simple wave diminishes.

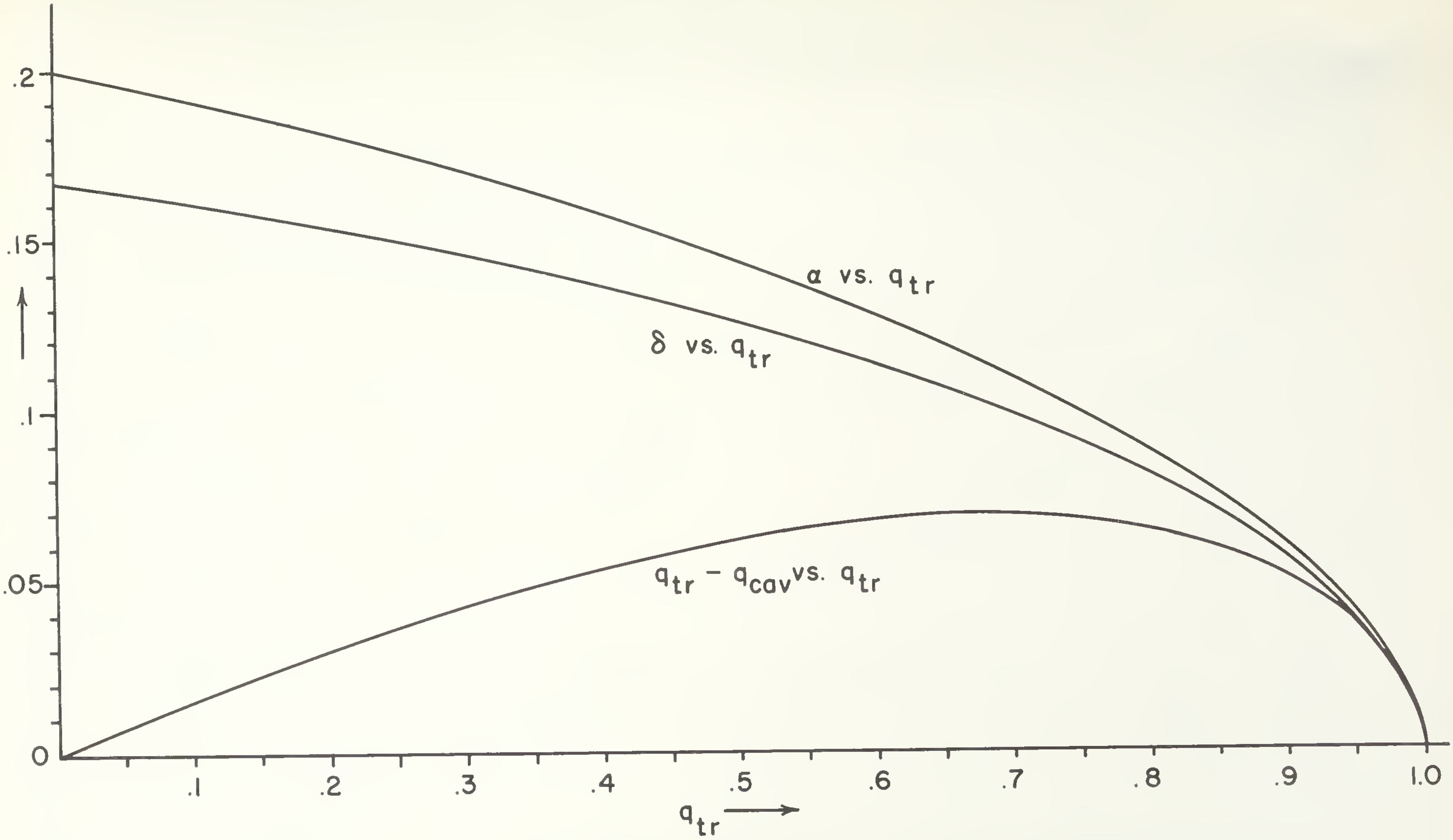

FIG. 8. Graph of the variation of the quantities $\alpha = (q_{tr}-q_{cav})/q_{cav}$, $\delta = (q_{tr}-q_{cav})/q_{tr}$ and $q_{tr} - q_{cav}$ with $q_{tr}$. The abscissa, $q_{tr}$, is that value of the square ratio, $q = (c_s/a)^2$, where $c_s$ is the slow disturbance speed and a is the sound speed, which corresponds to taking $c_s$ equal to the Alfvẽn disturbance speed. For each $q_{tr}$, $q_{cav}$ is the value of q in the relation $s = s(q, q_{tr}; 5)$ [see (4.13)] for which s vanishes.

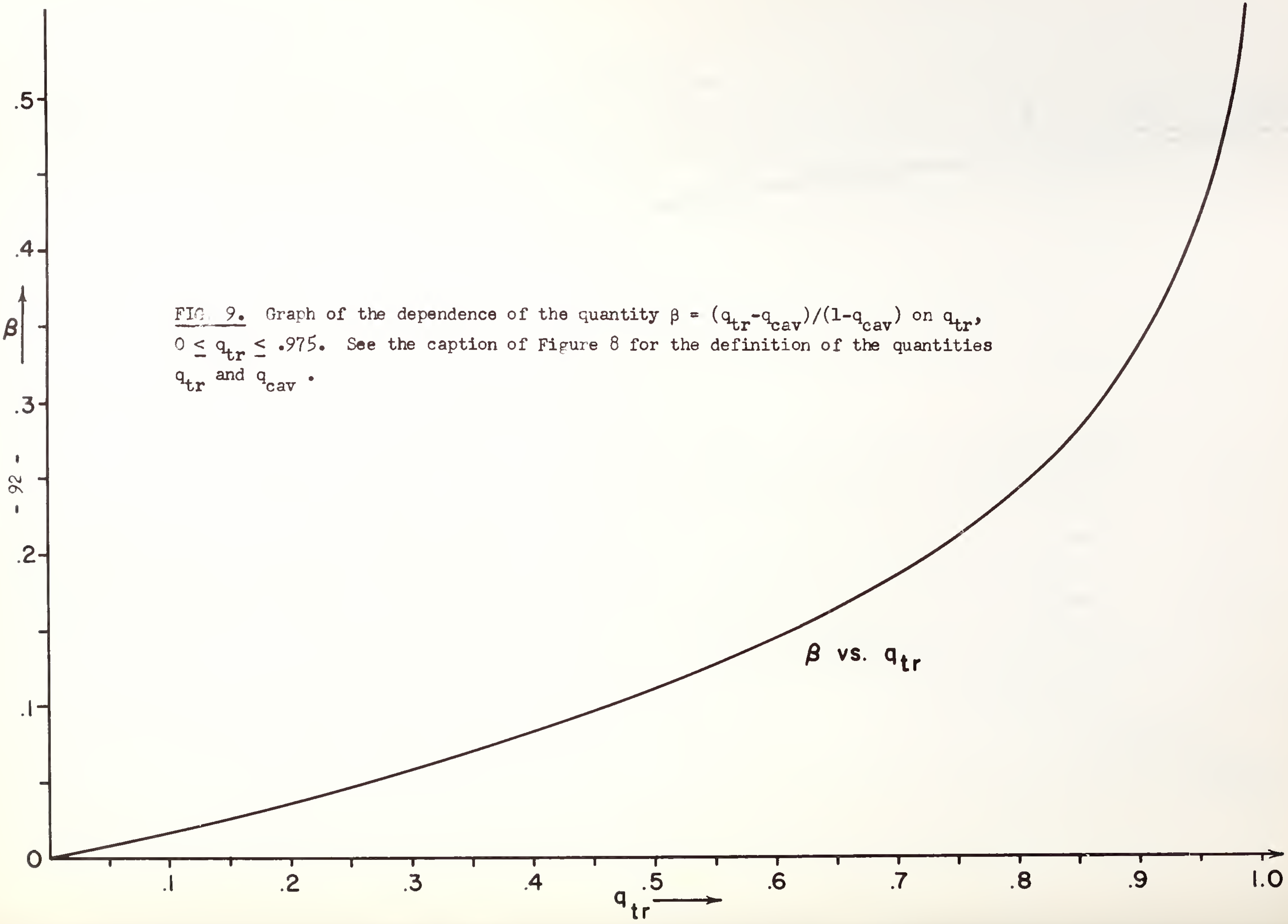

FIG. 9. Graph of the dependence of the quantity $\beta = (q_{tr}-q_{cav})/(1-q_{cav})$ on $q_{tr}$, $0 \leq q_{tr} \leq .975$. See the caption of Figure 8 for the definition of the quantities $q_{tr}$ and $q_{cav}$.

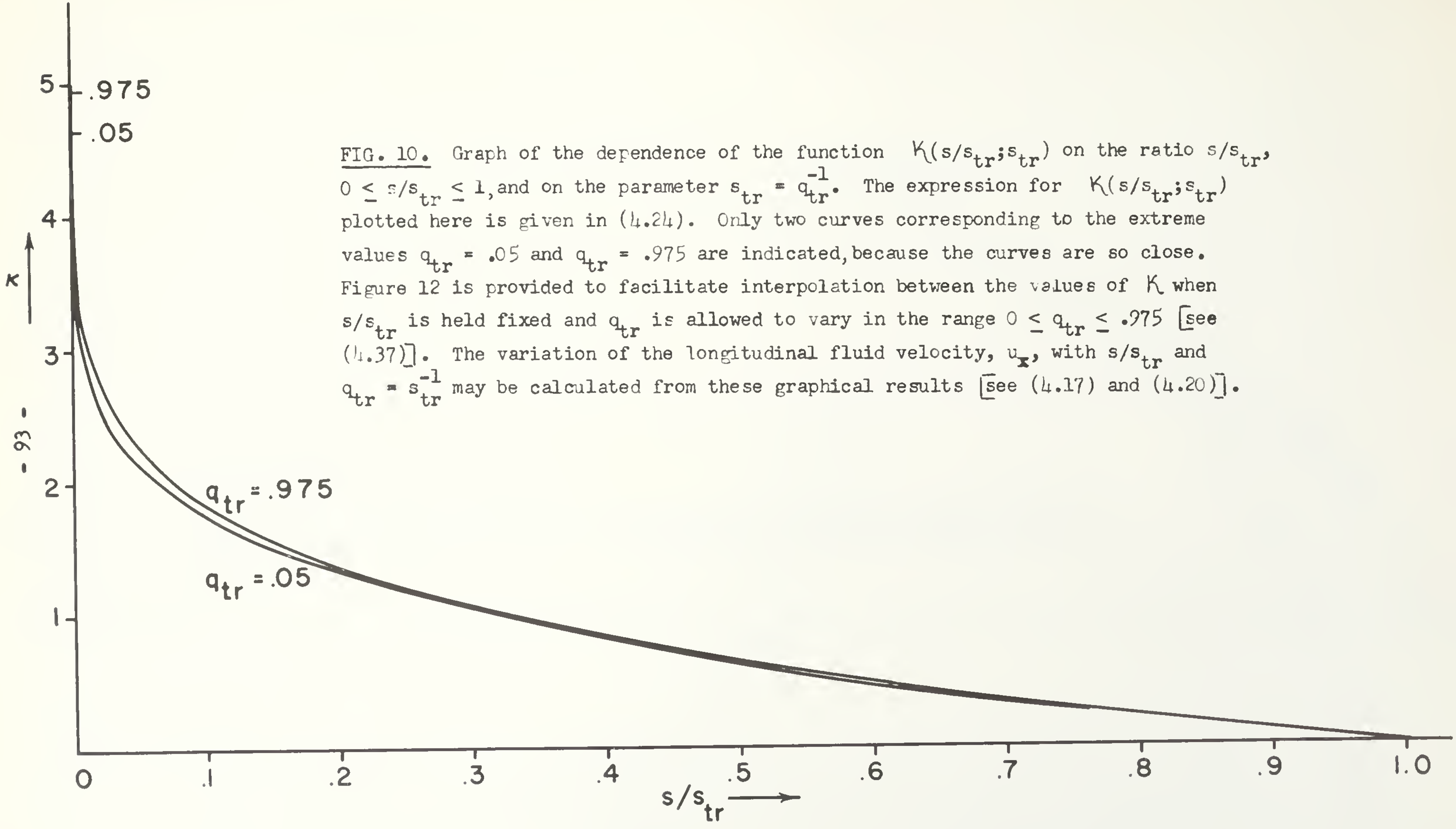

FIG. 10. Graph of the dependence of the function $\kappa(s/s_{tr};s_{tr})$ on the ratio $s/s_{tr}$, $0 \leq s/s_{tr} \leq 1$, and on the parameter $s_{tr} = q_{tr}^{-1}$. The expression for $\kappa(s/s_{tr};s_{tr})$ plotted here is given in (4.24). Only two curves corresponding to the extreme values $q_{tr} = .05$ and $q_{tr} = .975$ are indicated, because the curves are so close. Figure 12 is provided to facilitate interpolation between the values of $\kappa$ when $s/s_{tr}$ is held fixed and $q_{tr}$ is allowed to vary in the range $0 \leq q_{tr} \leq .975$ [see (4.37)]. The variation of the longitudinal fluid velocity, $u_x$, with $s/s_{tr}$ and $q_{tr} = s_{tr}^{-1}$ may be calculated from these graphical results [see (4.17) and (4.20)].

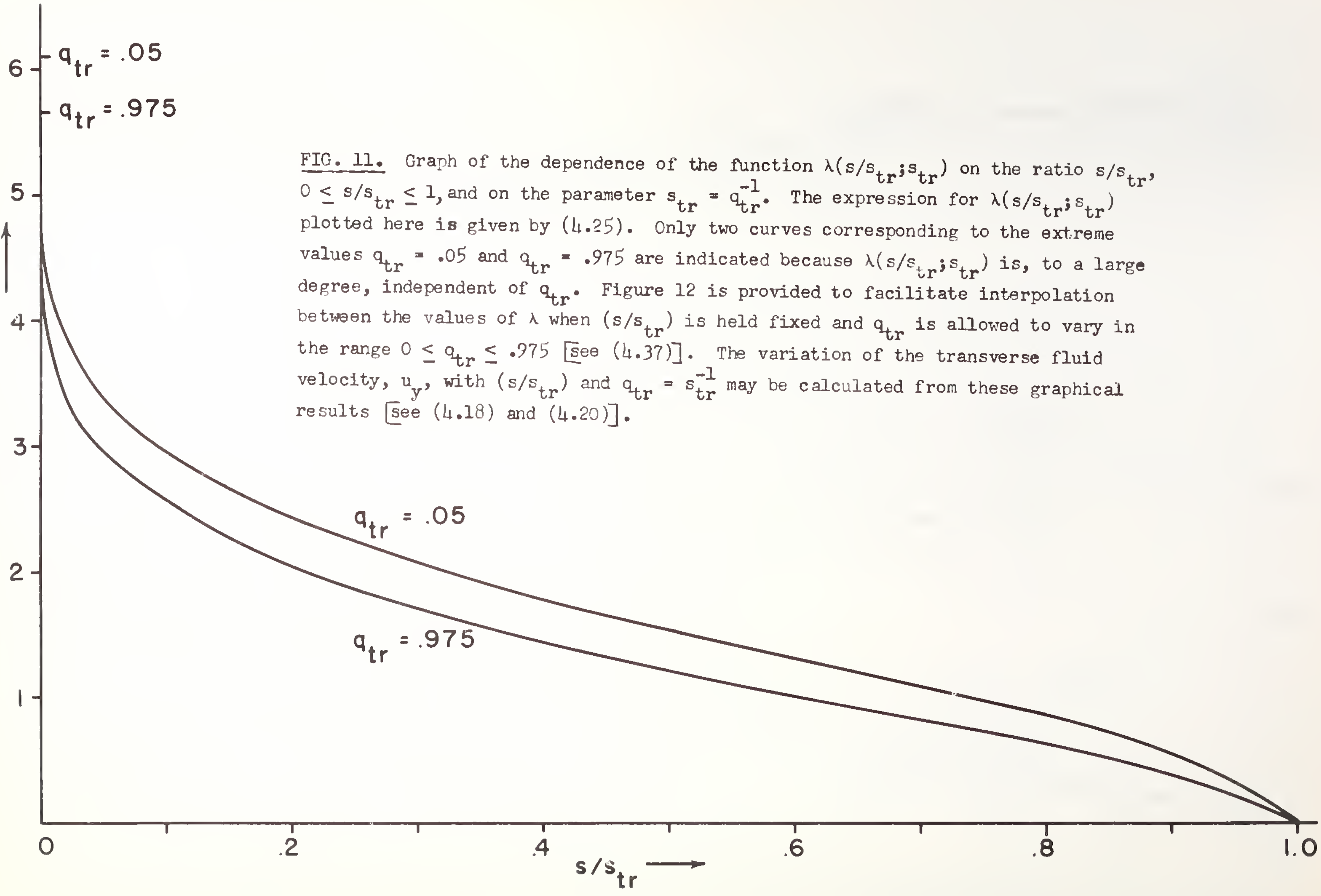

FIG. 11. Graph of the dependence of the function $\lambda(s/s_{tr};s_{tr})$ on the ratio $s/s_{tr}$, $0 \leq s/s_{tr} \leq 1$, and on the parameter $s_{tr} = q_{tr}^{-1}$. The expression for $\lambda(s/s_{tr};s_{tr})$ plotted here is given by (4.25). Only two curves corresponding to the extreme values $q_{tr} = .05$ and $q_{tr} = .975$ are indicated because $\lambda(s/s_{tr};s_{tr})$ is, to a large degree, independent of $q_{tr}$. Figure 12 is provided to facilitate interpolation between the values of λ when $(s/s_{tr})$ is held fixed and $q_{tr}$ is allowed to vary in the range $0 \leq q_{tr} \leq .975$ [see (4.37)]. The variation of the transverse fluid velocity, $u_y$, with $(s/s_{tr})$ and $q_{tr} = s_{tr}^{-1}$ may be calculated from these graphical results [see (4.18) and (4.20)].

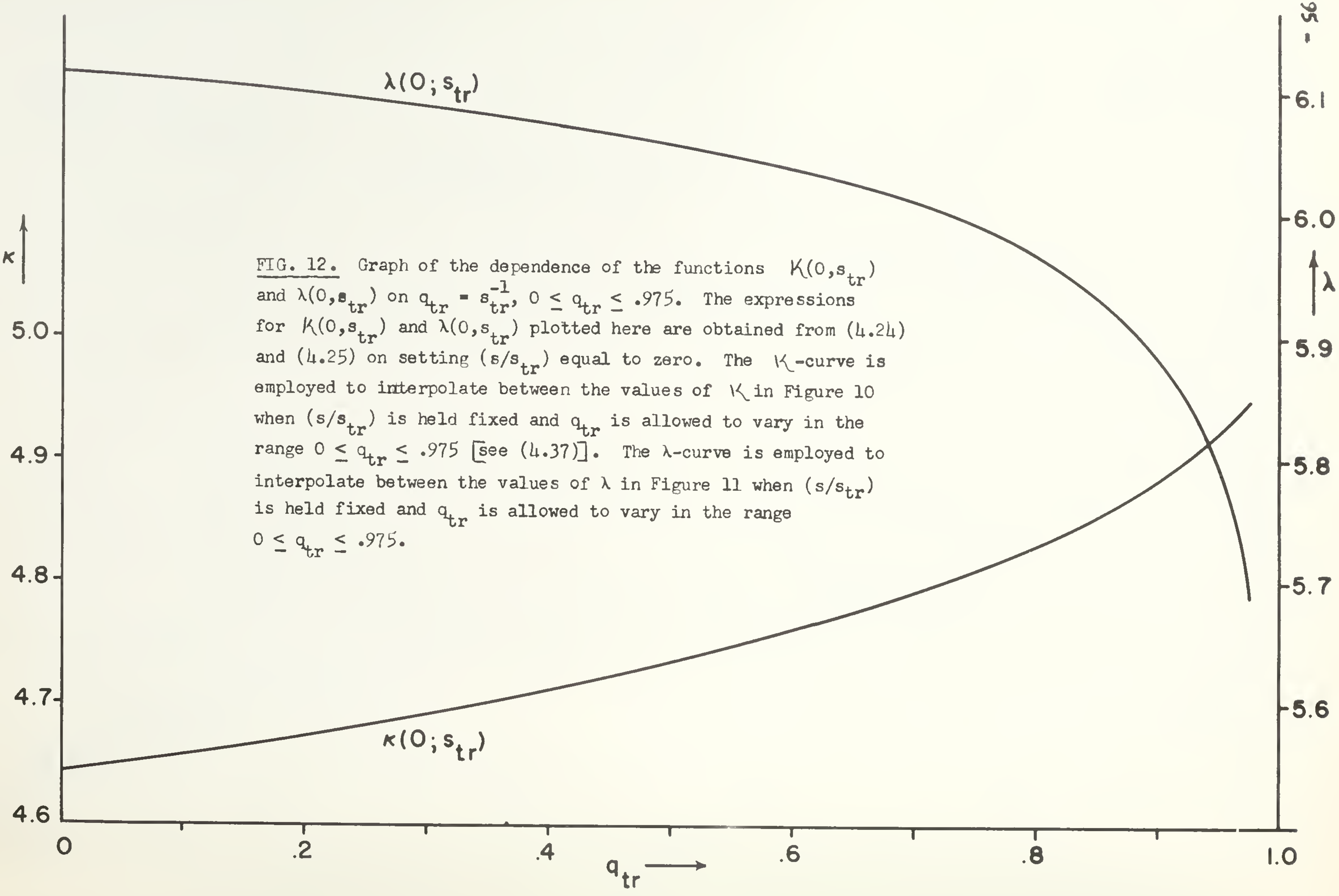

FIG. 12. Graph of the dependence of the functions $\kappa(0,s_{tr})$ and $\lambda(0,s_{tr})$ on $q_{tr} = s_{tr}^{-1}$, $0 \leq q_{tr} \leq .975$. The expressions for $\kappa(0,s_{tr})$ and $\lambda(0,s_{tr})$ plotted here are obtained from (4.24) and (4.25) on setting $(s/s_{tr})$ equal to zero. The $\kappa$-curve is employed to interpolate between the values of $\kappa$ in Figure 10 when $(s/s_{tr})$ is held fixed and $q_{tr}$ is allowed to vary in the range $0 \leq q_{tr} \leq .975$ [see (4.37)]. The $\lambda$-curve is employed to interpolate between the values of $\lambda$ in Figure 11 when $(s/s_{tr})$ is held fixed and $q_{tr}$ is allowed to vary in the range $0 \leq q_{tr} \leq .975$.

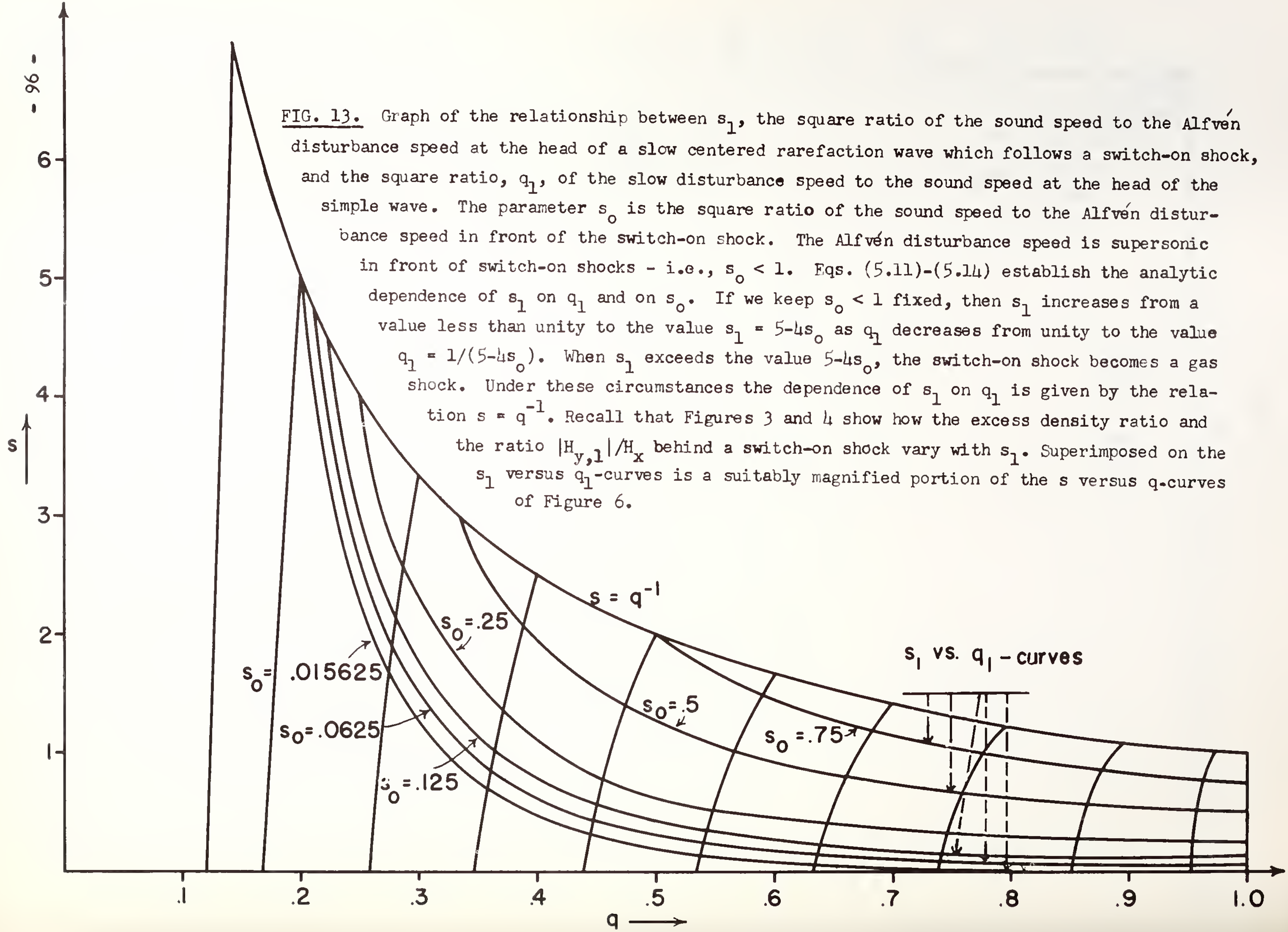

FIG. 13. Graph of the relationship between $s_1$, the square ratio of the sound speed to the Alfvén disturbance speed at the head of a slow centered rarefaction wave which follows a switch-on shock, and the square ratio, $q_1$, of the slow disturbance speed to the sound speed at the head of the simple wave. The parameter $s_o$ is the square ratio of the sound speed to the Alfvén disturbance speed in front of the switch-on shock. The Alfvén disturbance speed is supersonic in front of switch-on shocks - i.e., $s_o < 1$. Eqs. (5.11)-(5.14) establish the analytic dependence of $s_1$ on $q_1$ and on $s_o$. If we keep $s_o < 1$ fixed, then $s_1$ increases from a value less than unity to the value $s_1 = 5-4s_o$ as $q_1$ decreases from unity to the value $q_1 = 1/(5-4s_o)$. When $s_1$ exceeds the value $5-4s_o$, the switch-on shock becomes a gas shock. Under these circumstances the dependence of $s_1$ on $q_1$ is given by the relation $s = q^{-1}$. Recall that Figures 3 and 4 show how the excess density ratio and the ratio $|H_{y,1}|/H_x$ behind a switch-on shock vary with $s_1$. Superimposed on the $s_1$ versus $q_1$-curves is a suitably magnified portion of the s versus q-curves of Figure 6.

FIG. 15a. See caption on following page.

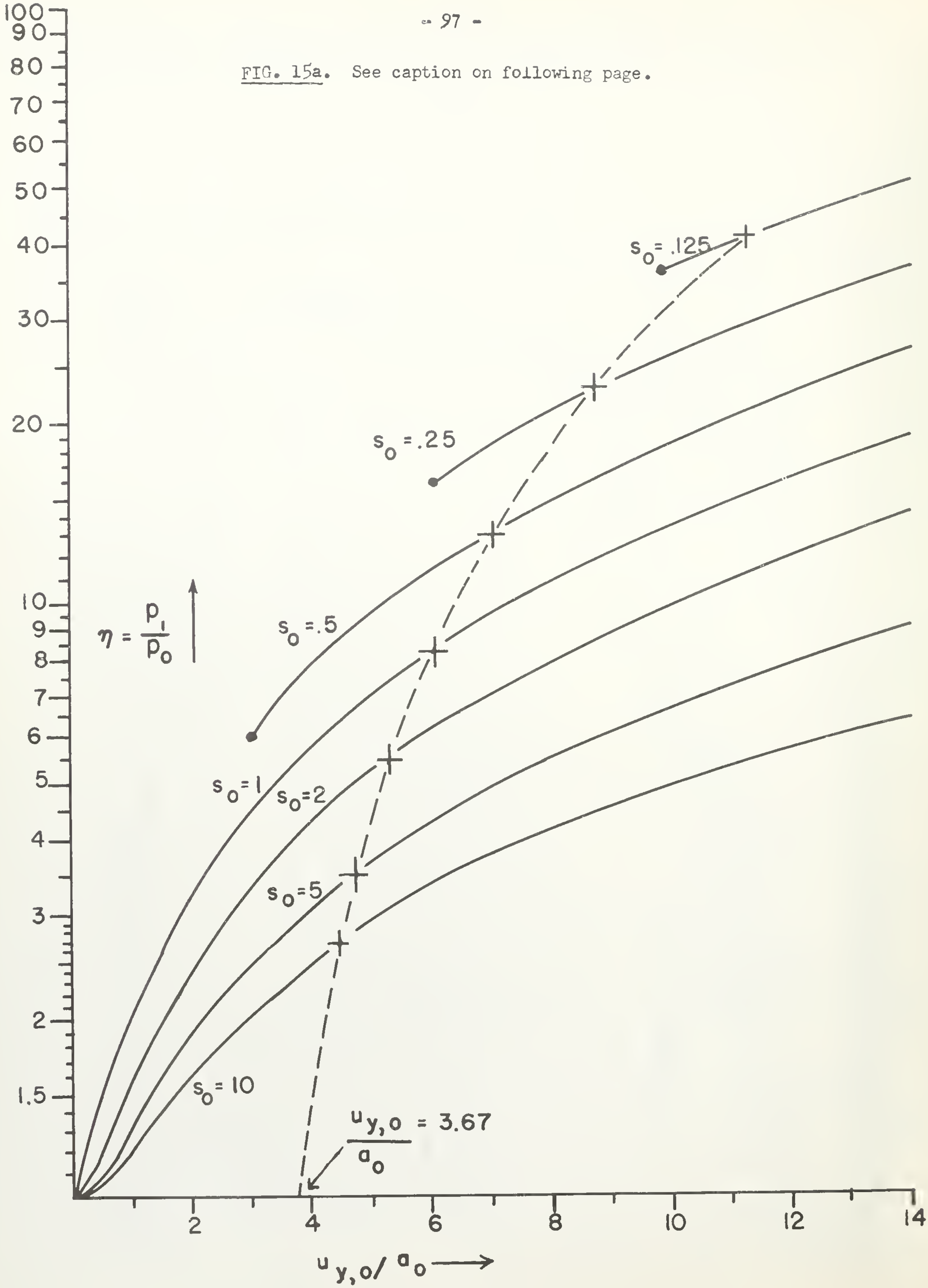

FIG. 15a. Graph of the relationship between the ratio $\eta = (p_1/p_0)$, where $p_1$ is the pressure behind the pure gas shocks and $p_0$ is the pressure in front, and the ratio $(u_{y,0}/a_0)$, where $u_{y,0}$ is (half) the initial discontinuity in the transverse velocity and $a_0$ is the sound speed in front of the shock. The parameter $s_0$ is the square ratio of the sound speed to the Alfvén disturbance speed in front of the shock. On each curve, indexed by $s_0$, the point corresponding to the minimum value of $u_{y,0}/a_0$ at which cavitation is produced is indicated by a plus (+) sign. The dashed curve is the locus of these points. The point on each of the incomplete curves corresponding to the " critical" values of $u_{y,0}/a_0$ and $\eta$, - that is, to the point at which the switch-on shock in the resolution reduces to a pure gas shock, is indicated by a dot (the lowest point of the curves indexed by values of $s_0$ less than unity). The remaining parts of these curves, the portions below the critical point, are shown in Figure 15b. The scale on the left is logarithmic.

FIG. 15b. See caption on following page.

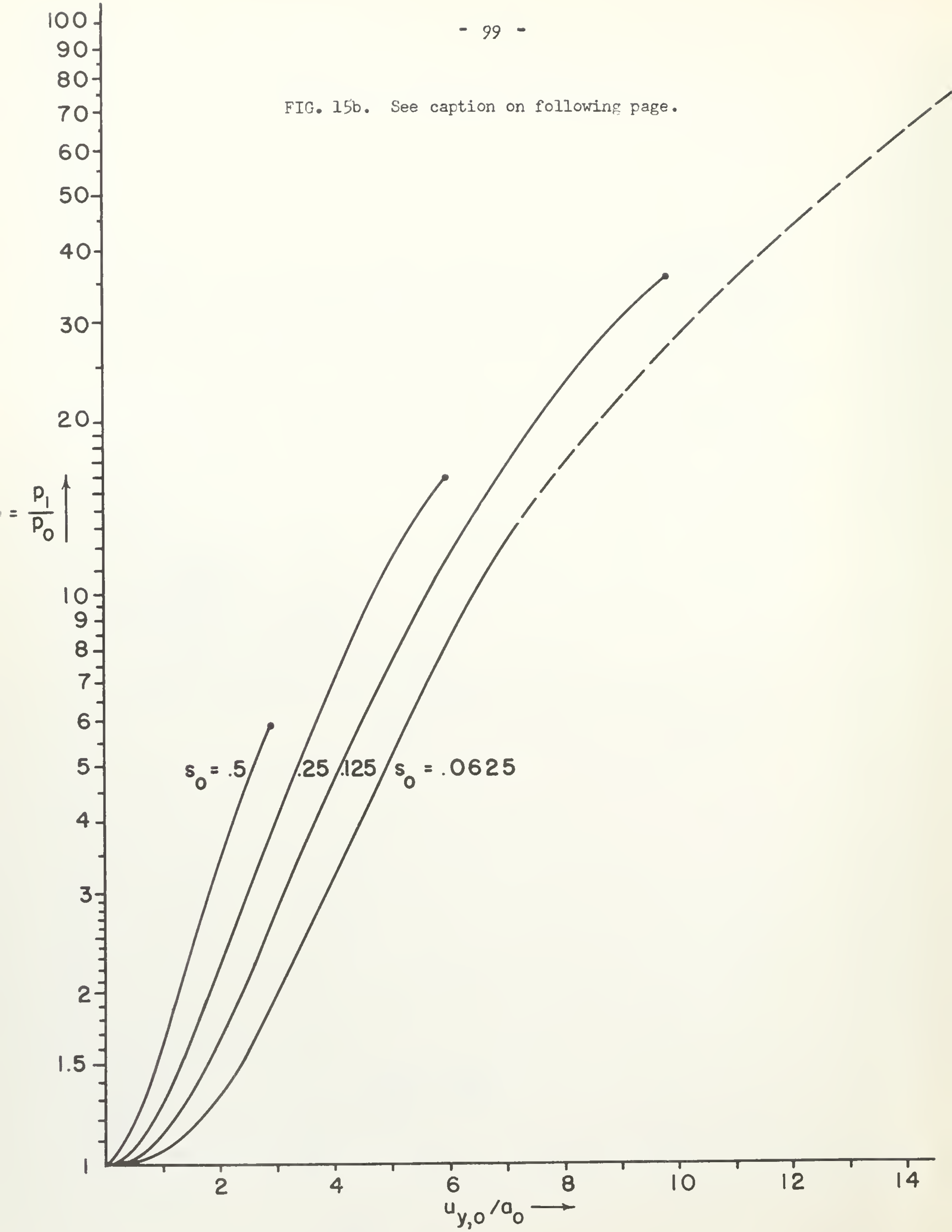

FIG. 15b. Graph of the relationship between the ratio $\eta = (p_1/p_0)$, where $p_1$ is the pressure behind the switch-on shocks and $p_0$ is the pressure in front, and the ratio $(u_{y,0}/a_0)$ of (half) the initial discontinuity in the transverse velocity to the sound speed $a_0$ in front of the shocks. The parameter $s_0$ is the square ratio of the sound speed to the Alfvén disturbance speed in front of the switch-on shocks; the presence of these shocks implies that $s_0$ is less than unity. The dot at the upper end of each curve corresponds to the "critical" point $(u_{y,0}/a_0, \eta)$ at which the switch-on shocks reduce to pure gas shocks.

The curves depicted here should be regarded as the continuations of the incompleted curves of Figure 15a. The upper portion of the .0625-curve has been sketched in roughly. The scale on the left is logarithmic.

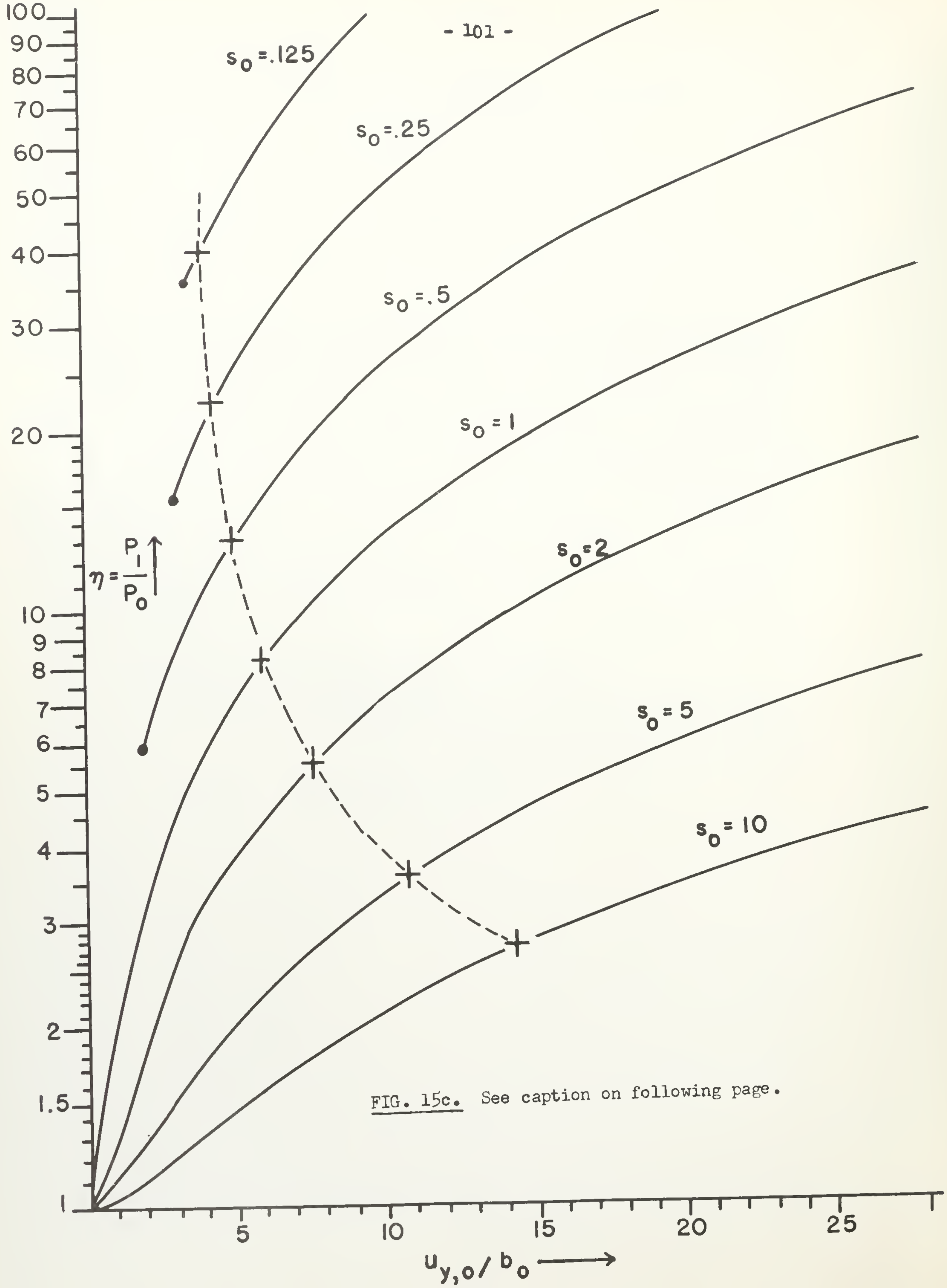

FIG. 15c. See caption on following page.

FIG. 15c. Graph of the relationship between the ratio $\eta = (p_1/p_0)$, where $p_1$ is the pressure behind the pure gas shocks and $p_0$ is the pressure in front, and the ratio $u_{y,0}/b_0$, where $u_{y,0}$ is (half) the initial discontinuity in the transverse velocity and $b_0$ is the Alfvén disturbance speed in front of the shocks. The parameter $s_0$ is the square ratio of the sound speed to the Alfvén disturbance speed in front of the shocks. These curves may be obtained from the corresponding curves of Figure 15a by employing the relation $(u_{y,0}/b_0) = (u_{y,0}/a_0)\sqrt{s_0}$ and vice verea. The scale on the left is logarithmic.

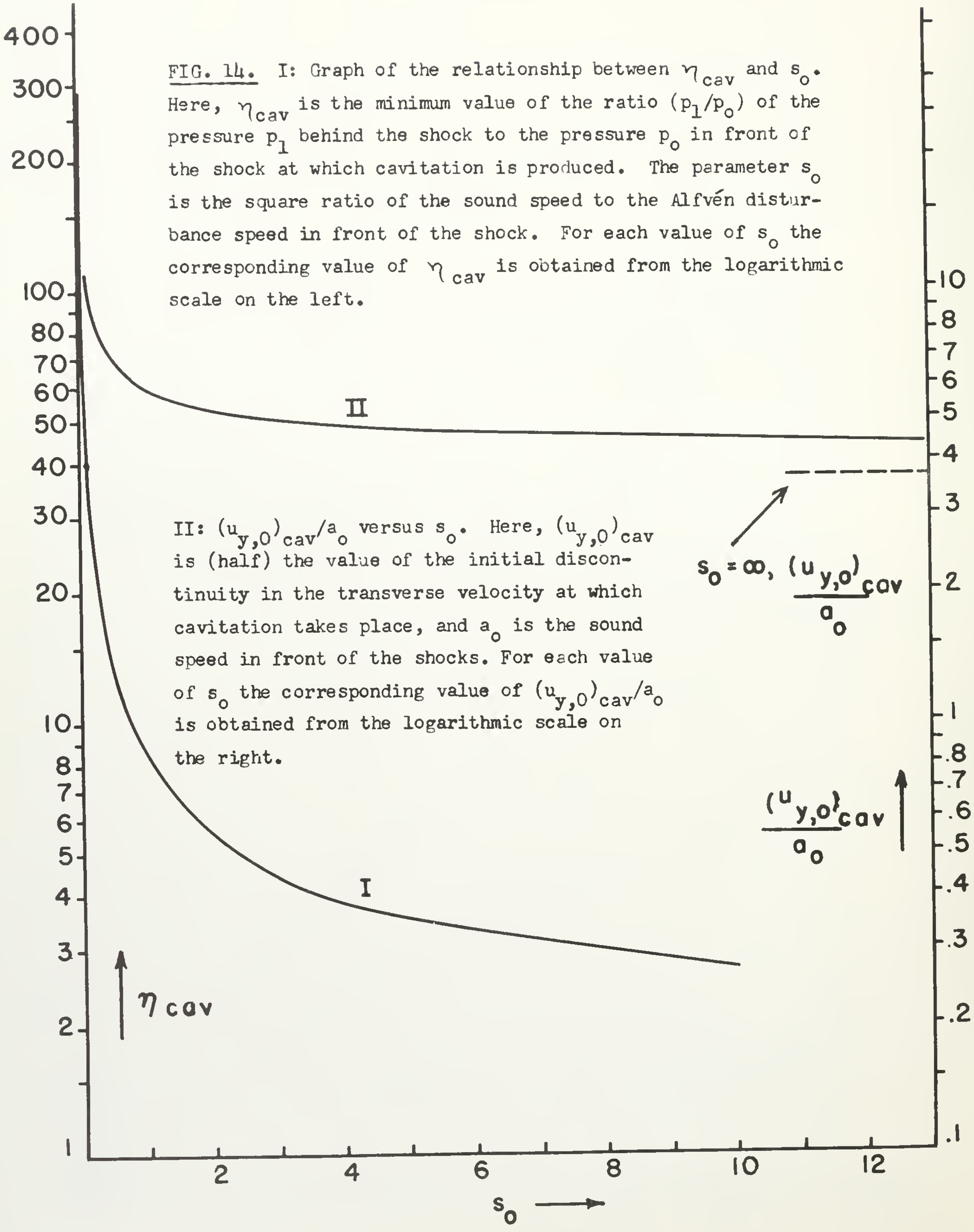

FIG. 14. I: Graph of the relationship between $\eta_{cav}$ and $s_o$. Here, $\eta_{cav}$ is the minimum value of the ratio $(p_1/p_o)$ of the pressure $p_1$ behind the shock to the pressure $p_o$ in front of the shock at which cavitation is produced. The parameter $s_o$ is the square ratio of the sound speed to the Alfvén disturbance speed in front of the shock. For each value of $s_o$ the corresponding value of $\eta_{cav}$ is obtained from the logarithmic scale on the left.

II: $(u_{y,0})_{cav}/a_o$ versus $s_o$. Here, $(u_{y,0})_{cav}$ is (half) the value of the initial discontinuity in the transverse velocity at which cavitation takes place, and $a_o$ is the sound speed in front of the shocks. For each value of $s_o$ the corresponding value of $(u_{y,0})_{cav}/a_o$ is obtained from the logarithmic scale on the right.

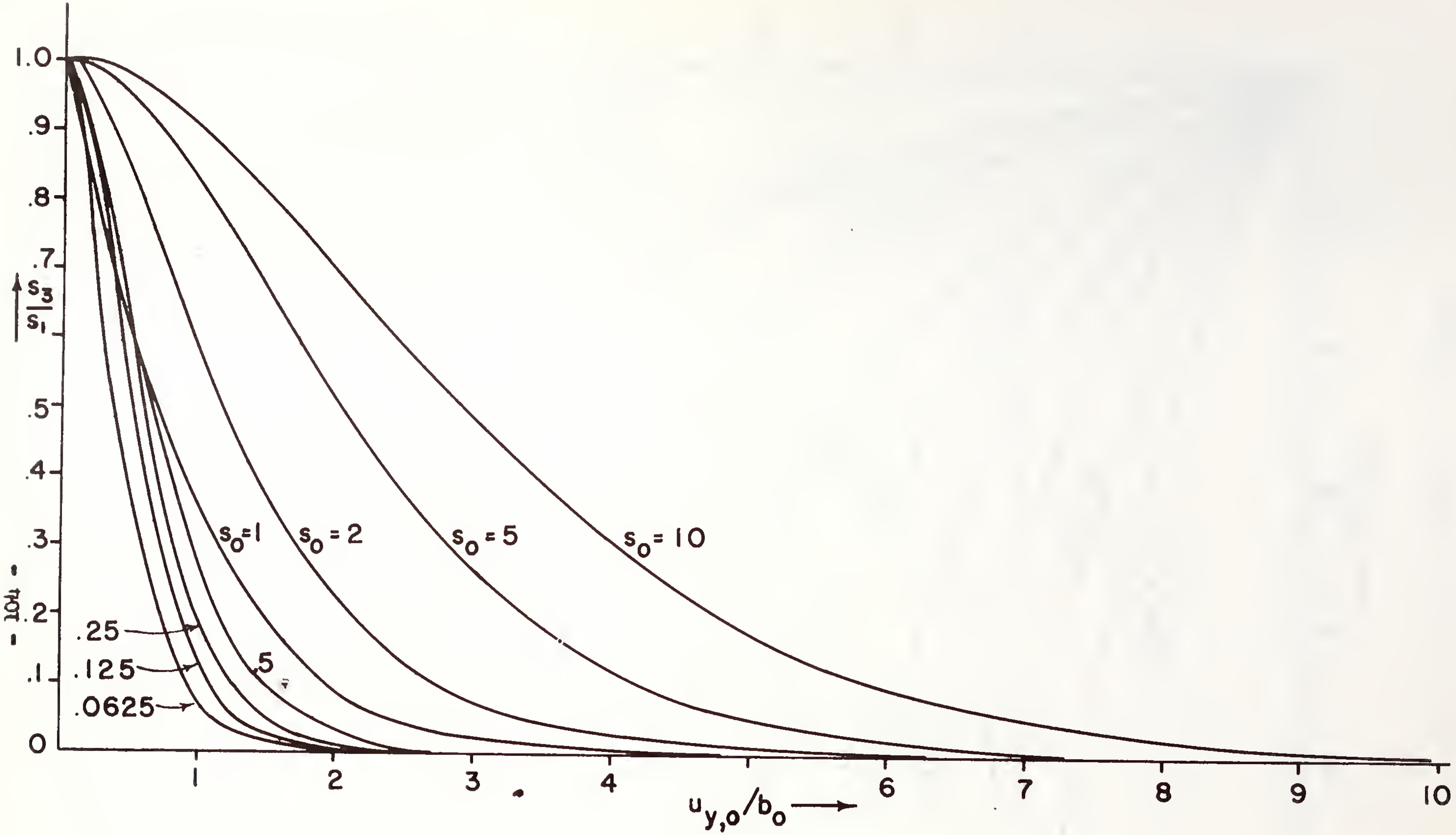

FIG. 16. Graph of the relationship between $(s_3/s_1) = (p_3/p_1)$ and $(u_{y,0}/b_o)$ for several values of the parameter $s_o$. Here, $s_o$ and $s_1$ are the square ratios of the sound speed to the Alfvén disturbance speed in front of and behind the shocks and $s_3$ the same square ratio at the tails of the rarefaction waves. The quantity $p_1$ is the pressure at the heads, and $p_3$ is the pressure at the tails of the rarefaction waves. The abscissa is the ratio between (half) the magnitude of the initial discontinuity in the transverse velocity $u_{y,0}$ and the Alfvén disturbance speed in front of the shocks.

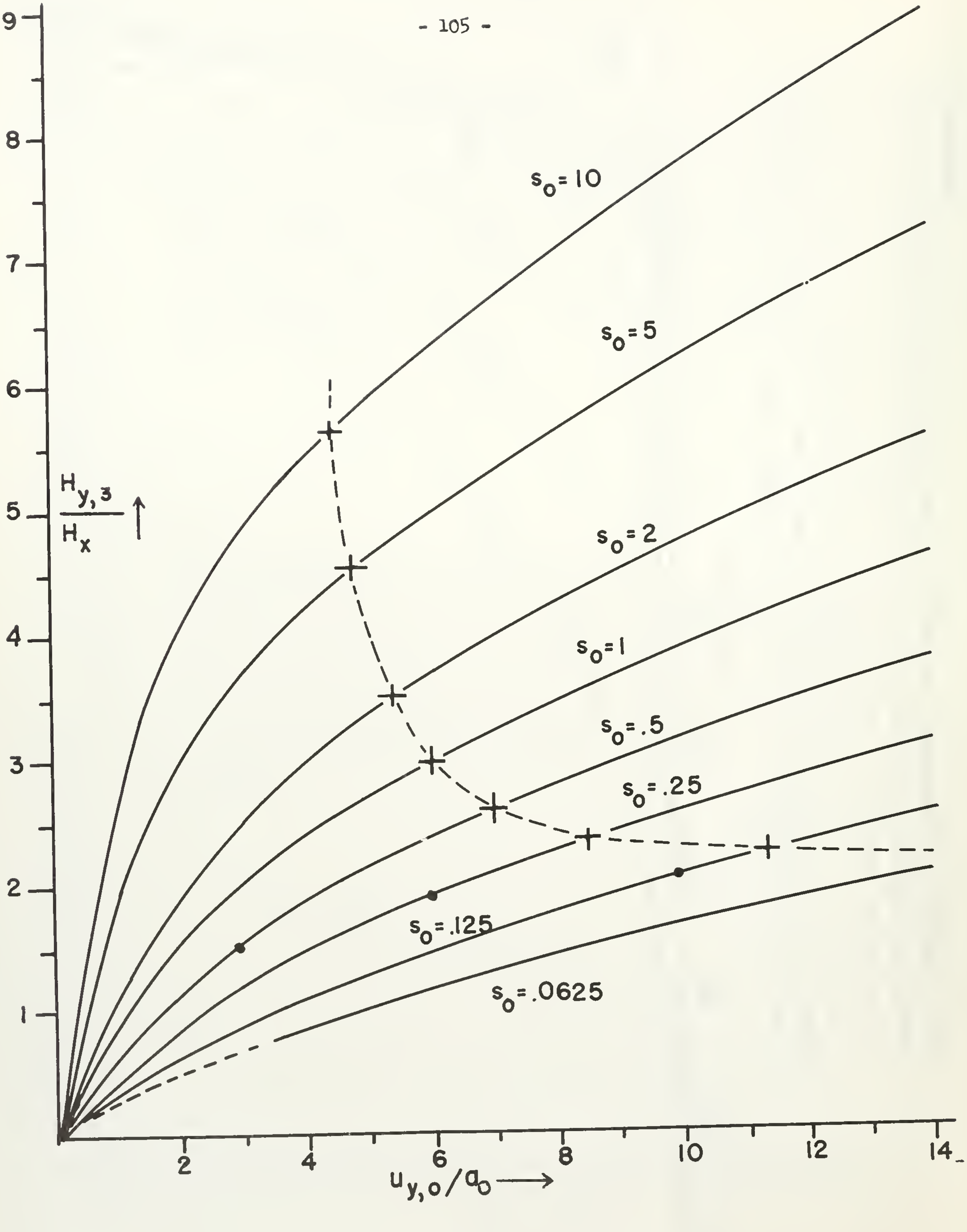

FIG. 17a. See caption on following page.

FIG. 17a. Graph of the relationship between the ratio $(H_{y,3}/H_x)$, where $H_{y,3}$ is the transverse magnetic field component in the region between the rarefaction waves and $H_x$ is the fixed, longitudinal magnetic field component, and the ratio $(u_{y,0}/a_o)$, where $u_{y,0}$ is (half) the magnitude of the initial discontinuity in the transverse velocity and $a_o$ is the sound speed in front of the shocks. The parameter $s_o$ is the square ratio $(a_o/b_o)^2$ of the sound $a_o$ to the Alfvén disturbance speed $b_o$ in front of the shocks. On each curve, indexed by $s_o$, the point corresponding to the minimum value of $u_{y,0}/a_o$ at which cavitation is produced is indicated by a plus (+) sign. The dashed curve is the locus of these points. The point on the curves indexed by values of $s_o$ less than unity, which corresponds to the " critical' values of $u_{y,0}/a_o$ and $\eta$ - that is, the point at which the switch-on shock in the resolution reduces to a pure gas shock, is indicated by a dot. It is easy to deduce from these curves that, for fixed values of $u_{y,0}$ and fixed pressure $p_o$ and density $\rho_o$ in front of the shocks, $H_{y,3}$ is a non-decreasing function of $H_x$.

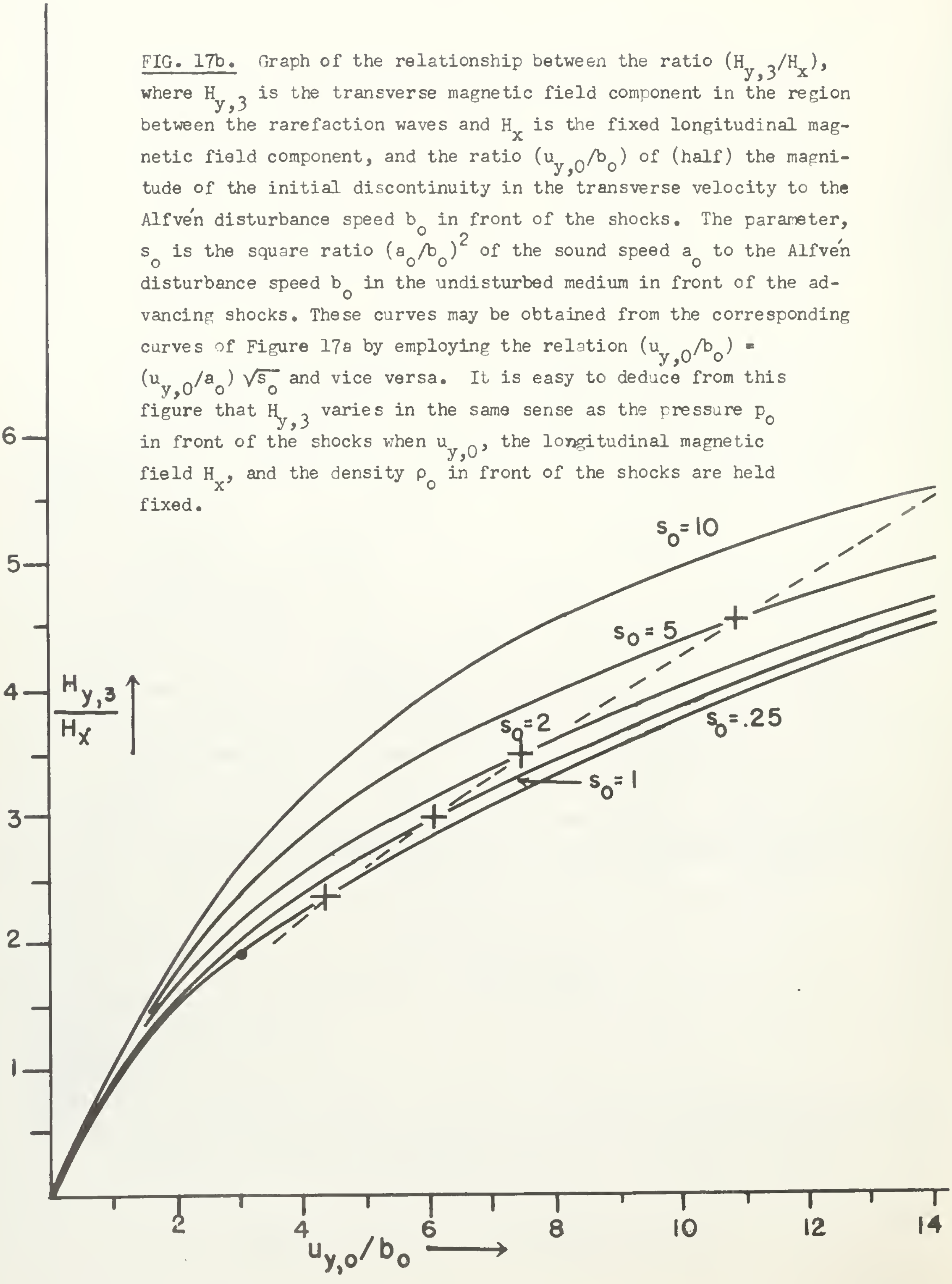

FIG. 17b. Graph of the relationship between the ratio $(H_{y,3}/H_x)$, where $H_{y,3}$ is the transverse magnetic field component in the region between the rarefaction waves and $H_x$ is the fixed longitudinal magnetic field component, and the ratio $(u_{y,0}/b_o)$ of (half) the magnitude of the initial discontinuity in the transverse velocity to the Alfvén disturbance speed $b_o$ in front of the shocks. The parameter, $s_o$ is the square ratio $(a_o/b_o)^2$ of the sound speed $a_o$ to the Alfvén disturbance speed $b_o$ in the undisturbed medium in front of the advancing shocks. These curves may be obtained from the corresponding curves of Figure 17a by employing the relation $(u_{y,0}/b_o) = (u_{y,0}/a_o)\sqrt{s_o}$ and vice versa. It is easy to deduce from this figure that $H_{y,3}$ varies in the same sense as the pressure $p_o$ in front of the shocks when $u_{y,0}$, the longitudinal magnetic field $H_x$, and the density $\rho_o$ in front of the shocks are held fixed.

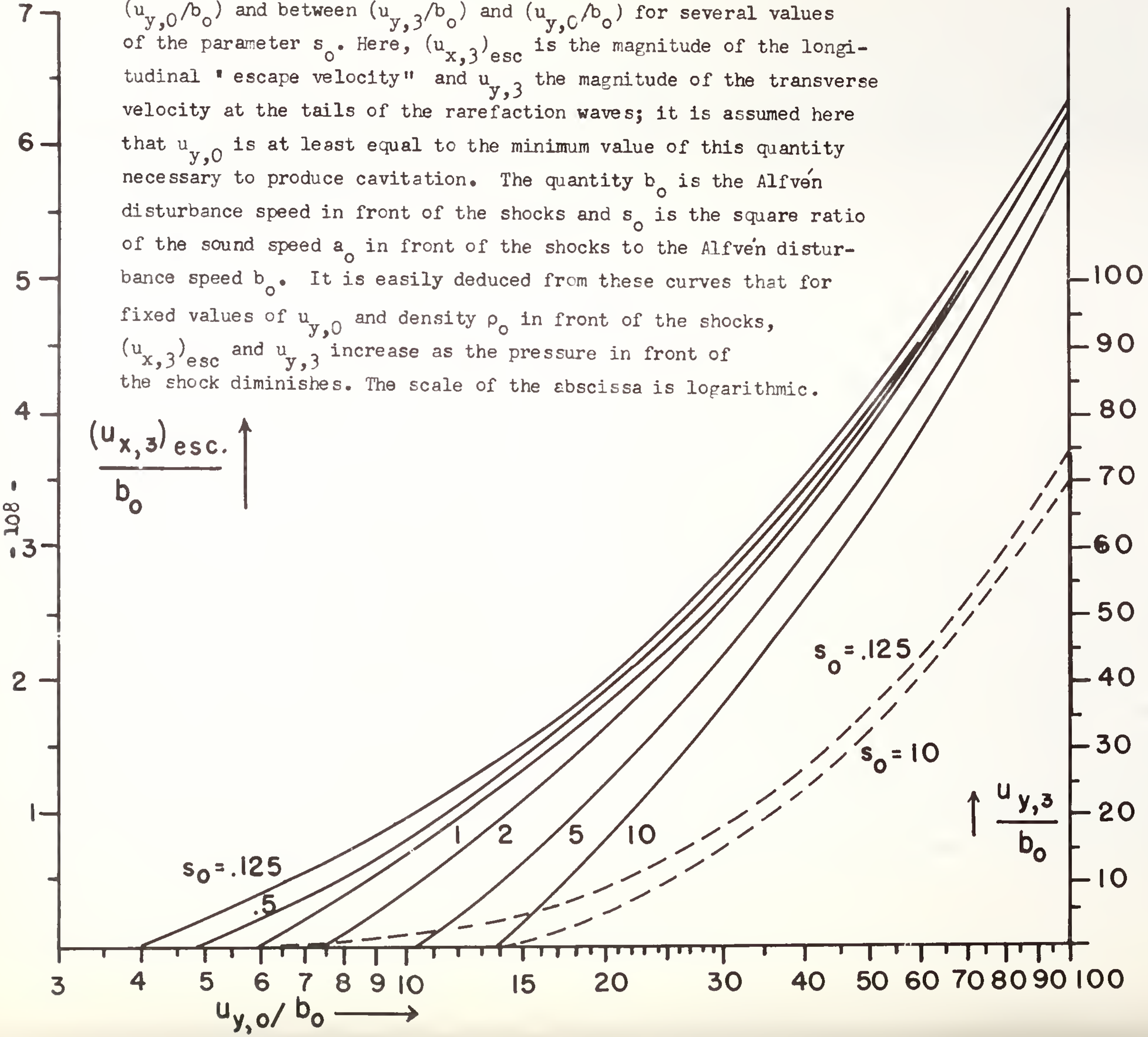

FIG. 18. Graph of the relationships between $((u_{x,3})_{esc}/b_o)$ and $(u_{y,0}/b_o)$ and between $(u_{y,3}/b_o)$ and $(u_{y,0}/b_o)$ for several values of the parameter $s_o$. Here, $(u_{x,3})_{esc}$ is the magnitude of the longitudinal "escape velocity" and $u_{y,3}$ the magnitude of the transverse velocity at the tails of the rarefaction waves; it is assumed here that $u_{y,0}$ is at least equal to the minimum value of this quantity necessary to produce cavitation. The quantity $b_o$ is the Alfvén disturbance speed in front of the shocks and $s_o$ is the square ratio of the sound speed $a_o$ in front of the shocks to the Alfvén disturbance speed $b_o$. It is easily deduced from these curves that for fixed values of $u_{y,0}$ and density $\rho_o$ in front of the shocks, $(u_{x,3})_{esc}$ and $u_{y,3}$ increase as the pressure in front of the shock diminishes. The scale of the abscissa is logarithmic.

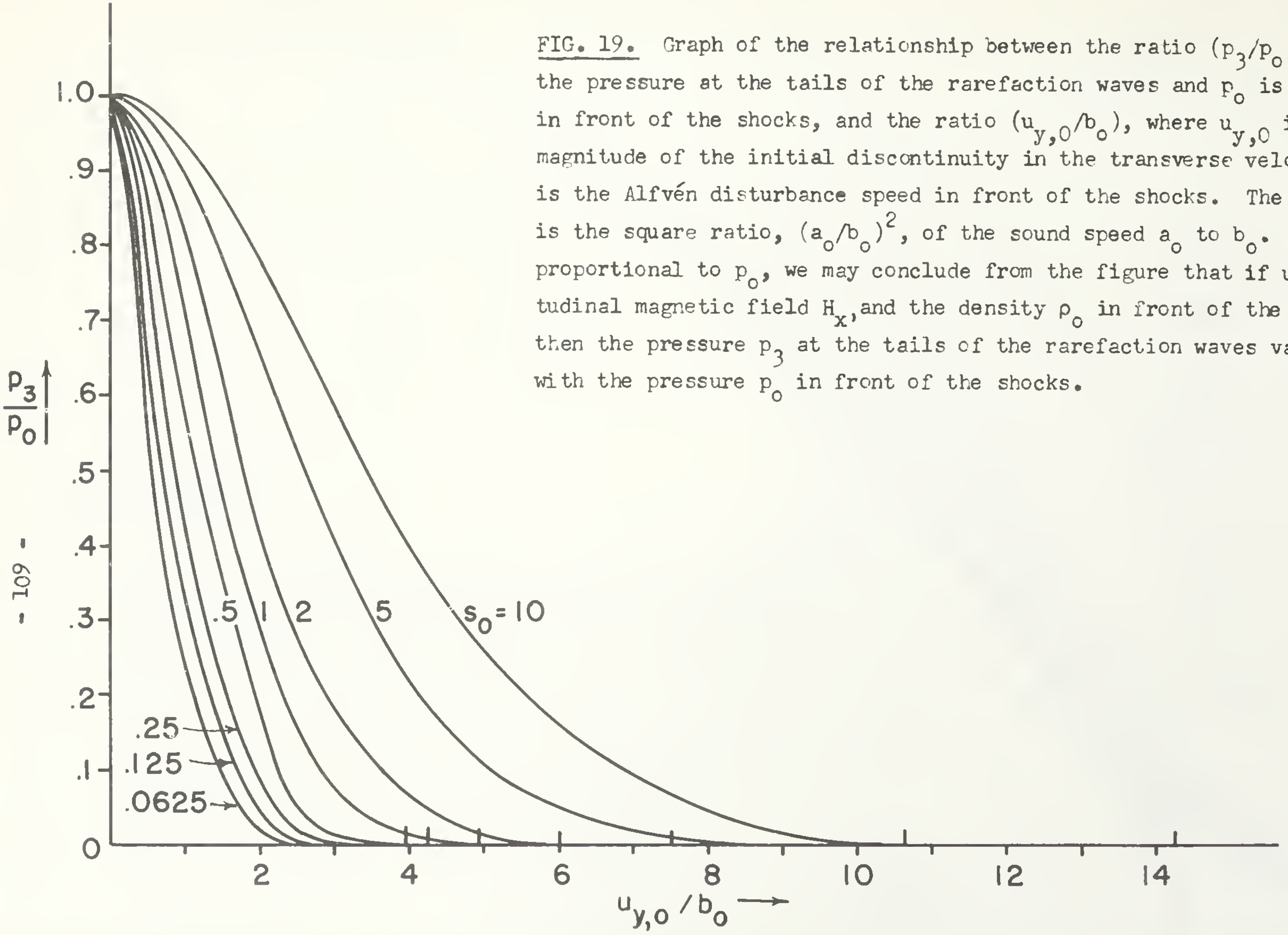

FIG. 19. Graph of the relationship between the ratio $(p_3/p_o)$, where $p_3$ is the pressure at the tails of the rarefaction waves and $p_o$ is the pressure in front of the shocks, and the ratio $(u_{y,0}/b_o)$, where $u_{y,0}$ is (half) the magnitude of the initial discontinuity in the transverse velocity and $b_o$ is the Alfvén disturbance speed in front of the shocks. The parameter $s_o$ is the square ratio, $(a_o/b_o)^2$, of the sound speed $a_o$ to $b_o$. Since $s_o$ is proportional to $p_o$, we may conclude from the figure that if $u_{y,0}$, the longitudinal magnetic field $H_x$, and the density $\rho_o$ in front of the shocks is fixed, then the pressure $p_3$ at the tails of the rarefaction waves varies directly with the pressure $p_o$ in front of the shocks.

## Appendix I

### The Rankine-Hugoniot conditions at the boundary of a perfectly conducting neutral medium which expands into a vacuum.

Let D(t) be an arbitrary time-dependent domain which contains part of the boundary, S(t) say, that separates the medium from free space. Let $\sum(t)$ be the entire surface of D(t). Consider the following system of equations:

$$(a_1) \qquad \int_{\sum(t)} \bar{E}\cdot\bar{n} = 0, \qquad \int_{\sum(t)} \bar{H}\cdot\bar{n} = 0$$

$$(a_2) \qquad \frac{d}{dt}\int_{D(t)} \bar{H}\, dV = \int_{\sum(t)} \bar{H}\,\bar{U}\cdot\bar{n}\, d\sigma - \int_{\sum(t)} \bar{n}\times\bar{E}\, d\sigma$$

(I-1)

$$(a_3) \qquad \int_{D(t)} \bar{J}\, dV + \int_{S(t)} \bar{\mathfrak{J}}\, ds = \int_{\sum(t)} \bar{n}\times\bar{H}\, d\sigma$$

$$(a_4) \qquad \frac{d}{dt}\int_{D(t)} \rho\,\bar{u}\, dV = \int_{\sum(t)} \rho\,\bar{u}\,(\bar{u}\cdot n - U\cdot n)\, d\sigma - \int_{\sum(t)} p\,\bar{n}\, d\sigma + \int_{\sum(t)} \bar{n}\cdot\bar{\bar{S}}^{(m)} d\sigma$$

$$(a_5) \qquad \frac{d}{dt}\int_{D(t)} \rho\, dV = \int_{\sum(t)} \rho(\bar{u}\cdot\bar{n} - U\cdot n)\, d\sigma\,.$$

Here, $\bar{E}$ and $\bar{H}$ are the electric and magnetic field vectors, $\bar{J}$ the volume current density within the medium, $\bar{\mathfrak{J}}$ the surface current density on S(t), $\rho$ the density, p the pressure, $\bar{u}$ the velocity of the fluid, $\bar{n}$ the outward normal to $\sum(t)$, $\bar{U}\cdot\bar{n}$ the speed of the surface in the direction $\bar{n}$, $d\sigma$ the differential element of area on $\sum(t)$ and ds the differential element of area on S(t). $\bar{\bar{S}}^{(m)}$ is the magnetic stress tensor. If $\bar{n}$ is any direction in space, $\bar{n} \cdot \bar{\bar{S}}^{(m)}$ is given by the following expression:

$$\bar{n} \cdot \bar{\bar{S}}^{(m)} = \mu(\bar{H} \cdot \bar{n})\, \bar{H} - \frac{\mu}{2} H^2\, \bar{n}\,, \tag{I-2}$$

where $\mu$ is the magnetic specific inductive capacity of free space. Moreover, $\nabla \cdot \bar{\bar{S}}^{(m)}$ is given by the following well-known identity:

$$\nabla \cdot \bar{\bar{S}}^{(m)} = \mu(\nabla \times \bar{H}) \times \bar{H} + \mu\bar{H}\, \nabla \cdot \bar{H}\,. \tag{I-3}$$

In the medium we assume that the electric field vector is given by

$$\bar{E} = \mu\bar{H} \times \bar{u}\,. \tag{I-4}$$

In the following we shall suppose that dependent variables are continuous and have continuous space and time derivatives everywhere except possibly across S(t). Let $D_o(t)$ be a region contained entirely within the medium. Then, the system (I-1) applies in $D_o(t)$ if we set $\bar{J}$, the surface current density, equal to zero. If we use the identities[†]

$$\begin{aligned} &\frac{d}{dt} \int A\,dV = \int_{D(t)} \frac{\partial A}{\partial t}\, dV + \int_{\sum(t)} A\, \bar{U} \cdot \bar{n}\, d\sigma \\ &\int_{D(t)} \nabla * Q\, dV = \int_{\sum(t)} \bar{n} * Q\, d\sigma\,, \end{aligned} \tag{I-5}$$

where A is a scalar and Q a scalar, vector, or tensor quantity for which the operation " * " makes sense, then, on taking into account (I-3) and (I-4), the system (I-1) reduces to the following set of partial differential equations in $D_o(t)$:

---

[†] The quantities A and Q are assumed to be continuous; $\frac{\partial A}{\partial t}$ and $\nabla \times Q$ are assumed to be integrable in the domain over which the integration is extended.

$$(b_1) \qquad \nabla \cdot \bar{E} = 0, \qquad \nabla \cdot \bar{H} = 0$$

$$(b_2) \qquad \frac{\partial \bar{H}}{\partial t} + \nabla \times (\bar{H} \times \bar{u}) = 0$$

$$(b_3) \qquad \nabla \times \bar{H} = J$$

(I-6)

$$(b_4) \qquad \rho\left( \frac{\partial \bar{u}}{\partial t} + \bar{u} \cdot \nabla \bar{u}\right) + \nabla p + \mu(\nabla \times \bar{H}) \times \bar{H} = 0$$

$$(b_5) \qquad \frac{\partial \rho}{\partial t} + \nabla \cdot (\rho \bar{u}) = 0.$$

Similarly, if $D_1(t)$ is a region contained entirely within empty space we find:

$$(c_1) \qquad \nabla \cdot \bar{E} = 0, \qquad \nabla \cdot \bar{H} = 0$$

$$(I\text{-}7) \quad (c_2) \qquad \nabla \times E + \mu \frac{\partial \bar{H}}{\partial t} = 0$$

$$(c_3) \qquad \nabla \times \bar{H} = 0.$$

Thus the system (I-1) is equivalent to Lundquist's equations within the medium and to the quasistatic approximation to Maxwell's equations in free space.

Now let us apply (I-1) to D(t), the first domain discussed in this Appendix. Let S(t) separate D(t) into $D_o(t)$ and $D_1(t)$, $D_1(t)$ being the region in free space. Then after applying (I-1) to $D_o(t)$ and $D_1(t)$ separately and subtracting the resulting equations from the corresponding equation over D(t), we get, since the volume terms cancel, the following integral relations over the surface S(t):

$$(d_1) \qquad \int_{S(t)} \bar{n} \times \left[\bar{E}\right] ds = 0, \qquad \int_{S(t)} \bar{n} \times \left[\bar{H}\right] ds = 0$$

$$(d_2) \qquad \int_{S(t)} \left\{ \bar{U} \cdot \bar{n} \, [H] - \bar{n} \times [E] \right\} ds = 0$$

(I-8)

$$(d_3) \qquad \int_{S(t)} \left\{ \bar{n} \times [H] - \bar{j} \right\} ds = 0$$

(I-8 cont'd)

$$(d_4) \qquad \int_{S(t)} \left[\rho\, \bar{u}(\bar{u} \cdot \bar{n} - \bar{U} \cdot n)\right] ds - \int_{S(t)} p\, \bar{n}\, ds - \int_{S(t)} \bar{n} \cdot \bar{\bar{S}}^{(m)} ds$$

$$(d_5) \qquad \int_{S(t)} \left[\rho(u \cdot \bar{n} - \bar{U} \cdot n)\right] ds = 0.$$

Here, the normal to $S(t)$, $\bar{n}$, is assumed directed into $D_o(t)$, and if $Q$ is any quantity (scalar or vector) then

(I-9)
$$[\,Q\,] = Q_1 - Q_o \,.$$

Since $D(t)$ is arbitrary, $S(t)$, which by definition is that part of the boundary of the total domain contained in $D(t)$, may be chosen arbitrarily small. From (I-8) we therefore obtain the following jump relations across $S(t)$:

(I-10)

$$(e_1) \qquad [\,\bar{E}\,] \cdot \bar{n} = 0, \qquad [\,\bar{H}\,] \cdot \bar{n} = 0$$

$$(e_2) \qquad [\,\bar{H}\,]\, \bar{U} \cdot \bar{n} - n \times [\,E\,] = 0$$

$$(e_3) \qquad \bar{n} \times [\,H\,] = \bar{j}$$

$$(e_4) \qquad [\,m\bar{u}\,] - [\,p\,]\bar{n} - \frac{\mu}{2}\,[\,\bar{H}^2\,]\,\bar{n} + \mu(\bar{H} \cdot \bar{n})\,[\,\bar{H}\,]$$

$$(e_5) \qquad [\,m\,] = 0, \quad m_j = \rho_j(\bar{u}_j \cdot \bar{n} - \bar{U} \cdot \bar{n}), \qquad j = 0, 1.$$

Now since $\rho_1$ vanishes in free space we have, using $(e_5)$,

(I-11)
$$m_1 = m_o = 0$$

It follows from the transverse part of $(e_4)$ and the second relation of $(e_1)$ that $[\,H\,]$ vanishes*. Consequently, from $(e_1)$, $(e_2)$ and $(e_3)$ we conclude that $[\,E\,]$ and $\bar{j}$ vanish. Moreover, the longitudinal part of $(e_4)$ and $[\,H\,] = 0$ implies that $[p]$ vanishes. Hence, since $p_1 = 0$, we find that $p_o$ vanishes. Since, in addition, $\rho_o$ is related to $p_o$ by means of the adiabatic equation of state it follows that $\rho_o$ also vanishes.

---

* It is assumed here, that $\bar{H}_1 \cdot \bar{n}$ ($= H_2 \cdot \bar{n}$) does not vanish.

The relations

$$\text{(I-12)} \qquad \rho_o = 0 , \quad p_o = 0 , \quad [\bar{E}] = 0, \quad [\bar{H}] = 0$$

are the desired "jump" conditions at the boundary surface $S(t)$.

It should be observed that the Rankine-Hugoniot conditions noted in the text may be derived in a similar manner.

## Appendix II

### The relation of $q_{cav}$ to $q_{tr}$ and $1-q_{cav}$ to $1-q_{tr}$ as $q_{tr}$ approaches zero and unity respectively.

In (4.13) set $s = 0$ and $q = q_{cav}$. We then have

$$0 = \frac{1}{q_{tr}}\left(\frac{1-q_{cav}}{1-q_{tr}}\right)^{\theta}$$

$$\text{(II-1)} \qquad = \theta(1-q_{cav})^{\theta}\left[(\theta+1)\log\left\{\frac{q_{tr}(1-q_{cav})}{q_{cav}(1-q_{tr})}\right\} + \frac{1}{q_{cav}} - \frac{1}{q_{tr}} + \sum_{k=1}^{\theta}\left(\frac{\theta+1-k}{k}\right)\left\{\frac{1}{(1-q_{tr})^{\theta}} - \frac{1}{(1-q_{cav})^{\theta}}\right\}\right].$$

Let $q_{tr}$ and hence $q_{cav}$ $(< q_{tr})$ approach zero. Neglecting higher-order terms, in particular the logarithmic and sum terms, we get

$$\text{(II-2)} \qquad \frac{1}{q_{tr}} - \theta\left(\frac{1}{q_{cav}} - \frac{1}{q_{tr}}\right) = 0.$$

Solving for $q_{cav}$ we have

$$\text{(II-3)} \qquad q_{cav} \sim \frac{\theta}{\theta+1}\, q_{tr}\,, \quad q_{tr} \to 0.$$

Now let $q_{tr}$ approach unity. Neglecting the first two terms in the braces in (I-1) and the first three terms in the summation (it is assumed that $\theta$ is 5) we have, after suitably rearranging terms,

$$\text{(II-4)} \qquad \left[\frac{1}{1-q_{tr}}\left(\frac{1-q_{tr}}{1-q_{cav}}\right) + 2.5\right] - \left(\frac{1-q_{cav}}{1-q_{tr}}\right)^{4}\left(\frac{2.5q_{tr}-1}{q_{tr}}\right) = 0.$$

Setting

$$\text{(II-5)} \qquad \omega = \frac{1-q_{tr}}{1-q_{cav}}\,,$$

we then have

(II-6) $$\omega^5 + \frac{3}{2}(1-q_{tr})\omega^4 - (1-q_{tr})\left[\frac{3/2\ q_{tr}-1}{q_{tr}}\right] = 0.$$

Assuming, subject to later verification, that ratio of the first to the second term is very small compared to unity, i.e., that

(II-7) $$\frac{(3/2)(1-q_{tr})}{\omega} << 1,$$

we get

(II-8) $$\omega^5 = (1-q_{tr})\left[\frac{(3/2)q_{tr}-1}{q_{tr}}\right]$$

and hence

(II-9) $$\omega = (1-q_{tr})^{1/5}\left[\frac{(3/2)q_{tr}-1}{q_{tr}}\right]^{1/5} \qquad q_{tr} \rightarrow 1 .$$

Clearly, the relation (II-7) is satisfied. Employing (II-5), we have finally

(II-10) $$1 - q_{cav} \sim (1-q_{tr})^{4/5}\,(2/3)^{1/5}. \qquad q_{tr} \rightarrow 1 .$$

## References

[1] Alfvén, H. - Cosmological electrodynamics; Oxford (Clarendon Press), 1950.

[2] De Hoffman, F. and Teller, E. - Magneto-hydrodynamic shocks; Phys. Rev., 80, 629 (1950).

[3] Helfer, L.H. - Magneto-hydrodynamic shock waves; Astrophysical Journal, 117, 177, (1952).

[4] Lüst, R. - (a) Magneto-hydrodynamische Stosswellen in einen Plasma unendlicher Leitfähigkeit; Zeit. für Naturforchung, 8a 277 (1953).

(b) Stationäre magneto-hydrodynamische Stosswellen beliebiger Stärke; Zeitschrift für Naturforschung, 10a, 125, (1955).

[5] Courant, R. and Friedrichs, K.O. - Supersonic flow and shock waves; Interscience Publishers, New York, 1948.

[6] Lax, P.D. - Initial-value problems for non-linear hyperbolic equations; Conference on Partial Differential Equations, Technical Report 14, Univ. of Kansas, 1954.

[7] Friedrichs, K.O. - Non-linear wave motion in magneto-hydrodynamics; a Los Alamos Report, 1954.

[8] Lundquist, S. - Studies in magneto-hydrodynamics; Arkiv for Fysik, 5, 297, (1952).

[9] Owens, O.G. - One-dimensional compressible flows of magneto-hydrodynamics; Technical Memorandum of the Sandia Corporation, September, 1955.

[10] Pearson, K. - Tables of the incomplete beta-function; the Biometrika Office, University College, London, 1934.